RWTH AACHEN

RHEINISCH-WESTFÄLISCHE TECHNISCHE HOCHSCHULE AACHEN

Institut für Mathematik

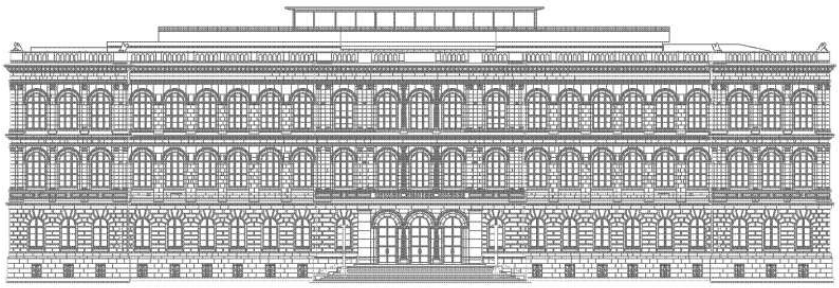
Structure of the Attractor of the Cahn-Hilliard Equation on a Square

by

Stanislaus Maier-Paape
Konstantin Mischaikow
Thomas Wanner

Report No. **5** 2005

Oktober 2005



Institute for Mathematics, RWTH Aachen University

Templergraben 55, D-52062 Aachen
Germany

Structure of the Attractor of the Cahn-Hilliard Equation on a Square

Stanislaus Maier-Paape
Institut für Mathematik
RWTH Aachen
Templergraben 55
52062 Aachen, Germany
maier@instmath.rwth-aachen.de

Konstantin Mischaikow
Center for Dynamical Systems and Nonlinear Studies
Georgia Institute of Technology
Atlanta, GA 30332-0190, USA
mischaik@math.gatech.edu

Thomas Wanner
Department of Mathematical Sciences
George Mason University
Fairfax, VA 22030, USA
wanner@math.gmu.edu

December 22, 2005

Abstract

We describe the fine structure of the global attractor of the Cahn-Hilliard equation on two–dimensional square domains. This is accomplished by combining recent numerical results on the set of equilibrium solutions due to Maier-Paape and Miller [27] with algebraic Conley index techniques. Using the information on the set of equilibria as assumption, we build Morse decompositions and connection matrices. The latter imply existence of heteroclinic connections between the equilibria inside the attractor. While path following the parameter range of Cahn–Hilliard, we find more and more complicated dynamical behavior. One of our main results describes the fine structure of the attractor for mean mass zero with four stable cosine structured equilibria and eight other stable equilibria that have a quarter circle nodal line. Besides that, we also study the attractor in symmetry fixed point spaces where we e.g. find nonunique connection matrices and saddle–saddle connections of Morse sets.

AMS subject classifications: 35B40, 35B41, 35K55

Keywords: Cahn-Hilliard equation, global attractor, equilibrium structure, heteroclinic connections, Conley index, connection matrix, transition matrix

Contents

1 Introduction **3**

2 Equilibrium Structure **7**
2.1 Basic Hypotheses and Notation 7
2.2 Bifurcation Points and Center Manifold Reductions 8
2.3 Numerical Results 13
2.4 Numerically Motivated Hypotheses 18

3 Conley Index Theory **19**

4 The Attractor before the Secondary Bifurcation **24**
4.1 Morse Decompositions and Admissible Orders 25
4.2 Connection Matrices 26

5 The Attractor after the Secondary Bifurcation **30**
5.1 Morse Decompositions and Admissible Orders 30
5.2 The Zero Mass Case 34
5.3 Global Bifurcations 40

6 The Attractor with stable Quarter Circle Solutions **46**
6.1 Numerically Motivated Hypotheses 46
6.2 Situation with Non–resolved Chessboard Solutions 49
6.3 Resolved Chessboard Solutions in a Fixed Point Space 53
6.4 Symmetry with respect to Both Diagonals 63

List of Figures **66**

References **68**

1 Introduction

For many dissipative equations arising in applications, the long-time behavior of their solutions is determined by a compact global attractor. Understanding the dynamics on the attractor is therefore crucial to a deeper understanding of the underlying model. There exist numerous results on establishing the existence of attractors, both for specific examples and for general classes of problems. We refer the reader to the by now standard references Babin, Vishik [1], Hale [20], and Temam [41], as well as the literature cited therein. Nevertheless, results which actually describe the dynamics on the attractor are not quite as common. See for example Brunovský, Fiedler [3, 4], McCord, Mischaikow [32], Kokubu, Mischaikow, Nishiura, Oka, Takaishi [25], Grinfeld, Novick-Cohen [19], and Fiedler, Rocha [13], just to name a few. Common to all of these papers is that they restrict their attention to evolution problems for functions which are defined on one–dimensional domains. This restriction is necessary, since the results crucially rely on describing the evolution of the lap or zero number of the solutions. Combining this knowledge with precise information on the structure of the equilibrium set and with Conley index theory, then furnishes the description of the dynamics on the global attractor. A somewhat different approach was presented by Mischaikow [34], who assumes the existence of a very specific Morse decomposition of the attractor. Again, this assumption has been verified for certain one–dimensional problems only.

In this paper we present some insight into the dynamics on the attractor for a specific partial differential equation model on a two–dimensional square domain. This will be accomplished by Conley index methods, in combination with rigorous mathematical results and certain assumptions on the equilibrium structure of the problem — where the latter assumptions have been verified numerically. Although we rely on numerical information, we make use only of robust properties, i.e. properties which are stable under perturbation like existence and uniqueness of hyperbolic equilibria or heteroclinic connections that lie in transverse sections of invariant manifolds of hyperbolic equilibria. Since such robust objects may, in principle, be rigorously proved by numerically supported methods (see e.g. Mischaikow, Zgliczyński [42], Maier–Paape et al. [28], Day et al. [10] or Korostyshevskiy [26]), we are only one or two steps short of rigorously proving more or less complete fine structure in global attractors even for PDE on two–dimensional square domains. To the best of our knowledge, this is the first time that such a result on two–dimensional domains has been achieved.

Specifically, we consider the Cahn-Hilliard equation

$$\begin{aligned} u_t &= -\Delta(\varepsilon^2\Delta u + f(u)) \quad \text{in} \quad \Omega\,, \\ &\qquad \frac{\partial u}{\partial \nu} = \frac{\partial \Delta u}{\partial \nu} = 0 \quad \text{on} \quad \partial\Omega\,, \end{aligned} \tag{1}$$

which was proposed by Cahn and Hilliard [5, 6] as a model for phase separation processes in binary metal alloys. We assume that $\Omega = (0,1)^2 \subset \mathbb{R}^2$, and that the function $-f$ is the derivative of a double-well potential F, the standard example being the cubic function $f(u) = u - u^3$ with double-well potential $F(u) = (u^2-1)^2/4$. In

the model, ε is a small positive parameter modeling interaction length. Furthermore, the variable u represents the concentration of one of the two components of the alloy, subject to an affine transformation such that the concentrations 0 or 1 correspond to u being -1 or 1, respectively. The Cahn-Hilliard equation is mass-conserving, i.e., the total concentration $m = \int_\Omega u dx$ remains constant along any solution u. Moreover, (1) is an $H_0^{-1}(\Omega)$-gradient system with respect to the van der Waals free energy functional

$$E_\varepsilon[u] := \int_\Omega \left(\frac{\varepsilon^2}{2} \cdot |\nabla u|^2 + F(u) \right) dx \,, \tag{2}$$

where F is the primitive of $-f$ as mentioned above. See Fife [14].

Using the methods of Henry [21], it can be shown that the Cahn-Hilliard equation generates a nonlinear semiflow on the affine space of $H^2(\Omega)$-functions with fixed mass m satisfying Neumann boundary conditions. As for the long-time behavior of solutions of (1), the existence of a global, connected attractor $\mathcal{A} = \mathcal{A}_{\varepsilon,m}$ which is compact, and attracts all bounded sets, has been established by Nicolaenko, Scheurer, and Temam [36]. See also Temam [41]. Furthermore, it is known that every solution of the Cahn-Hilliard equation converges to an equilibrium as $t \to \infty$. See Zheng [43] and Rybka, Hoffmann [38]. More detailed information on the structure of the attractor exists only for one–dimensional domains. See Mischaikow [34], Bai et al. [2], Elliott, Stuart [12], as well as Grinfeld, Novick-Cohen [19].

For gradient systems such as Cahn–Hilliard it is known that the global attractor consists of equilibrium solutions, as well as orbits connecting them (see Temam [41]). A significant obstacle to generalizing the above results to higher–dimensional domains Ω has been the lack of knowledge about the structure of the set of equilibria. Only few rigorous analytical results are available. See for example Fife et al. [15], Maier-Paape, Wanner [29], and Kielhöfer [23], [24] for certain two–dimensional domains. However, a complete rigorous description seems to be out of reach.

Recently, Maier-Paape and Miller [27] obtained numerical results in the range $\varepsilon \geq 1/\sqrt{230}$ describing the set of equilibria for the special case of Ω being the unit square $(0,1)^2 \subset \mathbb{R}^2$, using path-following techniques. These results were in parts (i.e. for $\varepsilon \geq 1/\sqrt{60}$ and away from the bifurcation points) even made rigorous by Maier–Paape, Miller, Mischaikow and Wanner [28] using computer assisted proofs based on Conley index theory. Using their results, we are able to obtain a description of the attractor of the Cahn-Hilliard equation (1) with $\Omega = (0,1)^2$ as long as $\varepsilon \geq \bar{\varepsilon}$ where $\bar{\varepsilon}$ depends on the specific case of the attractor.

More precisely, we establish homology based connection matrices for Morse decompositions of the attractor $\mathcal{A}_{\varepsilon,m}$ of (1). Since nontrivial entries in connection matrices can be linked to the existence of heteroclinic connections, we get a rough idea of how the dynamics inside the global attractor is organized and thereby establish a "lower bound" on the complexity of the flow on the attractor. We are, however, one step short of establishing semi–conjugacies from the global attractor onto certain finite–dimensional dynamical systems. Nevertheless, we think in further studies this should be achievable. Even though the range of considered ε-values seems to be rather small, we already identify interesting phenomena. To describe those in more detail, we want

to introduce some of the main equilibrium branches of (1) with mean mass $m = 0$ (see Figure 1).

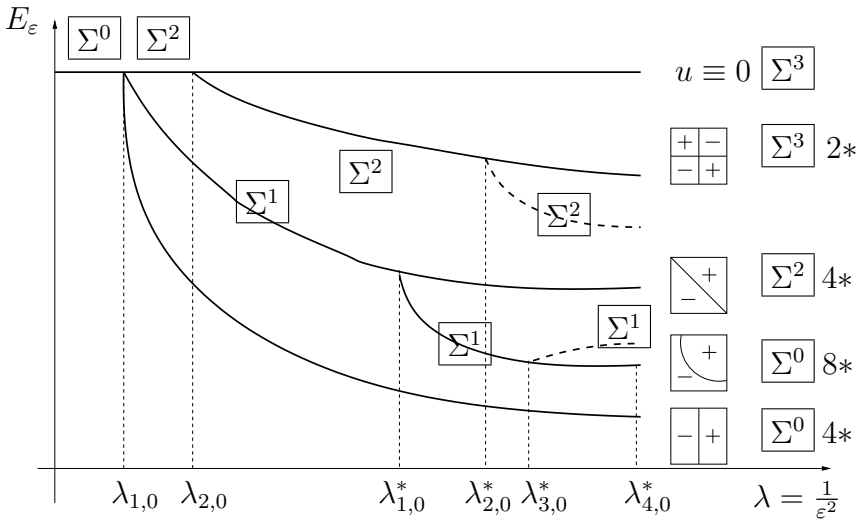


Figure 1: Sketch of the bifurcation diagram and energy values for $m = 0$

Notice that from now on we sometimes use the new parameter $\lambda = 1/\varepsilon^2$. For the main branches in Figure 1 we have sketched the nodal line structure of the solutions which is globally preserved in λ. Furthermore Σ^i indicates a branch of hyperbolic equilibria with Morse index i and $k*$ means that by symmetry this branch has a total of k similar looking branches. In Figure 2 we give numerical contour plots of the four main branches from the energy diagram Figure 1.

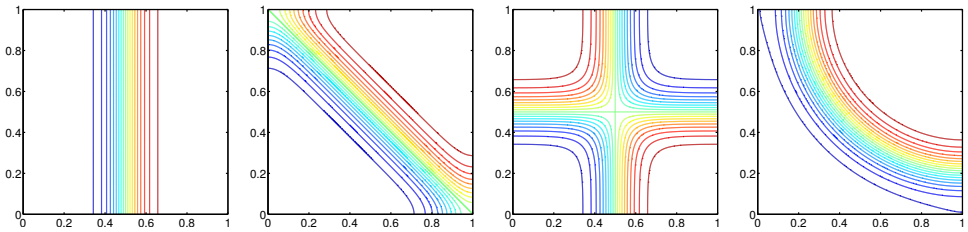


Figure 2: Contour plots of the four main branches at $\lambda = 150$

One of our main results is the description of the global attractor in the full phase space for mass $m = 0$ after the bifurcation point $\lambda^*_{3,0} \approx 118$. At this point the branches of solutions with a quarter circle nodal line bifurcate and give birth to solutions with no more symmetry. As a consequence of that bifurcation, the quarter circle solutions become stable. Besides those stable quarter circle solutions, there are also stable solutions of the respective ODE problem with cosine structure and one straight nodal line. This main result is presented in Subsection 6.2 (see Figure 29).

We believe that this result describes the mechanism to answer an open question stated in Bai et al. [2] concerning Figure 6.4(ii) therein: this figure shows a trajectory of the Cahn–Hilliard equation for $\varepsilon = 0.01$ which finally settles in a quarter circle solution. Consequently Bai et al. ask the question whether the quarter circle steady

state might be stable. Even though $\varepsilon = 0.01$ is far from the regime where our numerical assumptions have been verified, in principle the attractor structure of Figure 29 may very well still hold at $\varepsilon = 0.01$ or even for smaller ε values. Further studies to confirm this would be desirable.

Since the complexity of the set of equilibria increases considerably as ε decreases, we also discuss the attractor for $m = 0$ in certain fixed point spaces where all solutions have some additional symmetry (cf. Subsections 6.3 and 6.4; in particular Figures 34 and 37). We think that some of these dynamical descriptions of the attractor even hold in the range $\varepsilon < 1/\sqrt{230}$.

This paper is organized as follows. In Section 2, we present both rigorous and numerical results on the structure of the equilibrium set of (1). After setting the framework in Section 2.1, we present rigorous results on the equilibrium structure near the homogeneous equilibrium in Section 2.2. These results are obtained using a center manifold reduction. The numerical results of Maier-Paape and Miller [27] are briefly reviewed in Section 2.3. Together with the previous bifurcation analysis, they provide a fairly detailed picture of the structure of the equilibrium set (see in particular the bifurcation/energy diagrams Figures 10 and 11). Finally, based on these numerical results we formulate additional hypotheses on the structure of the equilibrium set in Subsection 2.4. In the next Section 3 we briefly review the basics of Conley index theory and formulate some lemmas and propositions that are helpful later when it comes to establishing entries in connection matrices. For instance we review the notion of transition matrices that are used to continue connection matrices for the energy induced order. A more subtle point is the continuation of known interval information at bifurcation points. Here we often could apply Proposition 3.7 after switching to the flow induced order.

The remaining three sections address the attractor structure. In Section 4 we obtain precise results for arbitrary mass m. These results are valid as long as none of the bifurcating primary branches exhibits a secondary bifurcation. Then in Section 5 we address the attractor structure after the first secondary bifurcation at $\lambda^*_{1,0}$ (see the attractor in Figure 17 for $m = 0$). These results can be extended even beyond the secondary bifurcation of the chessboard solutions at $\lambda^*_{2,0}$ by not resolving that respective Morse set any further after the bifurcation point. Using this ansatz we are able to reach the point were the quarter circle solutions become stable. This part is described in Section 6 and was mentioned above. Finally, we want to mention some results in Subsection 5.3, where we discuss global bifurcations and possible attractor dynamics for $m \neq 0$, but after the first secondary bifurcation at $\lambda^*_{1,0}$. We can describe possible dynamics in that range as far as the assumed Morse decompositions continue, but we have not yet enough numerical information on the existence of certain heteroclinic connections to precisely establish which connection matrices are in fact assumed in that range.

We close this introduction with a remark on the underlying numerical assumptions from which we start our analysis. Based on our numerical observations we have formulated hypotheses like (H1) to (H6) in Subsection 2.4 or the various modifications in Section 6. In order to rigorously verify these hypotheses the following tasks have to be performed:

- rigorous computation of branches of hyperbolic equilibria (e.g. (H3)); at bifurcation points the structure of the bifurcation has to be resolved rigorously (for instance (H4)).

As noted before, at least for some branches of hyperbolic equilibria rigorous computations have already been worked out (cf. [28]). Further tasks are:

- continuation of isolated invariant sets and verification of energy related estimates concerning the elements of that set (like in (H5) or (H3b)' of Subsection 6.1; in particular (46)).
- completeness of the set of equilibria (for instance (H6)).

The latter point boils down to verifying that no additional equilibria - apart from the ones already found - are present. Such questions have recently been discussed in Day et al. [10] for the Swift–Hohenberg equation. One last point on our to do list is:

- rigorous verification of transverse heteroclinic connections (e.g. like in (42)).

Non–rigorous computations of some of the needed transverse heteroclinic connections may be found under http://www.instmath.rwth-aachen.de/∼maier.

All the above hypotheses share the property that they are stable under perturbation. Therefore, in principle it is possible to use computer assisted proofs to establish them. In conclusion, there is hope that at some point our result might be verified to hold even without extra hypotheses.

Acknowledgements

S. Maier–Paape would like to thank the Department of Mathematical Sciences at George Mason University for its hospitality during his sabbatical in spring 2005 when these results were worked out. He was supported by the *Deutsche Forschungsgemeinschaft* MA 1587/4–1 and KON 594/2005. Konstantin Mischaikow was partially supported by NSF grants DMS–0511115 and DMS–0107396, DOE grant 97891, and DARPA. The work of Thomas Wanner was partially supported by NSF grant DMS–0406231 and the U.S. Department of Energy under Contract DE–FG02–05ER25712.

2 Equilibrium Structure

2.1 Basic Hypotheses and Notation

In this section we present both theoretical and numerical results which describe the set of equilibria of the Cahn-Hilliard equation for a range of certain ε-values. Throughout, we assume that the following hypothesis is satisfied.

(H1) Consider the Cahn-Hilliard equation (1) on the unit square $\Omega = (0,1)^2 \subset \mathbb{R}^2$ for the specific nonlinearity $f(u) = u - u^3$. The total mass m is a fixed real number

in the spinodal region satisfying

$$0 \le m^2 < \frac{1}{25} \, .$$

Finally, we use the abbreviation $\lambda = \varepsilon^{-2}$.

We note that the above constraint on m is only satisfied in a part of the spinodal region $\{u\colon |u| < 1/\sqrt{3}\}$. It can readily be verified that under this hypothesis, the equilibrium solutions of (1) are precisely the solutions of the semilinear elliptic problem

$$\begin{aligned} \varepsilon^2 \Delta u + f(u) &= c \qquad \text{in} \quad \Omega \, , \\ \frac{\partial u}{\partial \nu} &= 0 \qquad \text{on} \quad \partial\Omega \, , \\ \int_\Omega u \, dx &= m \, , \end{aligned} \tag{3}$$

where the real constant c depends on the solution u. In fact, one has $c = \int_\Omega f(u)\, dx$.

The special choice of the domain Ω and the function f implies several symmetry properties of solutions of (3). By slightly abusing notation, let us assume that the orthogonal group $O(2)$ is acting on $\mathbb{R}^2$ with respect to the new origin $(1/2, 1/2)$, i.e., with respect to the center of our domain Ω. Then the symmetry group of Ω is the dihedral group D_4 consisting of four rotations and four reflections, and we adopt the following notation.

(H2) Assume that the orthogonal group $O(2)$ acts on $\mathbb{R}^2$ with respect to the center of the square $\Omega = (0,1)^2$. Then for $k = 0, \dots, 3$, we denote by $\gamma_k \in O(2)$ the counter-clockwise rotation about $k \cdot \pi/2$. Furthermore, let γ_x and γ_y denote the reflections about parallels to the x- and y-axis through $(1/2, 1/2)$, respectively, and let γ_a and γ_b denote the reflections about the diagonals $y = x$ and $y = 1 - x$, respectively.

All of these elements of D_4 act on functions $u : \Omega \to \mathbb{R}$ in the obvious way, i.e., we define $(\gamma u)(z) = u(\gamma^{-1} z)$ for all $z \in \Omega$ and $\gamma \in D_4$.

It is easy to verify that if u is a solution of (3) and $\gamma \in D_4$ is arbitrary, then the function γu is also a solution of (3) with the same mass m. Furthermore, the oddness of the nonlinearity f immediately implies that if u is an equilibrium of the Cahn-Hilliard equation with mass m, then $-u$ is a solution of (3) with mass $-m$. This action will be denoted by $\gamma_m\colon\ u \mapsto -u$.

We already mentioned in the introduction that the Cahn-Hilliard equation (1) has a compact global attractor $\mathcal{A}_\lambda^m$ for arbitrary $\lambda > 0$, where we choose m as in (H1). As a first part of this attractor we study the set of equilibria in the following.

2.2 Bifurcation Points and Center Manifold Reductions

Obviously, the constant function m is an equilibrium solution for all $\varepsilon > 0$. In the following, we determine the structure of nontrivial solution branches of (3) bifurcating from this trivial solution branch.

We begin in this subsection with a description of the first two bifurcation points on the trivial solution branch $\{(\varepsilon, m, c) : \varepsilon > 0, c = f(m)\}$ as ε decreases towards 0. In addition, the dynamics of the Cahn-Hilliard equation (1) close to the trivial solution is determined using a center manifold reduction. All of these results are mathematically rigorous.

It is well-known that the eigenvalues of $-\Delta$ on the square domain $\Omega = (0,1)^2$ and subject to homogeneous Neumann boundary conditions are given by

$$\kappa_{k,\ell} = \left(k^2 + \ell^2\right) \cdot \pi^2 \,, \qquad \text{for} \qquad k, \ell \in \mathbb{N}_0 \,, \tag{4}$$

with corresponding eigenfunctions

$$\varphi_{k,\ell}(x,y) = \cos(k\pi x) \cdot \cos(\ell \pi y) \,. \tag{5}$$

In view of hypothesis (H1), the linearization of (3) at the homogeneous equilibrium m has a nontrivial kernel if and only if

$$\lambda = \frac{1}{\varepsilon^2} = \frac{\kappa_{k,\ell}}{f'(m)} \,, \qquad \text{for some} \qquad (k,\ell) \in \mathbb{N}_0^2 \setminus \{(0,0)\} \,. \tag{6}$$

We are particularly interested in the first two bifurcation points, given by

$$\lambda_{1,m} = \frac{1}{\varepsilon_{1,m}^2} = \frac{\pi^2}{f'(m)} \,, \qquad \text{and} \qquad \lambda_{2,m} = \frac{1}{\varepsilon_{2,m}^2} = \frac{2\pi^2}{f'(m)} \,. \tag{7}$$

We begin our discussion of the dynamics of the Cahn-Hilliard equation (1) near the homogeneous equilibrium m by considering ε close to the second bifurcation point $\varepsilon_{2,m}$. In this case, the linearization of (3) has a one–dimensional kernel, and one can hope to apply the celebrated result due to Crandall and Rabinowitz [9], or some variant thereof. This is indeed possible and leads to the following result.

Lemma 2.1 *Assume that (H1) and (H2) hold, and consider ε-values close to the bifurcation point $\varepsilon_{2,m}$ defined in (7). Then as ε decreases through $\varepsilon = \varepsilon_{2,m}$, two non-trivial solutions $\mathbf{c}_0^m = \mathbf{c}_0^m(\varepsilon)$ and $\mathbf{c}_1^m = \mathbf{c}_1^m(\varepsilon)$ of (3) bifurcate from the trivial solution m. For definiteness, we assume that $\mathbf{c}_0^m - m < 0$ close to $(0,0)$. Both of these solutions have Morse index Σ^2, and for $i = 0, 1$ they satisfy*

$$\begin{array}{rclcrcl} \gamma_0 \mathbf{c}_i^m &=& \gamma_2 \mathbf{c}_i^m &=& \mathbf{c}_i^m \,, & \qquad \gamma_1 \mathbf{c}_i^m &=& \gamma_3 \mathbf{c}_i^m &=& \mathbf{c}_{1-i}^m \,, \\ \gamma_a \mathbf{c}_i^m &=& \gamma_b \mathbf{c}_i^m &=& \mathbf{c}_i^m \,, & \qquad \gamma_x \mathbf{c}_i^m &=& \gamma_y \mathbf{c}_i^m &=& \mathbf{c}_{1-i}^m \,, \end{array} \tag{8}$$

as well as

$$\mathbf{c}_i^{-m} = -\mathbf{c}_{1-i}^m \,.$$

Moreover, there exist two heteroclinic orbits connecting the homogeneous equilibrium m to either of the new equilibria for $\varepsilon < \varepsilon_{2,m}$, provided $\varepsilon \approx \varepsilon_{2,m}$. These heteroclinic orbits arise as transverse intersections of the unstable manifold of m and the stable manifolds of the $\mathbf{c}_i^m$. Through this bifurcation, the Morse index of the homogeneous equilibrium m changes from Σ^2 to Σ^3. See also Figure 3 where the case $m = 0$ is depicted.

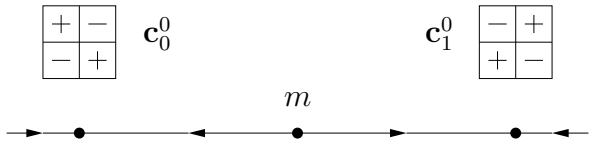


Figure 3: Dynamics near the bifurcation point $\varepsilon = \varepsilon_{2,m}$ for $m = 0$

As introduced before Σ^k is used to denote an equilibrium with Morse index k. The corresponding bifurcation can be found in Figures 10 and 11 at $\lambda_{2,0}$ and $\lambda_{2,m}$, respectively.

Proof: Assume that $\varepsilon^2 = \varepsilon_{2,m}^2$. Then the linearization of (1) at the homogeneous equilibrium m has a one–dimensional kernel, spanned by the function $\varphi_{1,1}$ defined in (5). One can easily verify that the result by Crandall and Rabinowitz [9] is applicable, which immediately implies the occurrence of the bifurcation and the transversality of the invariant manifolds.

In order to more precisely describe the flow, we augment the Cahn-Hilliard equation (1) by the ordinary differential equation

$$\dot{\varepsilon} = 0 \; . \tag{9}$$

Then standard results imply the existence of a smooth two–dimensional center manifold for (1), (9) in a neighborhood of $(m, \varepsilon_{2,m}^2)$. If we write

$$\varepsilon^2 = \varepsilon_{2,m}^2 + \eta$$

and

$$\begin{aligned} u = m + \alpha\varphi_{1,1} + w \quad & \text{where} \quad \alpha \in \mathbb{R} \\ & \text{and} \quad (w,1)_{L^2} = (w,\varphi_{1,1})_{L^2} = 0 \; , \end{aligned}$$

then the center manifold is given as the graph of a smooth function $\Phi = \Phi(\alpha, \eta)$, which is defined in a neighborhood of $(0,0) \in \mathbb{R}^2$. Following Henry [21, Section 6.2], it can be shown that the flow on this center manifold is given by $\dot{\eta} = 0$ and

$$\dot{\alpha} = -\alpha \cdot \left(4\pi^4 \cdot \eta + \frac{3\pi^2}{8} \cdot \frac{3 - 35m^2}{1 - 3m^2} \cdot \alpha^2 \right) + |\alpha| \cdot O\left(|(\alpha,\eta)|^3 \right) \; . \tag{10}$$

From this the assertions of Lemma 2.1 follow easily. ◇

The above proof remains true as long as we only assume $m^2 < 3/35$. The stronger assumption in hypothesis (H1) will be needed later. In the case $m^2 > 3/35$, equation (10) implies that two non-trivial solutions bifurcate from the homogeneous equilibrium for $\varepsilon^2 > \varepsilon_{2,m}^2$. Furthermore, the direction of the flow on the center manifold is reversed. In other words, the bifurcation changes from a supercritical to a subcritical

pitchfork bifurcation in terms of the parameter $\lambda = 1/\varepsilon^2$. This also corresponds to the formation of a turning point on the bifurcation branches, which is similar to the one–dimensional case studied by Grinfeld, Novick-Cohen [18].

Let us now turn our attention to the first bifurcation point $\varepsilon_{1,m}$. It can readily be verified that the linearization of (3) at the homogeneous equilibrium m has a two–dimensional kernel, spanned by the functions $\varphi_{1,0}$ and $\varphi_{0,1}$ — and resulting in a far more interesting bifurcation picture. More precisely, we obtain the following result.

Lemma 2.2 *Assume that (H1) and (H2) hold, and consider ε-values close to the bifurcation point $\varepsilon_{1,m}$ defined in (7). Then as ε decreases through $\varepsilon = \varepsilon_{1,m}$, eight non-trivial solutions bifurcate from the trivial solution m, which can be described as follows.*

(a) The four solutions $\mathbf{d}_i^m = \mathbf{d}_i^m(\varepsilon)$ for $i = 0, \ldots, 3$ have Morse index Σ^1, and their geometry is qualitatively like $m \pm \varphi_{1,0} \pm \varphi_{0,1}$, i.e., their m-level sets are close to either one of the two diagonals of Ω. For definiteness, we assume that $\mathbf{d}_0^m - m < 0$ close to $(0,0)$, as well as $\mathbf{d}_i^m = \gamma_i \mathbf{d}_0^m$ for $i = 1, 2, 3$. Furthermore, the solutions exhibit the following symmetries for $i = 0$ and $i = 2$:

$$\begin{array}{llll} \gamma_a \mathbf{d}_i^m = \mathbf{d}_i^m , & \gamma_b \mathbf{d}_{i+1}^m = \mathbf{d}_{i+1}^m , & & \\ \gamma_x \mathbf{d}_0^m = \mathbf{d}_3^m , & \gamma_y \mathbf{d}_0^m = \mathbf{d}_1^m , & \mathbf{d}_0^{-m} = -\mathbf{d}_2^m . & \end{array} \tag{11}$$

(b) The four solutions $\mathbf{x}_i^m = \mathbf{x}_i^m(\varepsilon)$ for $i = 0, \ldots, 3$ have Morse index Σ^0, and their geometry is qualitatively like $m \pm \varphi_{1,0}$ or $m \pm \varphi_{0,1}$, i.e., their m-level sets are close to either the horizontal or the vertical line through the center of Ω. For definiteness, we assume that $\mathbf{x}_0^m - m < 0$ close to $(0,0)$ and $(0,1)$, as well as $\mathbf{x}_i^m = \gamma_i \mathbf{x}_0^m$ for $i = 1, 2, 3$. Furthermore, the solutions exhibit the following symmetries for $i = 0$ and $i = 2$:

$$\begin{array}{llll} \gamma_x \mathbf{x}_i^m = \mathbf{x}_i^m , & \gamma_y \mathbf{x}_{i+1}^m = \mathbf{x}_{i+1}^m , & & \\ \gamma_a \mathbf{x}_0^m = \mathbf{x}_1^m , & \gamma_b \mathbf{x}_0^m = \mathbf{x}_3^m , & \mathbf{x}_0^{-m} = -\mathbf{x}_2^m . & \end{array} \tag{12}$$

Moreover, the Morse index of the trivial solution m changes from Σ^0 to Σ^2. The flow of (1) close to m is qualitatively given as shown in Figure 4 for the case $m = 0$. For $m \neq 0$ the flow is qualitatively the same, but the level sets of the equilibria change. The heteroclinic orbits between the homogeneous equilibrium m and the $\mathbf{d}_i^m$, as well as the ones between the $\mathbf{d}_i^m$ and the $\mathbf{x}_j^m$ arise as transverse intersections of the respective unstable and stable manifolds.

Proof: Assume $\varepsilon^2 = \varepsilon_{1,m}^2$. The linearization of (1) at the homogeneous equilibrium m has a two–dimensional kernel, spanned by the functions $\varphi_{1,0}$ and $\varphi_{0,1}$ defined in (5). As in the proof of Lemma 2.1, we augment the Cahn-Hilliard equation (1) by $\dot{\varepsilon} = 0$, i.e., by the ordinary differential equation (9). Then (1), (9) has a smooth three–dimensional center manifold in a neighborhood of $(m, \varepsilon_{1,m}^2)$. Again we introduce new coordinates. Let

$$\varepsilon^2 = \varepsilon_{1,m}^2 + \eta$$

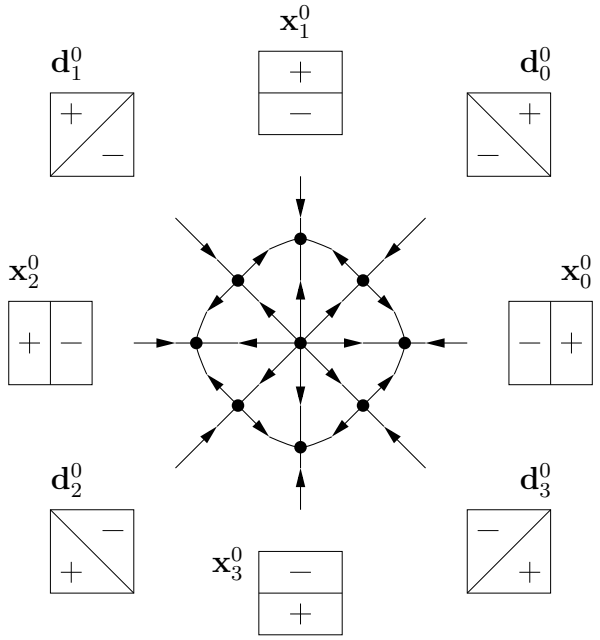


Figure 4: Dynamics near the bifurcation point $\varepsilon = \varepsilon_{1,m}$ for $m = 0$

and

$$u = m + \alpha\varphi_{1,0} + \beta\varphi_{0,1} + w \ , \quad \text{where} \quad \alpha, \beta \in \mathbb{R} \ , \quad \text{and} \quad (w,1)_{L^2} = (w,\varphi_{1,0})_{L^2} = (w,\varphi_{0,1})_{L^2} = 0 \ .$$

Then the center manifold is given as the graph of a smooth function $\Phi = \Phi(\alpha, \beta, \eta)$, defined in a neighborhood of $(0,0,0) \in \mathbb{R}^3$, and using the method of Henry [21, Section 6.2] one can show that the flow on this center manifold is given by $\dot{\eta} = 0$ and

$$\dot{\alpha} = -\alpha \cdot \left(\pi^4 \cdot \eta + c_1(m) \cdot \alpha^2 + c_2(m) \cdot \beta^2\right) + R_\alpha(\alpha, \beta, \eta) \ , \tag{13}$$

$$\dot{\beta} = -\beta \cdot \left(\pi^4 \cdot \eta + c_2(m) \cdot \alpha^2 + c_1(m) \cdot \beta^2\right) + R_\beta(\alpha, \beta, \eta) \ , \tag{14}$$

where

$$c_1(m) = \frac{3\pi^2(1-5m^2)}{4(1-3m^2)} \quad \text{and} \quad c_2(m) = \frac{3\pi^2(1-15m^2)}{2(1-3m^2)} \ .$$

Moreover, R_α and R_β are smooth functions satisfying

$$R_{\alpha/\beta}(\alpha, \beta, \eta) = |(\alpha, \beta)| \cdot O\left(|(\alpha, \beta, \eta)|^3\right) \ .$$

In order to obtain the assertions of the lemma we employ scaling methods as described in Chow and Hale [7, Chapter 7].

Notice first that due to (H1) we have $m^2 < 1/25$. This implies $c_1(m) \neq c_2(m)$, as well as $c_1(m) > 0$ and $c_2(m) > 0$. Similar to the proof of Lemma 2.1 in [7, Chapter 7] one can then show that there exists a constant $C > 0$ and a neighborhood V of $(0,0,0) \in \mathbb{R}^3$, such that the following is true: If $(\alpha, \beta, \eta) \in V$ is an equilibrium of the flow (13-14) on the center manifold, then

$$|(\alpha, \beta)| \leq C\sqrt{|\eta|} \ .$$

Thus, we can rescale both (13) and (14) by setting

$$\alpha = \tilde{\alpha} \cdot \tilde{\eta} \; , \qquad \beta = \tilde{\beta} \cdot \tilde{\eta} \; , \qquad \text{and} \qquad \eta = \sigma_\eta \cdot \tilde{\eta}^2 \; , \qquad \text{where} \qquad \sigma_\eta = \pm 1 \; . \tag{15}$$

In other words, we consider the cases $\eta > 0$ and $\eta < 0$ separately by setting $\sigma_\eta = +1$ or $\sigma_\eta = -1$, respectively.

Inserting (15) into (13) and (14), introducing the new time scale $\tau = t \cdot \tilde{\eta}^2$, and then dividing by $\tilde{\eta}^3$, furnishes for $\tilde{\eta} \neq 0$ the scaled system

$$\frac{d\tilde{\alpha}}{d\tau} = -\tilde{\alpha} \cdot \Big(\pi^4 \cdot \sigma_\eta + c_1(m) \cdot \tilde{\alpha}^2 + c_2(m) \cdot \tilde{\beta}^2 \Big) + \tilde{R}_{\tilde{\alpha}}(\tilde{\alpha}, \tilde{\beta}, \tilde{\eta}) \; , \tag{16}$$

$$\frac{d\tilde{\beta}}{d\tau} = -\tilde{\beta} \cdot \Big(\pi^4 \cdot \sigma_\eta + c_2(m) \cdot \tilde{\alpha}^2 + c_1(m) \cdot \tilde{\beta}^2 \Big) + \tilde{R}_{\tilde{\beta}}(\tilde{\alpha}, \tilde{\beta}, \tilde{\eta}) \; , \tag{17}$$

where $\tilde{R}_{\tilde{\alpha}/\tilde{\beta}}$ are smooth functions satisfying

$$\tilde{R}_{\tilde{\alpha}/\tilde{\beta}}(\tilde{\alpha}, \tilde{\beta}, \tilde{\eta}) = |(\tilde{\alpha}, \tilde{\beta})| \cdot |\tilde{\eta}| \cdot O(|(\tilde{\alpha}, \tilde{\beta}, \tilde{\eta})|^3) \; .$$

It is clear that for $\sigma_\eta = 1$ there are no non-trivial equilibrium solutions of the rescaled system (16), (17). This implies, that there are no non-trivial equilibria of the Cahn-Hilliard equation (1) close to m, provided $\varepsilon^2 > \varepsilon_{1,m}^2$ and $\varepsilon^2 \approx \varepsilon_{1,m}^2$.

Now assume $\sigma_\eta = -1$. For $\tilde{\eta} \to 0$ the system (16), (17) converges to a system which has eight non-trivial equilibria. These are given by

$$\left(0, \pm \frac{\pi^2}{\sqrt{c_1(m)}} \right) \; , \; \left(\pm \frac{\pi^2}{\sqrt{c_1(m)}}, 0 \right) \; , \; \left(\pm \frac{\pi^2}{\sqrt{c_1(m) + c_2(m)}}, \pm \frac{\pi^2}{\sqrt{c_1(m) + c_2(m)}} \right) \; .$$

Applying the implicit function theorem in each of these equilibria implies the existence of eight non-trivial equilibria of (16), (17) for sufficiently small $\tilde{\eta} > 0$. This in turn implies that the Cahn-Hilliard equation (1) has eight non-trivial equilibria close to m, provided $\varepsilon^2 < \varepsilon_{1,m}^2$ and $\varepsilon^2 \approx \varepsilon_{1,m}^2$. Furthermore, it is not hard to verify that these equilibrium solutions satisfy all the assertions of Lemma 2.2. See also Chow and Hale [7, Chapter 7]. This completes the proof. ◇

Notice that the results of Lemma 2.2 remain valid as long as the total mass satisfies $m^2 < 1/15$, as well as $m^2 \neq 1/25$. For $m^2 = 1/25$, one has $c_1(m) = c_2(m)$, i.e., the above proof breaks down since the limiting system exhibits infinitely many non-trivial equilibria which form a circle. In this case, higher-order approximations have to be employed. This is the reason for assuming $m^2 < 1/25$ in (H1).

Analogous to the above two results, it is possible to determine the dynamics of the Cahn-Hilliard equation (1) close to the homogeneous equilibrium m for arbitrary bifurcation values of $\varepsilon > 0$. However, this will not be needed for the main results of this paper.

2.3 Numerical Results

The results of the last subsection provide an accurate description of the flow of (1) in a neighborhood of the homogeneous equilibrium m, provided ε is close to the first or

second bifurcation point. However, these results are necessarily of a local nature, i.e., they do not provide any insight into the further behavior of the bifurcation branches.

In general, determining the complete global bifurcation structure of an infinite–dimensional problem is a difficult task, and has been achieved completely only in very few cases. In this subsection, we present recent numerical results for our situation. These were obtained by Maier-Paape and Miller [27] and recently extended by Deering et al. [11]. They furnish a clearer picture of the global structure of the solution branches from the last subsection, which were studied only locally there.

Consider the set of equations given in (3). Solutions of this system are exactly the equilibrium solutions of the Cahn-Hilliard equation (1) for the parameter $\varepsilon > 0$ and with total mass m. The parameter c is implicitly defined through the equilibrium solution as stated after (3). Nevertheless, introducing c as an additional parameter is exactly what allowed Maier-Paape and Miller [27] to obtain accurate numerical information on the solution structure by employing path-following techniques. More precisely, if we choose $c = f(m) = m - m^3$, then the constant function $u \equiv m$ satisfies (3), for any value of m. For certain m-values, non-trivial solutions will bifurcate from this trivial solution branch. Linearizing (3) at m shows that this happens if and only if (6) holds. Maier-Paape and Miller used a finite element method in combination with path-following techniques to numerically compute these non-trivial solution branches. Parts of these results, in particular in the range $\lambda \leq 60$, were recently even verified with a rigorous numerics method in Maier–Paape et al. [28].

Recall that in the one–dimensional Cahn-Hilliard equation discussed by Grinfeld, Novick-Cohen [18] all branches continue as smooth curves, and none of them exhibit secondary bifurcations. The numerics of Maier-Paape, Miller [27] and Deering et al. [11] show that this changes in the case of a square domain Ω. Most of the solution branches do exhibit secondary bifurcations, resulting in a considerably richer equilibrium structure. In particular, the following results were obtained.

(N1) **(The $\mathbf{c}_i^m$-branches)** For mass $m = 0$, the two branches of non-trivial solutions $\mathbf{c}_i^0$ described in Lemma 2.1 continue as smooth curves for $\lambda_{2,0} < \lambda \leq \lambda_{2,0}^* \approx 103.697$, i.e., the indices of the solutions do not change and are equal to Σ^2. At $\lambda = \lambda_{2,0}^*$, each of the two branches exhibits a supercritical pitchfork bifurcation leading to a total of four new solutions. The new solutions are denoted by $\mathbf{c}_i^{0,\pm}$, $i = 0, 1$, and have index Σ^2, while the index of the $\mathbf{c}_i^0$ changes to Σ^3. In order to distinguish matters this latter branch is noted $\mathbf{c}_i^{0,*}$ after the bifurcation point (cf. Figures 5 and 10). All of these solution branches continue as smooth curves keeping their qualitative nodal line structure and symmetries (8) for all $\lambda_{2,0}^* < \lambda \leq 230$ with the exception that the $\mathbf{c}_i^{0,\pm}$ undergo a further symmetry breaking bifurcation at $\lambda_{2,0}^{**} \approx 103.698$ giving birth to so called cluster solutions, which remain symmetric with respect to only one diagonal symmetry (cf. [11]), but we refrain from resolving this situation here.

For $m \neq 0$, the above pitchfork bifurcation at $\lambda_{2,0}^*$ is resolved by a generic saddle node bifurcation near the $m = 0$ branches at $\lambda_{2,m}^* > \lambda_{2,0}^*$, leaving the original branch $\mathbf{c}_i^m$ smooth and unchanged. These bifurcations generate four new solutions, two each of index Σ^3 and of index Σ^2. In order to keep the notation com-

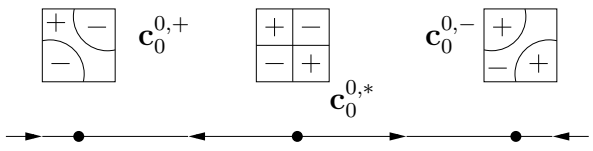


Figure 5: $\mathbf{c}_0^{0,*}$ bifurcates to $\mathbf{c}_0^{0,+}$ and $\mathbf{c}_0^{0,-}$ at $\lambda_{2,0}^*$

patible with the case $m = 0$, we denote the new solutions of index Σ^3 by $\mathbf{c}_i^{m,*}$, the new solutions of index Σ^2 by $\mathbf{c}_i^{m,-}$ for $m > 0$ and $\mathbf{c}_i^{m,+}$ for $m < 0$. Furthermore, at $\lambda = \lambda_{2,m}^*$ we change the notation for the solutions on the branches bifurcating from the trivial solution from $\mathbf{c}_i^m$ to $\mathbf{c}_i^{m,+}$ for $m > 0$ and $\mathbf{c}_i^{m,-}$ for $m < 0$ (see Figure 11).

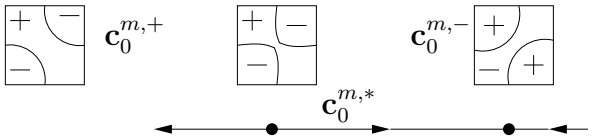


Figure 6: $\mathbf{c}_0^{m,+}$ and the saddle node branch ($\mathbf{c}_0^{m,*}$ and $\mathbf{c}_0^{m,-}$) for $m > 0$

Note that $\mathbf{c}_0^{m,+}$ in Figure 6 has the least energy of these three equilibria. To fix notation we set $\mathbf{c}_1^{m,*} := \gamma_1 \mathbf{c}_0^{m,*}$, $\mathbf{c}_1^{m,\pm} := \gamma_1 \mathbf{c}_0^{m,\pm}$, and the relations

$$\mathbf{c}_i^{-m,*} \;=\; -\mathbf{c}_{1-i}^{m,*}\,,\; \mathbf{c}_i^{-m,+} \;=\; -\mathbf{c}_{1-i}^{m,-}\,,\; \mathbf{c}_i^{-m,-} \;=\; -\mathbf{c}_{1-i}^{m,+}$$

give the equilibria with negative mass. All equilibria are fixed under the actions γ_2, γ_a, and γ_b. $\mathbf{c}_i^{0,*}$ is in addition fixed under $\gamma_1 \cdot (-1)$. All branches $\mathbf{c}_i^{m,*}$ and $\mathbf{c}_i^{m,\pm}$ persist as smooth curves for $\lambda_{2,m}^* < \lambda < 230$, with the exception that $\mathbf{c}_i^{m,\pm}$ have one further symmetry breaking bifurcation at $\lambda_{2,m}^{**,\pm} > \lambda_{2,0}^{**}$ yielding new branches with less symmetry (see cluster solutions in [11] which, however, are not important for our purposes).
Furthermore, the original branch of course also persists as smooth curve $\mathbf{c}_i^m$ in $\lambda_{2,m} < \lambda < \lambda_{2,m}^*$ with the properties (8).

(N2) **(The $\mathbf{x}_j^m$-branches)** The four branches of non-trivial solutions $\mathbf{x}_j^m$, $j = 0, ..., 3$, described in Lemma 2.2(b) continue as smooth curves for all $\lambda_{1,m} < \lambda \leq 230$, in particular we still have $\mathbf{x}_j^m = \gamma_j \mathbf{x}_0^m$, $j = 0, ..., 3$. There are no secondary bifurcations on any of these branches, i.e., the indices of the solutions do not change and are equal to Σ^0. Furthermore, the symmetries given in (12) remain and the qualitative nodal line structure is given in Figure 7.

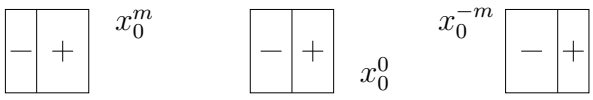


Figure 7: Nodal line structure of x_0^m, x_0^0 and x_0^{-m} for $m > 0$

(N3) **(The $\mathbf{d}_j^m$-branches)** For $m = 0$, the four branches of non-trivial solutions $\mathbf{d}_j^0$, $j = 0, ..., 3$, described in Lemma 2.2(a) exhibit secondary symmetry breaking bifurcations at $\lambda = \lambda_{1,0}^* \approx 50$ (cf. Figure 10). These bifurcations are supercritical pitchfork bifurcations and generate two new solutions $\mathbf{d}_j^{0,\pm}$, $j = 0, ..., 3$, for each of the four branches. We denote the original branch after the bifurcation by $\mathbf{d}_j^{0,*}$ (see Figure 8).

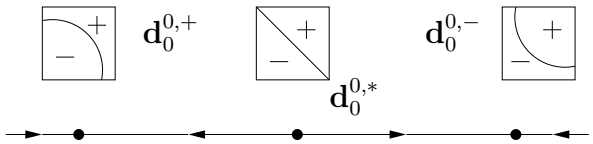


Figure 8: $\mathbf{d}_0^{0,*}$ bifurcates to $\mathbf{d}_0^{0,+}$ and $\mathbf{d}_0^{0,-}$ at $\lambda_{1,0}^*$

The three branches $\mathbf{d}_0^{0,*}$ and $\mathbf{d}_0^{0,\pm}$ are all invariant under the action γ_a and $\mathbf{d}_0^{0,*}$ possesses an additional symmetry $\gamma_b \cdot (-1)$. Each of the eight new solution branches continues as smooth curve for $\lambda_{1,0}^* < \lambda \leq \lambda_{3,0}^*$ with $\lambda_{3,0}^* \approx 117.63$. At that point $\mathbf{d}_j^{0,\pm}$ undergo a further supercritical pitchfork bifurcation which is described in more detail in Section 6. In the range $\lambda_{1,0}^* < \lambda \leq \lambda_{3,0}^*$ the $\mathbf{d}_j^{0,\pm}$ continue as smooth curves, whereas $\mathbf{d}_j^{0,*}$ continue all over $\lambda_{1,0}^* < \lambda \leq 230$ smoothly. The index of the solutions $\mathbf{d}_j^0$ equals Σ^1 for $\lambda < \lambda_{1,0}^*$, and changes to Σ^2 for $\mathbf{d}_j^{0,*}$ after the pitchfork bifurcation. The indices of the bifurcating solutions $\mathbf{d}_j^{0,\pm}$ are equal to Σ^1 in the range $\lambda_{1,0}^* < \lambda < \lambda_{3,0}^*$ and changes to Σ^0 afterwards.

For $m \neq 0$, the above pitchfork bifurcation at $\lambda_{1,0}^*$ is resolved by a generic saddle node bifurcation near the $m = 0$ branches at $\lambda_{1,m}^* > \lambda_{1,0}^*$, leaving the original branch $\mathbf{d}_j^m$ smooth and unchanged (see Figure 9).

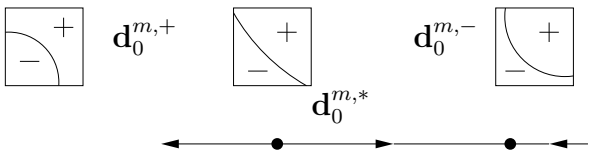


Figure 9: $\mathbf{d}_0^{m,+}$ and the saddle node branch ($\mathbf{d}_0^{m,*}$ and $\mathbf{d}_0^{m,-}$) for $m > 0$

The three branches $\mathbf{d}_0^{m,*}$ and $\mathbf{d}_0^{m,\pm}$ are still symmetric under the action of γ_a. These bifurcations generate eight new solutions, four each of index Σ^2 and of index Σ^1. To keep the notation compatible with the case $m = 0$, we denote the new solutions of index Σ^2 by $\mathbf{d}_j^{m,*}$, the new solutions of index Σ^1 by $\mathbf{d}_j^{m,-}$ $(m > 0)$ or $\mathbf{d}_j^{m,+}(m < 0)$. Furthermore, at $\lambda = \lambda_{1,m}^*$ we change the notation for the solutions on the branches bifurcating from the trivial solution from $\mathbf{d}_j^m$ to $\mathbf{d}_j^{m,+}(m > 0)$ or $\mathbf{d}_j^{m,-}(m < 0)$ (cf. Figure 11). In any case this original branch has the least energy of all branches stemming from $\mathbf{d}_j^m$. All of the branches $\mathbf{d}_j^{m,*}$, $\mathbf{d}_j^{m,\pm}$ persist as smooth curves for all $\lambda_{1,m}^* < \lambda < \lambda_{3,m}^*$, where $\mathbf{d}_j^{m,\pm}$ undergo a further bifurcation giving these branches stability, but for $m \neq 0$ this will not be needed in

this paper. To fix notation we set $\mathbf{d}_j^{m,*} := \gamma_1 \mathbf{d}_0^{m,*}$, $\mathbf{d}_j^{m,\pm} := \gamma_1 \mathbf{d}_0^{m,\pm}$ for $j = 1, ..., 3$. Using

$$\mathbf{d}_0^{-m,*} = -\mathbf{d}_2^{m,*},\ \mathbf{d}_0^{-m,+} = -\mathbf{d}_2^{m,-}, \quad \text{and} \quad \mathbf{d}_0^{-m,-} = -\mathbf{d}_2^{m,+}$$

we get the connection to negative mass. Furthermore, the original branch $\mathbf{d}_j^m$ persists as smooth curve for $\lambda_{1,m} < \lambda < \lambda_{1,m}^*$ with all the relations (11).

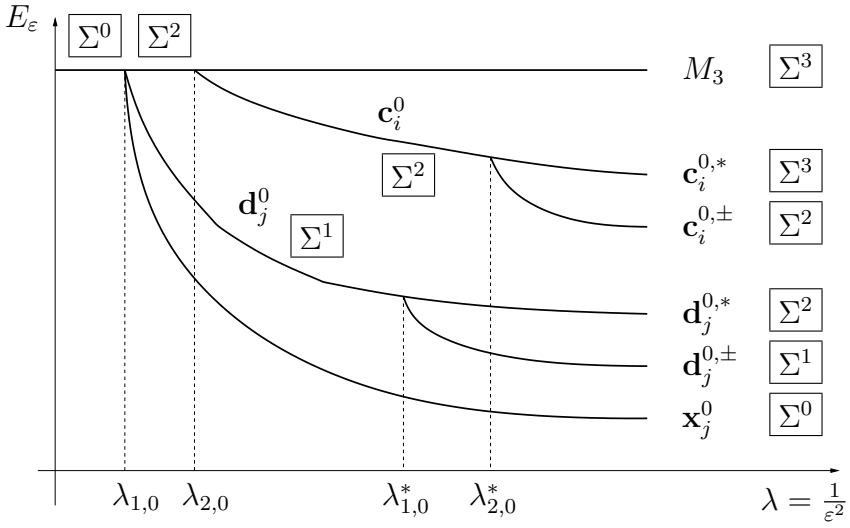


Figure 10: Partial bifurcation diagram and energy values for $m = 0$

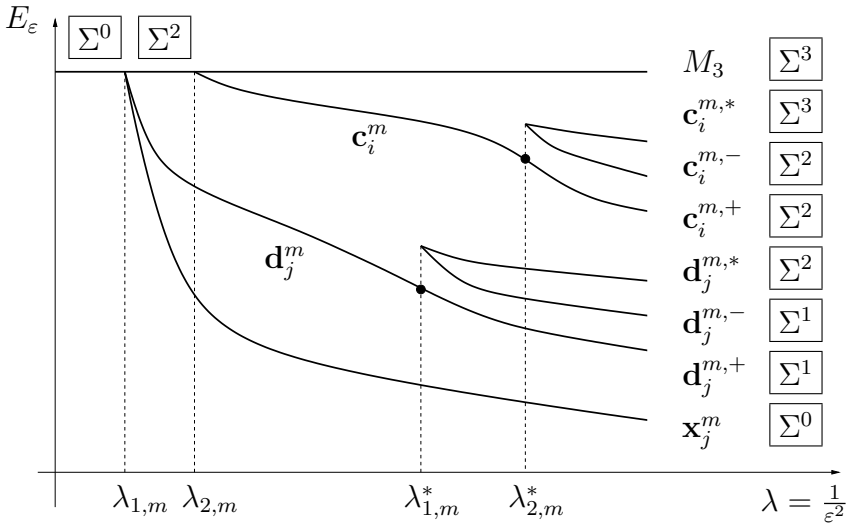


Figure 11: Partial bifurcation diagram and energy values for $m > 0$

These numerical results are summarized in Figures 10 and 11. Additionally, these figures contain information on the values of the energy functional E_ε defined in (2). It is clear that due to the symmetries of the equilibrium solutions we have $E_\varepsilon[\mathbf{c}_0^m] = E_\varepsilon[\mathbf{c}_1^m]$, as well as $E_\varepsilon[\mathbf{d}_0^m] = E_\varepsilon[\mathbf{d}_1^m] = E_\varepsilon[\mathbf{d}_2^m] = E_\varepsilon[\mathbf{d}_3^m]$, and similarly for the remaining branches, for every mass m. Furthermore, for $m = 0$ we obtain both $E_\varepsilon[\mathbf{c}_i^{0,+}] = E_\varepsilon[\mathbf{c}_i^{0,-}]$

and $E_\varepsilon[\mathbf{d}_j^{0,+}] = E_\varepsilon[\mathbf{d}_j^{0,-}]$, for all $i = 0, 1$ and $j = 0, 1, 2, 3$. As for energy inequalities between equilibria of different type, the following order follows from the numerics of [27]. For $m = 0$ the energies of the equilibria described in (N1), (N2), and (N3) are ordered as shown in Figure 10, where $j = 0, 1, 2, 3$ and $i = 0, 1$. On the other hand, for $m > 0$ the energies of the equilibria are ordered as shown in Figure 11. Similarly for $m < 0$. To the right hand side of $\lambda_{2,0}^*$ – and similarly $\lambda_{2,m}^*$ – will be further bifurcations on the $\mathbf{c}_i^{0,\pm}$ and $\mathbf{d}_j^{0,\pm}$ branches; we will describe that in more detail later once it is needed (cf. for instance Figure 23).

2.4 Numerically Motivated Hypotheses

In the next three sections we describe the structure of the attractor $\mathcal{A}_\lambda^m$ of (1) for a specific range of the parameter $\lambda = 1/\varepsilon^2$. Besides the basic hypotheses (H1) and (H2) from the beginning of Section 2.1 we will need to make further assumptions on the structure of the equilibrium set. These are based completely on the numerical results summarized in (N1), (N2), and (N3). We formulate here what is needed in Sections 4 and 5 concerning the range $0 < \lambda < \lambda_{2,m}^*$. A similar series of hypotheses to go beyond $\lambda_{2,0}^*$ (for $m = 0$ only) is given in Subsection 6.1.

(H3) **(Structure of the $\mathbf{x}_j^m$- and $\mathbf{c}_i^m$-branches)** For m as in (H1), the solution branches corresponding to the solutions $\mathbf{x}_j^m$, $j = 0, ..., 3$, and $\mathbf{c}_i^m$, $i = 0, 1$ (described in (N1) and (N2)), continue as smooth curves for $\lambda_{1,m} < \lambda < \lambda_{2,m}^*$ and $\lambda_{2,m} < \lambda < \lambda_{2,m}^*$, respectively, without any secondary bifurcations.

(H4) **(Structure of the $\mathbf{d}_j^m$-branches)** For $m = 0$, the solution branches corresponding to the solutions $\mathbf{d}_j^0$ (described in (N3)) continue as smooth curves for $\lambda_{1,0} < \lambda < \lambda_{1,0}^*$, at which point they undergo a generic supercritical pitchfork bifurcation yielding the branches $\mathbf{d}_j^{0,*}$ and $\mathbf{d}_j^{0,\pm}$. The bifurcating branches continue without secondary bifurcations for $\lambda_{1,0}^* < \lambda < \lambda_{2,0}^*$, and the indices of the solutions are as shown in Figure 10.

For $m \neq 0$ and as in (H1) the branches corresponding to the solutions $\mathbf{d}_j^m$ continue as smooth curves for $\lambda_{1,m} < \lambda < \lambda_{1,m}^*$. At $\lambda_{1,m}^*$ in a saddle node bifurcation as described in (N3) eight new branches are born giving a total of twelve branches $\mathbf{d}_j^{m,*}$ and $\mathbf{d}_j^{m,\pm}$ (cf. Figure 11). All branches continue as smooth curves for $\lambda_{1,m}^* < \lambda < \lambda_{2,m}^*$.

(H5) **(Continuation of the trivial Morse set)** For every $\lambda_{2,m} < \lambda < \lambda_{2,m}^*$ there exists an isolated invariant set $M_3 = M_{3,m}(\lambda)$ with Conley index Σ^3 which contains the trivial solution $u \equiv m$ and all equilibria bifurcating from the trivial solution at values $\lambda > \lambda_{2,m}$ including any connecting orbits between them. M_3 has all symmetries of $u \equiv m$, i.e., D_4, and for $m = 0$ additionally multiplication with -1. In the range $\lambda_{2,m} < \lambda \leq \lambda_{1,m}^*$ we assume that the set consisting of M_3 and the respective equilibria indicated in Figures 10 and 11 constitute a Morse decomposition of the attractor $\mathcal{A}_\lambda^m$ of (1) for m as in (H1).

For $\lambda \geq \lambda^*_{1,m}$ assume additionally that all the equilibria in M_3 have energy larger then $\mathbf{c}^m_i$ and the energy level of the other equilibria are ordered as illustrated in Figures 10 and 11.

(H6) **(Completeness of the bifurcation diagrams)** The bifurcation diagrams shown in Figures 10 and 11 are complete for all $0 < \lambda < \lambda^*_{2,m}$.

Basically, the above hypotheses state that for $\lambda \leq \lambda^*_{2,m}$ the complete bifurcation diagrams of (1) for m as in (H1) are as shown in Figures 10 and 11, and that the Morse set M_3 can be adapted for increasing λ in such a way that it "swallows" all subsequent bifurcations from the homogeneous equilibrium m — of which there are several. Notice, however, that we do not assume any energy inequalities between the respective equilibria for $\lambda < \lambda^*_{1,m}$. These will be a consequence of our algebraic approach. Only for $\lambda \geq \lambda^*_{1,m}$ we have to work with the energy induced order (including $\mathbf{c}^m_i < M_3$) which is always an admissible order.

Apparently the order of the energy levels may be computed robustly, since the involved energy values are significantly different. This includes the verification of the order $\mathbf{c}^m_i < M_3$. Therefore, by means of relying on numerical verification where robust computations are possible, we will derive rigorous results for situations where computations would be delicate. These results are the subject of the main Sections 4 – 6 of this paper.

3 Conley Index Theory

In this section we briefly recall a few definitions from Conley index theory. For more details we refer the reader to Conley [8], Salamon [39], Rybakowski [37], Smoller [40], Mischaikow [33], or Mischaikow and Mrozek [35].

Consider a flow $\varphi : \mathbb{R} \times X \to X$, where X denotes a locally compact topological space. Then a compact set $N \subset X$ is called an *isolating neighborhood* if its maximal invariant subset $S = Inv(N, \varphi)$ is contained in the interior of N, where

$$Inv(N, \varphi) = \{u \in N \ : \ \varphi(\mathbb{R}, u) \subset N\} \ .$$

In this situation, S is called an *isolated invariant set*. In order to describe the dynamics within such sets further, Conley introduced the concept of a Morse decomposition. Let S denote an isolated invariant set, and let

$$\mathcal{M}(S) = \{M_p \ : \ p \in \mathcal{P}\}$$

denote a finite collection of disjoint compact invariant subsets of S. The collection $\mathcal{M}(S)$ is called a *Morse decomposition*, if there exists a partial order $>$ on $\mathcal{P}$ such that for every $u \in S$ we have either

$$u \in M_p \quad \text{for some} \quad p \in \mathcal{P} \ ,$$

$$\text{or otherwise there exist } \; p, q \in \mathcal{P} \; \text{ with } \; p > q \; \text{ such that} \tag{18}$$

$$u \in \mathcal{C}\left(M_p, M_q\right) \; := \; \{w \in S \; : \; \alpha(w) \subset M_p \; \text{ and } \; \omega(w) \subset M_q\} \; .$$

In this case, the sets M_p are called *Morse sets*, and the partial order $>$ on $\mathcal{P}$ is called *admissible*. In general, there exist many admissible partial orders on the index set $\mathcal{P}$ of a given Morse decomposition. The uniquely determined minimal partial order is called the *flow–defined order* $>_\varphi$. It can easily be verified that we have $p >_\varphi q$ if and only if there exists a sequence of distinct elements $p = p_0, \ldots, p_{n+1} = q$ such that the sets of connecting orbits $\mathcal{C}(M_{p_k}, M_{p_{k+1}}) \neq \emptyset$ for $k = 0, \ldots, n$.

While it is clear that the Morse sets in a Morse decomposition are isolated invariant sets themselves, there are generally many more. For this, consider an admissible order $>$ on the index set $\mathcal{P}$, and let $I \subset \mathcal{P}$. Then I is called an *interval*, if for any choice of $p, q \in I$ and $r \in \mathcal{P}$ with $p > r > q$ we have $r \in I$. In this case, the set

$$M_I = \left(\bigcup_{p \in I} M_p \right) \; \cup \; \left(\bigcup_{p,q \in I} \mathcal{C}(M_p, M_q) \right) \tag{19}$$

is also an isolated invariant set (see [35, Proposition 2.12]).

In the following sections, we will describe the dynamics of the attractor of (1) for a certain parameter range. This will be accomplished by studying the Conley index of isolated invariant sets S. More precisely, we use the *homological Conley index* defined by

$$CH_*(S) := H_*(N/L, [L]) \approx H_*(N, L) \; ,$$

where the pair (N, L) denotes an appropriately selected *index pair* of S, and H_* denotes homology with $\mathbb{Z}_2$ coefficients. For more details we refer the reader to the introductory article by Mischaikow and Mrozek [35, Section 3.1]. In this paper, one can also find the following result, which will be needed later on.

Proposition 3.1 *Assume that S contains only a hyperbolic fixed point with an unstable manifold of dimension n. Then S is an isolated invariant set and*

$$CH_k(S) \approx \begin{cases} \mathbb{Z}_2 & \text{if } k = n \; , \\ 0 & \text{otherwise} \; . \end{cases}$$

For the remainder of this paper, we will abbreviate this statement by saying that the Conley index of S is equal to Σ^n.

In order to apply Conley's theory to Morse decompositions of the attractor, we need to know the Conley index of the attractor itself. This is the subject of the following result.

Proposition 3.2 *Let $\mathcal{A}_\lambda^m$ denote the global attractor of (1), where we set $\lambda = 1/\varepsilon^2$ and let m be as in (H1) of Subsection 2.1. Then for any $\lambda > 0$ we have*

$$CH_k\left(\mathcal{A}_\lambda^m\right) = \begin{cases} \mathbb{Z}_2 & \text{for} \quad k = 0 \; , \\ 0 & \text{for} \quad k \neq 0 \; . \end{cases}$$

We omit the proof of this result, since it is similar to the proof of Proposition 4.1 in McCord and Mischaikow [32].

Assume that we are given a Morse decomposition $\mathcal{M}(S)$ of an isolated invariant set S. The structure of the dynamics within S can be studied using the *connection matrix*

$$\Delta \; : \; \bigoplus_{p\in\mathcal{P}} CH_*(M_p) \to \bigoplus_{p\in\mathcal{P}} CH_*(M_p) \; .$$

We will write Δ as a matrix $\Delta = (\Delta(p,q))_{p,q\in\mathcal{P}}$, where $\Delta(p,q) : CH_*(M_q) \to CH_*(M_p)$ are linear mappings. Furthermore, if I denotes an interval in the partially ordered set $(\mathcal{P},>)$, we define

$$\Delta(I) \; = \; (\Delta(p,q))_{p,q\in I} \; : \; \bigoplus_{p\in I} CH_*(M_p) \to \bigoplus_{p\in I} CH_*(M_p) \; .$$

Using this notation, a connection matrix Δ has the following fundamental properties:

(C1) Δ is *upper triangular with respect to the partial order* $>$, i.e., for any pair of indices p and q a nontrivial map $\Delta(q,p) \neq 0$ implies either $p > q$ or $p = q$.

(C2) Δ is a *boundary operator*, i.e., we have $\Delta\circ\Delta = 0$, and Δ maps n-th level homology to $(n-1)$-st level homology.

(C3) For every interval I in $(\mathcal{P},>)$ we have

$$H_*\Delta(I) := \ker\Delta(I)/\mathrm{im}\Delta(I) \approx CH_*(M_I) \; .$$

An ordered pair (q,p) is called *adjacent* in $(\mathcal{P},>)$, if $\{q,p\} \subset \mathcal{P}$ is an interval with disjoint points and $q \not> p$.

(C4) If (q,p) are adjacent in $(\mathcal{P},>)$, and if $\Delta(q,p) \neq 0$, then the set of connecting orbits $\mathcal{C}(M_p, M_q)$ is not empty.

We want to point out that these properties do not characterize connection matrices. For the precise definition we refer the reader to Franzosa [16]. See also Mischaikow and Mrozek [35, Section 4.1.2]. Note that our definition of upper triangular goes back to [16, Definition 3.1]. Used for hyperbolic equilibria as Morse sets only, it is equivalent to the definition of upper triangular used in [35].

Furthermore, connection matrices are generally not unique, i.e., there may be many different connection matrices for a given Morse decomposition. There exists, however, always at least one. This fundamental result was proven by Franzosa [16].

The following lemma will be helpful later on.

Lemma 3.3 *Let $\mathcal{M}(S) = \{M_p : p \in \mathcal{P}\}$ be a Morse decomposition and let $>$ be any admissible order, i.e. $>$ has to be an extension of the flow–defined order. We denote by $\{\Delta^{>}\}$ the set of all possible connection matrices for that order. Then*

$$\{\Delta^{>_\varphi}\} \; \subset \{\Delta^{>}\} \; .$$

Proof: We just note that $>_\varphi$ might have less relations than $>$ and therefore $>_\varphi$ allows for more attractor repeller pairs. This yields more index triples and therefore more exact sequences which finally give more constraints on the connection matrices. (See the definition of connection matrices [16] or [33].) $\diamond$

In order to compute connection matrices and to relate their form to the existence of connecting orbits in S, we need the following result due to McCord [30].

Proposition 3.4 *Let (q,p) be adjacent in the partially ordered set $(\mathcal{P},>)$, and assume that the Morse sets M_p and M_q are hyperbolic equilibria whose unstable and stable manifolds intersect transversally. Furthermore, suppose that the dimensions of the unstable manifolds of M_p and M_q are given by $n+1$ and n, respectively, where $n \in \mathbb{N}_0$. Then $\Delta(q,p)$ equals the number of connecting orbits from M_p to M_q modulo 2.*

A further tool from Conley index theory necessary for our applications is the *algebraic transition matrix*. A transition matrix

$$T \; : \; \bigoplus_{p\in\mathcal{P}} CH_*(M_p) \to \bigoplus_{p\in\mathcal{P}} CH_*(M_p)$$

is an upper triangular isomorphism, which takes n-th level homology to n-th level homology. Furthermore, it relates the connection matrices of parameter-dependent Morse decompositions as the parameter varies. More precisely:

Proposition 3.5 *Let the flow $\varphi_\lambda : \mathbb{R}\times X \to \mathbb{R}$ be continuous in λ. Assume that we have a one-parameter family of Morse decompositions $\mathcal{M}_\lambda$, which continues over the interval $[\lambda_0,\lambda_1]$. Then if Δ_k denotes a connection matrix of $\mathcal{M}_{\lambda_k}$ for $k=0,1$, we have*

$$\Delta_1 = T^{-1}\circ\Delta_0\circ T \; ,$$

for some transition matrix T.

For more details we refer the reader to Franzosa and Mischaikow [17].

Remark 3.6 *In case the flow $\varphi_\lambda : \mathbb{R}\times X \to X$ is equivariant with respect to some symmetry action Γ on X, i.e.*

$$\varphi(t,\gamma x) \;=\; \gamma\,\varphi(t,x) \quad \textit{for all} \quad \gamma\in\Gamma\,,\, t\in\mathbb{R}\,,\, x\in X \; , \tag{20}$$

the entries of the connection and transition matrices have to respect this action as well. For instance if $\gamma M_p = M_{\tilde p}$ and $\gamma M_q = M_{\tilde q}$ then

$$\Delta(p,q) \;=\; \Delta(\tilde p,\tilde q) \; .$$

In order to prove this identity, one would have to introduce the definition of connection matrices. Basically, connection matrices are defined via index filtrations. In the case of equivariant dynamics one can always choose an index filtration whose sets lie on group orbits which give the desired symmetry. Since transition matrices can be viewed as special connection matrices, the same holds true for them. Further details will be given in an announced book by Kalies, Mischaikow and Vandervorst [22].

We finish this section with a result that discusses Morse decompositions in a neighborhood of a bifurcation point. In particular, we are interested in constructing finer Morse decompositions after the bifurcation from the given Morse decomposition at the bifurcation point. To do this, we need the following setup.

Let $\varphi_\lambda : \mathbb{R} \times X \to X$ be the flow of a parameter–dependent gradient system, continuous in λ, and $\mathcal{M}_{\lambda_0} = \{M_p^{\lambda_0}, p \in (\mathcal{P}_{\lambda_0}, >_{\varphi_{\lambda_0}})\}$ be a Morse decomposition of an isolated invariant set $S_{\lambda_0} \subset X$ at λ_0 with flow induced order . (21)

It is well known that the Morse decomposition continues for $|\lambda - \lambda_0| \leq \delta$ and some $\delta > 0$. Therefore the Morse sets continue as M_p^λ, $p \in \mathcal{P}_{\lambda_0}$ and the flow induced order persists, i.e. for all $|\lambda - \lambda_0| \leq \delta$

$$>_\lambda := >_{\varphi_{\lambda_0}} \tag{22}$$

is an admissible order. In particular S_{λ_0} continues to some $S_\lambda \subset X$ and $\mathcal{M}_\lambda := \{M_p^\lambda, p \in (\mathcal{P}_{\lambda_0}, >_{\varphi_\lambda})\}$ is a Morse decomposition of S_λ at λ for all $|\lambda - \lambda_0| \leq \delta$. Note that the same index set $\mathcal{P}_{\lambda_0}$ is used for all $\mathcal{M}_\lambda$. The goal of the following proposition is to handle bifurcations at λ_0 and construct finer Morse decompositions for $\lambda > \lambda_0$ as the one already known.

Proposition 3.7 *Given the situation (21) assume that $\mathcal{M}_{\lambda_0}$ continues as a Morse decomposition to $\mathcal{M}_\lambda = \{\mathcal{M}_p^\lambda, p \in (\mathcal{P}_{\lambda_0}, >_\lambda)\}$ for all λ with $|\lambda - \lambda_0| \leq \delta$ and that $I \subset \mathcal{P}_{\lambda_0}$ is an interval for $>_{lambda_0}$.*
Choose $|\lambda - \lambda_0| \leq \delta$ and let $\mathcal{M}(M_I^{\lambda_1}) = \{M_q^{\lambda_1}, q \in (\mathcal{Q}_{\lambda_1}, >_{\lambda_1}^I)\}$ be a Morse decomposition of $M_I^{\lambda_1}$ (cf. (19)). Then

$$\mathcal{M}_{\lambda_1}^2 = \{M_p^{\lambda_1}, p \in \mathcal{P}_{\lambda_0} \setminus I\} \cup \{M_q^{\lambda_1}, q \in \mathcal{Q}_{\lambda_1}\} \tag{23}$$

is a Morse decomposition of S_{λ_1} with flow induced order $>_{\lambda_1}^2$ and $\mathcal{Q}_{\lambda_1}$ is an interval in $((\mathcal{P}_{\lambda_0} \setminus I) \cup \mathcal{Q}_{\lambda_1}, >_{\varphi_{\lambda_1}}^2)$.

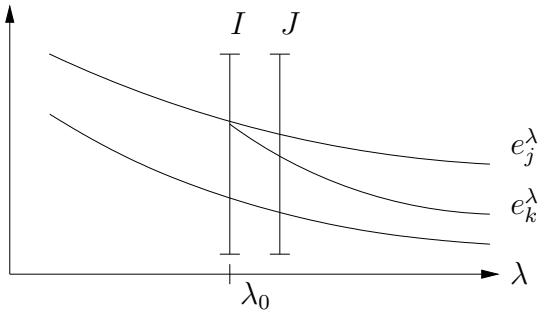


Figure 12: Intervals near the bifurcation point λ_0

Proof: Clearly the sets appearing in (23) are disjoint, compact and invariant sets and therefore Morse sets. Thus it is sufficient to show that there is a flow induced partial order on $M^2_{\lambda_1}$.

In order to see that we need a little construction. By assumption $\mathcal{M}_{\lambda_1} = \{M_p^{\lambda_1}, p \in \mathcal{P}_{\lambda_0}, >_{\lambda_1})\}$ with $>_{\lambda_1} = >_{\varphi_{\lambda_0}}$ is a Morse decomposition of S_{λ_1} and $I \subset \mathcal{P}_{\lambda_0}$ is an interval for $\mathcal{M}_{\lambda_0}$ with respect to $>_{\lambda_0} = >_{\varphi_{\lambda_0}}$
Then clearly I is also an interval for $\mathcal{M}_{\lambda_1}$ with respect to $>_{\lambda_1}$. Therefore $>_{\lambda_1}$ is an extension of the flow induced order $>_{\varphi_{\lambda_1}}$ on $\mathcal{M}_{\lambda_1}$ and I is still an interval for $>_{\varphi_{\lambda_1}}$.

Using e.g. Proposition 2.13 of [35]

$$\mathcal{M}'_{\lambda_1} := \{M_p^{\lambda_1}, p \in \mathcal{P}_{\lambda_0} \setminus I\} \cup \{M_I^{\lambda_1}\}$$

defines a new Morse decomposition of S_{λ_1} with admissible partial order $>'_{\lambda_1}$ given by

$$\begin{aligned} p >'_{\lambda_1} q &\iff p >_{\varphi_{\lambda_1}} q \qquad \text{if} \qquad p, q \in \mathcal{P}_{\lambda_0} \setminus I \\ p >'_{\lambda_1} I &\iff \exists\, q \in I \quad \text{such that} \quad p > q \\ I >'_{\lambda_1} I &\iff \exists\, q \in I \quad \text{such that} \quad q > p\,. \end{aligned} \tag{24}$$

One easily partial confirms that $>'_{\lambda_1}$ equals the flow induced order on M'_{λ_1}, i.e. $>'_{\lambda_1} = >'_{\varphi_{\lambda_1}}$.

Let us now discuss $\mathcal{M}^2_{\lambda_1}$. The first step is to show that if $u \in S_{\lambda_1} \setminus \mathcal{M}^2_{\lambda_1}$, then the alpha and omega limit sets of u lie in different elements of $\mathcal{M}^2_{\lambda_1}$. By definition of a Morse decomposition, if $u \in M_I^{\lambda_1} \setminus \mathcal{M}(M_p^{\lambda_1}$, then $\alpha(u) \subset M_q^{\lambda_1}$ and $\omega(u) \subset M_{q'}^{\lambda_1}$ where $q >^I_{\lambda_1} q'$. So assume $u \in S_{\lambda_1} \setminus (\mathcal{M}^2_{\lambda_1} \cup M_I^{\lambda_1})$. Again using the definition of a Morse decomposition for $\mathcal{M}'_{\lambda_1}$, we obtain $\alpha(u) \subset M_r^{\lambda_1}$ and $\omega(u) \subset M_{r'}^{\lambda_1}$ where $r, r' \in (\mathcal{P}_{\lambda_0} \setminus I) \subset \{I\}$ with $r >'_{\varphi_{\lambda_1}} r'$. If $r, r' \in \mathcal{P}_{\lambda_0} \setminus I$, then $r >^2_{\lambda_1} r'$.

If $r = I$, then $\alpha(u) \subset M_I^{\lambda_1}$. But then there has to exist some $q \in Q_{\lambda_1}$ with $\alpha(u) \subset M_q^{\lambda_1}$ sind since $M_I^{\lambda_1}$ has a Morse decomposition indexed with Q_{λ_1} and φ_{λ_1} is a strict gradient system. Again alpha and omega limit sets lie in different elements of $\mathcal{M}^2_{\lambda_1}$. A similar argument applies if $r' = I$. This concludes that there is a flow induced partial order $>^2_{\varphi_{\lambda_1}}$ on $\mathcal{M}^2_{\lambda_1}$.
It remains to show that Q_{λ_1} is an interval in $((\mathcal{P}_{\lambda_0} \setminus I) \cup Q_{\lambda_1}, >^2_{\varphi_{\lambda_1}})$, but this is straight forward using (24).

$\diamond$

4 The Attractor before the Secondary Bifurcation

Based on the hypotheses formulated in Sections 2.1 and 2.4, we give a precise description of the attractor $\mathcal{A}^m_\lambda$ of the Cahn-Hilliard equation (1) before the secondary

bifurcation occurs on (or near) the $\mathbf{d}_j^m$-branches. These results are valid for any mass m as in (H1) and any $\lambda \leq \lambda_{1,m}^*$. (See Figures 10 and 11.)

4.1 Morse Decompositions and Admissible Orders

As we pointed out in Section 3, the derivation of connection and transition matrices relies to some extent on knowing admissible partial orders on the index set of the corresponding Morse decompositions. While the energy information contained in Figures 10 and 11, combined with the fact that E_ε is a strict Lyapunov function for (1), readily implies such partial orders, we want to obtain our results with as few assumptions as possible. In fact, it turns out that the information on the bifurcation structure and the Morse indices contained in Figures 10 and 11 already suffices to obtain extremely precise information on the admissible orders.

We begin by considering the parameter interval $\lambda_{1,m} < \lambda \leq \lambda_{2,m}$. According to assumptions (H3) through (H6), a Morse decomposition $\mathcal{M}_\lambda^m$ of the attractor $\mathcal{A}_\lambda^m$ is given by the set

$$\mathcal{M}_\lambda^m := \left\{ \mathbf{x}_j^m \ , \ \mathbf{d}_j^m \ , \ m \ : \ j = 0, \ldots, 3 \right\} \ , \quad \text{for} \ \ \lambda_{1,m} < \lambda \leq \lambda_{2,m} \ . \tag{25}$$

By slightly abusing notation we will identify the index set $\mathcal{P}$ and the Morse decomposition $\mathcal{M}_\lambda^m$ in the following. The admissible orders (see (18)) for these Morse decompositions are the subject of the next proposition.

Proposition 4.1 *Assume that (H1) through (H6) are satisfied, and consider the parameter range $\lambda_{1,m} < \lambda \leq \lambda_{2,m}$. Furthermore, let $>$ be any partial order on $\mathcal{M}_\lambda^m$ satisfying both $m > \mathbf{d}_k^m$ and $\mathbf{d}_k^m > \mathbf{x}_j^m$ for arbitrary $k, j = 0, \ldots, 3$. Then $>$ is an admissible partial order for the Morse decomposition $\mathcal{M}_\lambda^m$.*

Proof: Fix $\lambda \in (\lambda_{1,m}, \lambda_{2,m}]$ and let $>_\varphi$ denote the flow–defined order for the Morse decomposition $\mathcal{M}_\lambda^m$ defined in (25). Then it obviously suffices to show that $>$ is an extension of the flow–defined partial order $>_\varphi$, i.e., for any pair $p, q \in \mathcal{M}_\lambda^m$ we have to verify that the inequality $p >_\varphi q$ implies $p > q$.

Let Δ denote an arbitrary connection matrix for the Morse decomposition $\mathcal{M}_\lambda^m$ equipped with the partial order $>_\varphi$. Due to the Morse indices of the Morse sets assumed in our hypotheses, Proposition 3.1, and property (C2) we must have

$$\Delta = \begin{bmatrix} 0 & D_0 & 0 \\ 0 & 0 & D_1 \\ 0 & 0 & 0 \end{bmatrix} \ ,$$

where $D_1 : \mathbb{Z}_2 \to \mathbb{Z}_2^4$ and $D_0 : \mathbb{Z}_2^4 \to \mathbb{Z}_2^4$ satisfy $D_0 \circ D_1 = 0$. Moreover, property (C3) and Proposition 3.2 imply

$$\ker D_1 \approx 0 \ , \quad \ker D_0 / \mathrm{im} D_1 \approx 0 \ , \quad \text{as well as} \quad \mathbb{Z}_2^4 / \mathrm{im} D_0 \approx \mathbb{Z}_2 \ .$$

Thus, the rank of D_1 has to be 1, and the rank of D_0 has to be 3. Together with property (C1) of a connection matrix we see that there has to be a connecting orbit

between m and some $\mathbf{d}_j^m$, as well as between some $\mathbf{d}_\ell^m$ and an $\mathbf{x}_k^m$. Since E_ε is a strict Lyapunov functional for (1), this implies $E_\varepsilon[m] > E_\varepsilon[\mathbf{d}_j^m]$ and $E_\varepsilon[\mathbf{d}_\ell^m] > E_\varepsilon[\mathbf{x}_k^m]$. Finally, using symmetry one obtains that $E_\varepsilon[\mathbf{d}_n^m] = E_\varepsilon[\mathbf{d}_{\tilde{n}}^m]$ and $E_\varepsilon[\mathbf{x}_n^m] = E_\varepsilon[\mathbf{x}_{\tilde{n}}^m]$ for arbitrary $n, \tilde{n} = 0, \ldots, 3$. Now the assertion of Proposition 4.1 follows easily. $\diamond$

Of particular interest to us is the minimal partial order satisfying the assumptions of the above result.

Definition 4.2 *In the situation of Proposition 4.1, we denote by $>_1$ the partial order on $\mathcal{M}_\lambda^m$ which is the transitive closure of the inequalities $m > \mathbf{d}_j^m$ and $\mathbf{d}_j^m > \mathbf{x}_k^m$ for arbitrary $j, k = 0, \ldots, 3$.*

The next result considers the interval $\lambda_{2,m} < \lambda \leq \lambda_{1,m}^*$. Due to assumptions (H3) through (H6), a Morse decomposition $\mathcal{M}_\lambda^m$ of the attractor $\mathcal{A}_\lambda^m$ is now given by

$$\mathcal{M}_\lambda^m := \left\{ \mathbf{x}_j^m \ , \ \mathbf{d}_j^m \ , \ \mathbf{c}_i^m \ , \ M_3 \ : \ i = 0, 1 \ , \ j = 0, \ldots, 3 \right\} \ , \quad \text{for} \ \ \lambda_{2,m} < \lambda \leq \lambda_{1,m}^* \ . \tag{26}$$

Similar to Proposition 4.1, one can prove the following result.

Proposition 4.3 *Assume that (H1) through (H6) are satisfied, and consider the parameter range $\lambda_{2,m} < \lambda \leq \lambda_{1,m}^*$. Furthermore, let $>$ be any partial order on $\mathcal{M}_\lambda^m$ satisfying $M_3 > \mathbf{c}_i^m$ for $i = 0, 1$, as well as both $\mathbf{c}_i^m > \mathbf{d}_j^m$ and $\mathbf{d}_j^m > \mathbf{x}_k^m$ for every choice of $i = 0, 1$ and $j, k = 0, \ldots, 3$. Then $>$ is an admissible partial order for the Morse decomposition $\mathcal{M}_\lambda^m$.*

Proof: The proof is analogous to the one of Proposition 4.1. This time, however, any connection matrix Δ corresponding to the flow-induced order has to be of the form

$$\Delta = \begin{bmatrix} 0 & D_0 & 0 & 0 \\ 0 & 0 & D_1 & 0 \\ 0 & 0 & 0 & D_2 \\ 0 & 0 & 0 & 0 \end{bmatrix} \ ,$$

where the matrices $D_2 : \mathbb{Z}_2 \to \mathbb{Z}_2^2$, $D_1 : \mathbb{Z}_2^2 \to \mathbb{Z}_2^4$, and $D_0 : \mathbb{Z}_2^4 \to \mathbb{Z}_2^4$ have ranks 1, 1, and 3, respectively. $\diamond$

Definition 4.4 *In the situation of Proposition 4.3, we denote by $>_2$ the partial order on $\mathcal{M}_\lambda^m$ which is the transitive closure of the inequalities $M_3 > \mathbf{c}_i^m$ for $i = 0, 1$, as well as both $\mathbf{c}_i^m > \mathbf{d}_j^m$ and $\mathbf{d}_j^m > \mathbf{x}_k^m$ for every choice of $i = 0, 1$ and $j, k = 0, \ldots, 3$.*

4.2 Connection Matrices

Now that we have precise information on the admissible orders for the Morse decompositions $\mathcal{M}_\lambda^m$ for $\lambda_{1,m} < \lambda \leq \lambda_{1,m}^*$, we can address the question of which connection matrices are supported. This will be accomplished by combining the rigorous local results from Section 2.2 with transition matrix methods. We begin by considering the parameter range $\lambda_{1,m} < \lambda \leq \lambda_{2,m}$.

Proposition 4.5 *Assume that hypotheses (H1) through (H6) are satisfied, and consider the parameter range $\lambda_{1,m} < \lambda \leq \lambda_{2,m}$. Furthermore, let $\mathcal{M}_\lambda^m$ denote the Morse decomposition of $\mathcal{A}_\lambda^m$ defined in (25), and let $>_1$ be the admissible order on $\mathcal{M}_\lambda^m$ from Definition 4.2. Then for every $\lambda_{1,m} < \lambda \leq \lambda_{2,m}$ the unique connection matrix Δ_λ^m is given by*

$$\Delta_\lambda^m = \begin{array}{|cccc|cccc|c|l}
\multicolumn{4}{c}{\mathbf{x}_0^m \ \mathbf{x}_1^m \ \mathbf{x}_2^m \ \mathbf{x}_3^m} & \multicolumn{4}{c}{\mathbf{d}_0^m \ \mathbf{d}_1^m \ \mathbf{d}_2^m \ \mathbf{d}_3^m} & m & \\
\hline
 & & & & 1 & 0 & 0 & 1 & & \mathbf{x}_0^m \\
 & & & & 1 & 1 & 0 & 0 & & \mathbf{x}_1^m \\
 & & & & 0 & 1 & 1 & 0 & & \mathbf{x}_2^m \\
 & & & & 0 & 0 & 1 & 1 & & \mathbf{x}_3^m \\
\hline
 & & & & & & & & 1 & \mathbf{d}_0^m \\
 & & & & & & & & 1 & \mathbf{d}_1^m \\
 & & & & & & & & 1 & \mathbf{d}_2^m \\
 & & & & & & & & 1 & \mathbf{d}_3^m \\
\hline
\multicolumn{9}{c}{} & m
\end{array} \tag{27}$$

where empty positions within the matrix are 0.

Proof: To begin with, let $\lambda > \lambda_{1,m}$ be sufficiently close to the bifurcation point $\lambda_{1,m}$ such that Lemma 2.2 holds. Then the connection matrix Δ_λ^m has to be of the form

$$\Delta_\lambda^m = \begin{bmatrix} 0 & D_0 & 0 \\ 0 & 0 & D_1 \\ 0 & 0 & 0 \end{bmatrix} ,$$

where $D_1 : \mathbb{Z}_2 \to \mathbb{Z}_2^4$ and $D_0 : \mathbb{Z}_2^4 \to \mathbb{Z}_2^4$ satisfy $D_0 \circ D_1 = 0$. As in the proof of Proposition 4.1 one can see that the ranks of D_0 and D_1 are given by 3 and 1, respectively. Furthermore, due to the transversality statement in Lemma 2.2 and Proposition 3.4, the entry of D_0 in the k-th row and j-th column equals the number of heteroclinic orbits from $\mathbf{d}_j^m$ to $\mathbf{x}_k^m$ modulo 2. Likewise, the entry of D_1 in the k-th row equals the number of heteroclinic orbits from m to $\mathbf{d}_k^m$ modulo 2. Together with Lemma 2.2 this immediately implies that the connection matrix Δ_λ^m necessarily has to be of the form given in the proposition, as long as $\lambda > \lambda_{1,m}$ is sufficiently close to $\lambda_{1,m}$.

Now let $\lambda_* > \lambda_{1,m}$ be sufficiently close to $\lambda_{1,m}$ as before, and let $\lambda_* < \lambda^* \leq \lambda_{2,m}$ be arbitrary. Let Δ_* denote the unique connection matrix at λ_*, and let Δ^* denote any connection matrix at λ^*. Due to Proposition 4.1, the Morse decomposition $\mathcal{M}_\lambda^m$ equipped with the partial order $>_1$ continues over the interval $[\lambda_*, \lambda^*]$. Therefore there exists an algebraic transition matrix T such that

$$\Delta^* = T^{-1} \circ \Delta_* \circ T \ .$$

Due to Definition 4.2 and the upper triangularity of transition matrices, the matrix T has to be the identity matrix. This immediately furnishes the result. ◇

The next result considers the interval $\lambda_{2,m} < \lambda \leq \lambda_{1,m}^*$. Also in this case there exists a unique connection matrix for the Morse decomposition $\mathcal{M}_\lambda^m$ of the attractor $\mathcal{A}_\lambda^m$.

Proposition 4.6 *Assume that hypotheses (H1) through (H6) are satisfied, and consider the parameter range $\lambda_{2,m} < \lambda \leq \lambda^*_{1,m}$. Furthermore, let $\mathcal{M}^m_\lambda$ denote the Morse decomposition of $\mathcal{A}^m_\lambda$ defined in (26), and let $>_2$ be the admissible order on $\mathcal{M}^m_\lambda$ from Definition 4.4. Then for every $\lambda_{2,m} < \lambda \leq \lambda^*_{1,m}$ the unique connection matrix Δ^m_λ is given by*

$$\Delta^m_\lambda = \begin{array}{c|cccc|cccc|cc|c|l}
 & \mathbf{x}^m_0 & \mathbf{x}^m_1 & \mathbf{x}^m_2 & \mathbf{x}^m_3 & \mathbf{d}^m_0 & \mathbf{d}^m_1 & \mathbf{d}^m_2 & \mathbf{d}^m_3 & \mathbf{c}^m_0 & \mathbf{c}^m_1 & M_3 & \\
\hline
 & & & & & 1 & 0 & 0 & 1 & & & & \mathbf{x}^m_0 \\
 & & & & & 1 & 1 & 0 & 0 & & & & \mathbf{x}^m_1 \\
 & & & & & 0 & 1 & 1 & 0 & & & & \mathbf{x}^m_2 \\
 & & & & & 0 & 0 & 1 & 1 & & & & \mathbf{x}^m_3 \\
\hline
 & & & & & & & & & 1 & 1 & & \mathbf{d}^m_0 \\
 & & & & & & & & & 1 & 1 & & \mathbf{d}^m_1 \\
 & & & & & & & & & 1 & 1 & & \mathbf{d}^m_2 \\
 & & & & & & & & & 1 & 1 & & \mathbf{d}^m_3 \\
\hline
 & & & & & & & & & & & 1 & \mathbf{c}^m_0 \\
 & & & & & & & & & & & 1 & \mathbf{c}^m_1 \\
\hline
 & & & & & & & & & & & & M_3
\end{array} \tag{28}$$

where empty positions within the matrix are 0.

Proof: Choose and fix $\lambda > \lambda_{2,m}$ sufficiently close to the bifurcation point $\lambda_{2,m}$ such that Lemma 2.1 can be applied. Then the connection matrix Δ^m_λ has to be of the form

$$\Delta = \begin{bmatrix} 0 & D_0 & 0 & 0 \\ 0 & 0 & D_1 & 0 \\ 0 & 0 & 0 & D_2 \\ 0 & 0 & 0 & 0 \end{bmatrix},$$

where the matrices $D_2 : \mathbb{Z}_2 \to \mathbb{Z}_2^2$, $D_1 : \mathbb{Z}_2^2 \to \mathbb{Z}_2^4$, and $D_0 : \mathbb{Z}_2^4 \to \mathbb{Z}_2^4$ have ranks 1, 1, and 3, respectively. Their specific forms are addressed separately.

We begin by considering D_0. The Morse sets $\mathbf{x}^m_j$ and $\mathbf{d}^m_j$, where $j = 0, \ldots, 3$, are an interval I in both the partial order $>_1$ and in the partial order $>_2$. Since the partial orders induced on I by either $>_1$ or $>_2$ coincide, this Morse decomposition continues over an λ-interval of the form $[\lambda_{2,m} - \varrho, \lambda_{2,m} + \varrho]$, for some $\varrho > 0$. A transition matrix argument similar to the one used in the proof of Proposition 4.5 now shows that D_0 has to coincide with the corresponding part of the connection matrix given in (27), which is exactly the form claimed in (28).

As for D_2, we recall that due to Lemma 2.1 and Proposition 3.4 the entry of D_2 in the i-th row equals the number of heteroclinic orbits from M_3 to $\mathbf{c}^m_i$ modulo 2. The rotational symmetry of the unit square, together with the equivariance of (1), then implies

$$D_2 = \begin{bmatrix} a \\ a \end{bmatrix},$$

for some $a \in \{0, 1\}$. Since D_2 has rank 1 we must have $a = 1$.

Finally, we turn our attention to D_1. Arguing as above using the rotational symmetry and the equivariance of (1) we see that

$$D_1 = \begin{bmatrix} b & c \\ c & b \\ b & c \\ c & b \end{bmatrix} .$$

According to property (C2) we have $\Delta_\lambda^m \circ \Delta_\lambda^m = 0$, which implies $D_1 \circ D_2 = 0$, and therefore $b + c = 0 \bmod 2$. Since D_1 has rank 1, this leaves $b = c = 1$ as the only possibility.

So far we have shown that the connection matrix Δ_λ^m necessarily has to be of the form given in (28), as long as $\lambda > \lambda_{2,m}$ is sufficiently close to $\lambda_{2,m}$. Using another transition matrix argument as in the proof of Proposition 4.5, one can easily show that this remains true for all $\lambda \in (\lambda_{2,m}, \lambda_{1,m}^*]$, and this completes the proof of the proposition. ◇

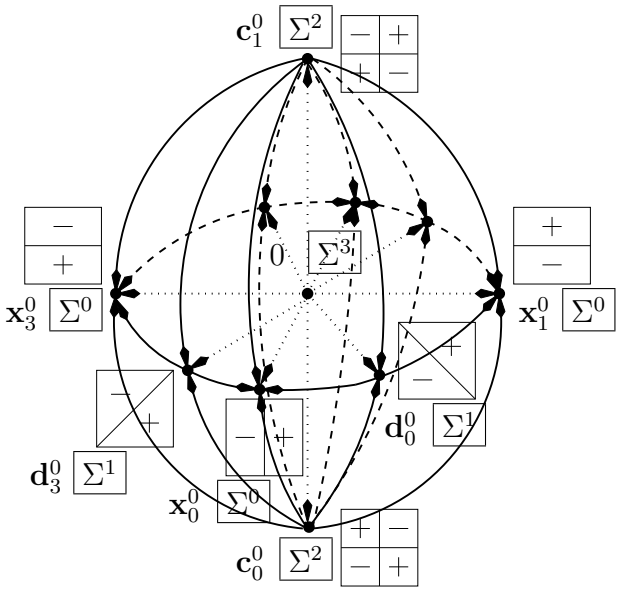


Figure 13: Sketch of the attractor $\mathcal{A}_\lambda^0$ for $\lambda \in (\lambda_{2,0}, \lambda_{1,0}^*)$

The connection matrix obtained in Proposition 4.6 suggests that the flow in $\mathcal{A}_\lambda^m$ for $\lambda \in (\lambda_{2,m}, \lambda_{1,m}^*)$ is as depicted in Figure 13. In fact, we think that methods in Kokubu et al. [25] or McCord [31] should be adaptable to establish semi–conjugacies of the flow on $\mathcal{A}_\lambda^m$ to the flow given in Figure 13. However, we do not pursue the issue of semi–conjugacies in this paper any further.

5 The Attractor after the Secondary Bifurcation

In this section we want to study the attractor of the Cahn–Hilliard equation (1) in the range $\lambda^*_{1,m} < \lambda \leq \lambda^*_{2,m}$, i.e. after the secondary bifurcation of the $\mathbf{d}^m_j$–branch, where the quarter circle solutions are born.

5.1 Morse Decompositions and Admissible Orders

In order to use connection and transition matrices we again need admissible orders on the index set of the corresponding Morse set. In contrast to Section 4, we now have to rely on energy information given by Figures 10 and 11, since we have equilibria with equal Morse indices on different energy levels. According to assumptions (H3) through (H6) for the parameter interval $\lambda^*_{1,m} < \lambda \leq \lambda^*_{2,m}$ the set

$$\mathcal{M}^m_\lambda \;:=\; \{\mathbf{x}^m_j,\, \mathbf{d}^{m,+}_j,\, \mathbf{d}^{m,-}_j,\, \mathbf{d}^{m,*}_j,\, \mathbf{c}^m_i,\, M_3 :\, i = 0, 1,\; j = 0, ..., 3\} \tag{29}$$

is a Morse decomposition of the attractor $\mathcal{A}^m_\lambda$. For λ up to $\lambda^*_{2,m}$ the Morse index of M_3 is 3, of $\mathbf{d}^{m,*}_j$ and $\mathbf{c}^m_i$ it is 2, whereas $\mathbf{d}^{m,\pm}_j$ have Morse index 1 and $\mathbf{x}^m_j$ have Morse index 0. The energy induced order for total mass $m > 0$ is

$$\mathbf{x}^m_j \;<\; \mathbf{d}^{m,+}_k \;<\; \mathbf{d}^{m,-}_j \;<\; \mathbf{d}^{m,*}_k \;<\; \mathbf{c}^m_i \;<\; M_3, \quad i = 0, 1,\; j, k = 0, ..., 3 \tag{30}$$

plus transitive closure. For $m = 0$ we have all as above, except that there is no relation between $\mathbf{d}^{m,-}_k$ and $\mathbf{d}^{m,+}_j$ since $E_\lambda(\mathbf{d}^{0,-}_k) = E_\lambda(\mathbf{d}^{0,+}_j)$. For $m < 0$ the order induced by energy between $\mathbf{d}^{m,-}_k$ and $\mathbf{d}^{m,+}_k$ is even reversed, i.e. here

$$\mathbf{x}^m_j \;<\; \mathbf{d}^{m,-}_k \;<\; \mathbf{d}^{m,+}_j \;<\; \mathbf{d}^{m,*}_k \;<\; \mathbf{c}^m_i \;<\; M_3, \quad i = 0, 1,\; j, k = 0, ..., 3 \tag{31}$$

plus transitive closure gives an admissible partial order for the Morse decomposition $\mathcal{M}^m_\lambda$. Given this partial order we intend to build connection matrices. According to (C2) any connection matrix Δ^m_λ has to be of the form

$$\Delta = \begin{bmatrix} 0 & D_0 & 0 & 0 \\ 0 & 0 & D_1 & 0 \\ 0 & 0 & 0 & D_2 \\ 0 & 0 & 0 & 0 \end{bmatrix}, \tag{32}$$

where, by (C3), the matrices

$$D_2 \colon\; \mathbb{Z}_2 \to \mathbb{Z}^6_2,\; D_1 \colon\; \mathbb{Z}^6_2 \to \mathbb{Z}^8_2, \text{ and } D_0 \colon\; \mathbb{Z}^8_2 \to \mathbb{Z}^4_2 \text{ have ranks } 1, 5, \text{and } 3\,, \tag{33}$$

respectively. Using symmetry we get

$$D_0 = \begin{array}{|cccccccc|l} \hline \mathbf{d}^{m,-}_0 & \mathbf{d}^{m,-}_1 & \mathbf{d}^{m,-}_2 & \mathbf{d}^{m,-}_3 & \mathbf{d}^{m,+}_0 & \mathbf{d}^{m,+}_1 & \mathbf{d}^{m,+}_2 & \mathbf{d}^{m,+}_3 & \\ \hline a & b & b & a & \tilde{a} & \tilde{b} & \tilde{b} & \tilde{a} & \mathbf{x}^m_0 \\ a & a & b & b & \tilde{a} & \tilde{a} & \tilde{b} & \tilde{b} & \mathbf{x}^m_1 \\ b & a & a & b & \tilde{b} & \tilde{a} & \tilde{a} & \tilde{b} & \mathbf{x}^m_2 \\ b & b & a & a & \tilde{b} & \tilde{b} & \tilde{a} & \tilde{a} & \mathbf{x}^m_3 \\ \hline \end{array} \tag{34}$$

and

$$D_1 = \begin{array}{|cccccc|l} \hline \mathbf{d}_0^{m,*} & \mathbf{d}_1^{m,*} & \mathbf{d}_2^{m,*} & \mathbf{d}_3^{m,*} & \mathbf{c}_0^{m} & \mathbf{c}_1^{m} & \\ \hline \alpha & \beta & \gamma & \beta & \mu & \nu & \mathbf{d}_0^{m,-} \\ \beta & \alpha & \beta & \gamma & \nu & \mu & \mathbf{d}_1^{m,-} \\ \gamma & \beta & \alpha & \beta & \mu & \nu & \mathbf{d}_2^{m,-} \\ \beta & \gamma & \beta & \alpha & \nu & \mu & \mathbf{d}_3^{m,-} \\ \tilde{\alpha} & \tilde{\beta} & \tilde{\gamma} & \tilde{\beta} & \tilde{\nu} & \tilde{\mu} & \mathbf{d}_0^{m,+} \\ \tilde{\beta} & \tilde{\alpha} & \tilde{\beta} & \tilde{\gamma} & \tilde{\mu} & \tilde{\nu} & \mathbf{d}_1^{m,+} \\ \tilde{\gamma} & \tilde{\beta} & \tilde{\alpha} & \tilde{\beta} & \tilde{\nu} & \tilde{\mu} & \mathbf{d}_2^{m,+} \\ \tilde{\beta} & \tilde{\gamma} & \tilde{\beta} & \tilde{\alpha} & \tilde{\mu} & \tilde{\nu} & \mathbf{d}_3^{m,+} \\ \hline \end{array} \qquad D_2 = \begin{array}{|c|l} \hline M_3 & \\ \hline r & \mathbf{d}_0^{m,*} \\ r & \mathbf{d}_1^{m,*} \\ r & \mathbf{d}_2^{m,*} \\ r & \mathbf{d}_3^{m,*} \\ s & \mathbf{c}_0^{m} \\ s & \mathbf{c}_1^{m} \\ \hline \end{array} \tag{35}$$

Lemma 5.1 *Assume $\Delta\colon \mathbb{Z}_2^{19} \to \mathbb{Z}_2^{19}$ is a connection matrix for some fixed value of $m > 0$ and $\lambda_{1,m}^* < \lambda \leq \lambda_{2,m}^*$. Then $\tilde{\Delta}$ with all non tilde entries exchanged with their respective tilde entries is a connection matrix for $-m$ and λ.*

Proof: By symmetry of the Cahn–Hilliard equation (1) any trajectory in $\mathcal{A}_\lambda^m$ gets mapped by $u \mapsto -u$ to a trajectory of $\mathcal{A}_\lambda^{-m}$. In particular, we can express the equilibria in $\mathcal{A}_\lambda^{-m}$ in the terms of equilibria of $\mathcal{A}_\lambda^m$. We gather from (N1) to (N3)

$$\mathbf{x}_0^{-m} = -\mathbf{x}_2^m,\ \mathbf{x}_1^{-m} = -\mathbf{x}_3^m,\ \mathbf{x}_2^{-m} = -\mathbf{x}_0^m,\ \mathbf{x}_3^{-m} = -\mathbf{x}_1^m\ ,$$

$$\mathbf{c}_0^{-m} = -\mathbf{c}_1^m,\ \mathbf{c}_1^{-m} = -\mathbf{c}_0^m\ ,$$

$$\mathbf{d}_0^{-m,*} = -\mathbf{d}_2^{m,*},\ \mathbf{d}_1^{-m,*} = -\mathbf{d}_3^{m,*},\ \mathbf{d}_2^{-m,*} = -\mathbf{d}_0^{m,*},\ \mathbf{d}_3^{-m,*} = -\mathbf{d}_1^{m,*},$$

and similarly

$$\mathbf{d}_0^{-m,+} = -\mathbf{d}_2^{m,-},\ \mathbf{d}_1^{-m,+} = -\mathbf{d}_3^{m,-},\ \mathbf{d}_2^{-m,+} = -\mathbf{d}_0^{m,-},\ \mathbf{d}_3^{-m,+} = -\mathbf{d}_1^{m,-},$$
$$\mathbf{d}_0^{-m,-} = -\mathbf{d}_2^{m,+},\ \mathbf{d}_1^{-m,-} = -\mathbf{d}_3^{m,+},\ \mathbf{d}_2^{-m,-} = -\mathbf{d}_0^{m,+},\ \mathbf{d}_3^{-m,-} = -\mathbf{d}_1^{m,+}\ .$$

Therefore, for instance a connection from $\mathbf{d}_0^{m,-}$ to $\mathbf{x}_0^m$ in $\mathcal{A}_\lambda^m$ implies a connection from $\mathbf{d}_2^{-m,+}$ to $\mathbf{x}_2^{-m}$ in $\mathcal{A}_\lambda^{-m}$, i.e. a and $\tilde{a}$ have to be exchanged. Similarly, b and $\tilde{b}$; α and $\tilde{\alpha}$ and so on have to be exchanged. ◇

Notice that, although we get a new connection matrix $\tilde{\Delta}$ at $-m$, the dynamics is actually conjugate to the one at $+m$, because for positive m the $\mathbf{d}_j^{m,+}$ have less energy than $\mathbf{d}_j^{m,-}$ and for negative m vice versa. Therefore the role of these equilibria changes as we go from m to $-m$. However, since we keep the numbering of our columns and rows as in (34) and (35) fixed, we do get a change of Δ to $\tilde{\Delta}$.

The conditions (C1) – (C4) on connection matrices yield a number of restrictions on Δ_λ^m, like for instance

$$D_0 \circ D_1 \;=\; 0 \quad \text{and} \quad D_1 \circ D_2 \;=\; 0$$

to get a boundary operator. But with 16 free parameters, it is not clear how the actually occurring connection matrices may be characterized.

At least close to the bifurcation point $\lambda_{1,m}^*$ we get some further restrictions.

Proposition 5.2 *Assume that the hypotheses (H1) to (H6) are satisfied. We consider $m \geq 0$ and $\lambda > \lambda_{1,m}^*$ but close to $\lambda_{1,m}^*$. Let $\mathcal{M}_\lambda^m$ be the Morse decomposition of $\mathcal{A}_\lambda^m$ from (29) with energy induced order. Then there exists some $\delta > 0$ such that any connection matrix Δ_λ^m for $\lambda \in (\lambda_{1,m}^*,\, \lambda_{1,m}^* + \delta)$ has the form (32) with (34), (35), and*

$$\alpha \;=\; s \;=\; 1\,, \quad \beta \;=\; \gamma \;=\; 0\,. \tag{36}$$

In case $m > 0$, we get additionally $\tilde{a} = 1$ and $\tilde{b} = 0$.

Proof: We start by proving $s = 1$. Apparently $A = \{\mathbf{c}_0^m\}$ and $R = \{M_3\}$ is an attractor repeller pair for all λ close to $\lambda_{1,m}^*$. Therefore the Conley index of the interval $I = \{\mathbf{c}_0^m,\, M_3\}$ continues. Since for $\lambda \leq \lambda_{1,m}^*$ due to Proposition 4.6 this index has to be trivial, we conclude with (C3) that s has to be 1 even for $\lambda > \lambda_{1,m}^*$ and close by.

ad $\alpha = 1$: For $m = 0$ we consider at $\lambda = \lambda_{1,0}^*$ an isolating neighborhood N of $\mathbf{d}_0^{0,*}$. Clearly left of the bifurcation point $CH_*(N) \approx \Sigma^1$ since there $\mathbf{d}_0^0$ has Morse index 1. Shortly after the bifurcation point, N is still an isolating neighborhood, now however for the interval $J = \{\mathbf{d}_0^{0,-},\, \mathbf{d}_0^{0,+},\, \mathbf{d}_0^{0,*}\}$ (cf. Figure 10) with connection matrix

$$\Delta(J) \;=\; \begin{array}{c|cc|c} \mathbf{d}_0^{0,-} & \mathbf{d}_0^{0,+} & \mathbf{d}_0^{0,*} & \\ \hline & & \alpha & \mathbf{d}_0^{0,-} \\ & & \tilde{\alpha} & \mathbf{d}_0^{0,+} \\ \hline & & & \mathbf{d}_0^{0,*} \end{array}$$

From the additional symmetry at $m = 0$ we obtain $\alpha = \tilde{\alpha}$. Using (C3) we conclude $\dim(\text{im } B) = 1$ for $B = \begin{pmatrix} \alpha \\ \alpha \end{pmatrix}$ and thus $\alpha = 1$.

For $m > 0$ we consider only the saddle–node bifurcation at $\lambda_{1,m}^*$ resulting in the two branches $\mathbf{d}_0^{m,*}$ and $\mathbf{d}_0^{m,-}$ with Morse indices 2 and 1, respectively. Since an isolating neighborhood N of $\mathbf{d}_0^{m,*}$ at $\lambda_{1,m}^*$ continues for λ close to $\lambda_{1,m}^*$ it has to have trivial Conley index, because for $\lambda < \lambda_{1,m}^*$ clearly $Inv(N, \varphi_\lambda) = \emptyset$. Reasoning as before for $\lambda > \lambda_{1,m}^*$ and close by we obtain $\alpha = 1$. Notice that we do not get information on $\tilde{\alpha}$.

ad $\beta = \gamma = 0$: We start again with the case $m = 0$. Here $I = \{\mathbf{d}_0^{0,*},\, \mathbf{d}_1^{0,*}\}$ is an interval at $\lambda = \lambda_{1,m}^*$. The continuation of M_I for $\lambda < \lambda_{1,m}^*$ has Conley index

$$CH_k\Big(M_I\Big) \;\approx\; \begin{cases} \mathbb{Z}_2\,, & \text{if } k \;=\; 1, \\ 0\,, & \text{else,} \end{cases}$$

since both equilibria there have Morse index Σ^1. After the bifurcation point an isolating neighborhood of M_I serves as an isolating neighborhood for M_J with $J = \{\mathbf{d}_0^{0,-}, \mathbf{d}_1^{0,-}, \mathbf{d}_0^{0,+}, \mathbf{d}_1^{0,+}, \mathbf{d}_0^{0,*}, \mathbf{d}_1^{0,*}\}$ (cf. Figure 14) and connection matrix

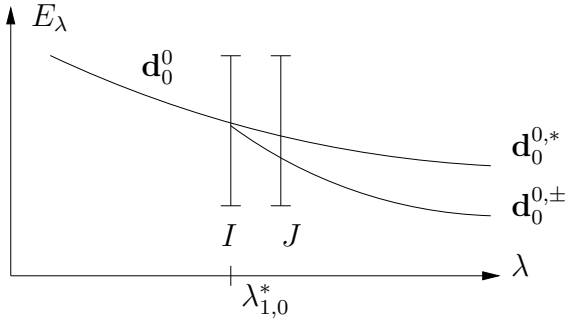


Figure 14: $\mathbf{d}_0^{0,*}$ and $\mathbf{d}_0^{0,\pm}$, $i = 0, 1$ intervals

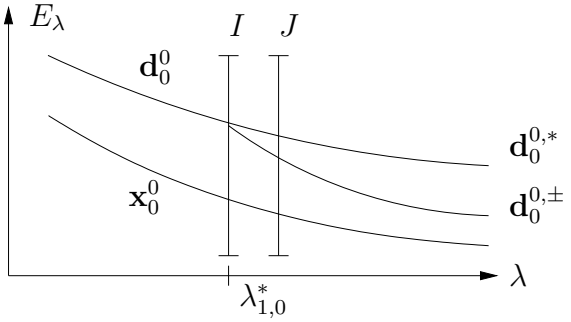


Figure 15: Intervals between $\mathbf{x}_0^0$ and $\mathbf{d}_0^{0,*}$

$$\Delta(J) \;=\; \begin{array}{c|cccc|cc|l} \mathbf{d}_0^{0,-} & \mathbf{d}_1^{0,-} & \mathbf{d}_0^{0,+} & \mathbf{d}_1^{0,+} & \mathbf{d}_0^{0,*} & \mathbf{d}_1^{0,*} & \\ \hline & & & & \alpha = 1 & \beta & \mathbf{d}_0^{0,-} \\ & & & & \beta & \alpha & \mathbf{d}_1^{0,-} \\ & & & & \alpha & \beta & \mathbf{d}_0^{0,+} \\ & & & & \beta & \alpha & \mathbf{d}_1^{0,+} \\ \hline & & & & & & \mathbf{d}_0^{0,*} \\ & & & & & & \mathbf{d}_1^{0,*} \end{array}$$

Denoting by B again the matrix with nontrivial entries in $\Delta(J)$ we get from (C3) $\dim(\text{im } B) = 2$ and hence $\beta = 0$. Similar reasoning with $\mathbf{d}_1^{0,\pm}$ and $\mathbf{d}_1^{0,*}$ replaced by $\mathbf{d}_2^{0,\pm}$ and $\mathbf{d}_2^{0,*}$, respectively, yields $\gamma = 0$.

In the case $m > 0$ is suffices to consider the interval $J = \{\mathbf{d}_0^{m,-}, \mathbf{d}_1^{m,-}, \mathbf{d}_0^{m,*}, \mathbf{d}_1^{m,*}\}$ with M_J closed to $\lambda_{1,m}^*$ being an isolated invariant set coming from two saddle–node bifurcations occurring at the same energy level. Notice that $CH_*(M_J) \approx 0$. The connection matrix for J has the form

$$\Delta(J) \;=\; \begin{array}{c|cc|cc|l} \mathbf{d}_0^{m,-} & \mathbf{d}_1^{m,-} & \mathbf{d}_0^{m,*} & \mathbf{d}_1^{m,*} & \\ \hline & & \alpha = 1 & \beta & \mathbf{d}_0^{m,-} \\ & & \beta & \alpha & \mathbf{d}_1^{m,-} \\ \hline & & & & \mathbf{d}_0^{m,*} \\ & & & & \mathbf{d}_1^{m,*} \end{array}$$

and (C3) gives as above $\beta = 0$. $\gamma = 0$ is again similarly derived.

To see that $\tilde{a} = 1$, we notice that for $m > 0$ the interval $I = \{\mathbf{x}_0^m, \mathbf{d}_0^m\}$ for $\lambda \le \lambda_{1,m}^*$ continues as interval $J = \{\mathbf{x}_0^m, \mathbf{d}_0^{m,+}\}$ for $\lambda > \lambda_{1,m}^*$, where the $\mathbf{d}_0^m/\mathbf{d}_0^{m,+}$ branch is actually unchanged, since we only changed notation (see $(N3)$). Therefore we obtain $\tilde{a} = 1$ from the respective entry in Δ_λ^m for $\lambda \le \lambda_{1,m}^*$ given in Proposition 4.6. From (C4) we gather that any nontrivial entry in the $\mathbf{d}_0^{m,+}$ column of D_0 implies a heteroclinic

connection to one of the $\mathbf{x}_k^m$ equilibria because $I = \{\mathbf{x}_k^m, \mathbf{d}_0^{m,+}\}$ is always on interval. Since $\mathbf{d}_0^{m,+}$ has Morse index 1, however, it has exactly two unstable directions. These have to connect to $\mathbf{x}_0^m$ and $\mathbf{x}_1^m$ given by $\tilde{a} = 1$. Therefore $\tilde{b} = 0$ is the only possibility left. $\diamond$

5.2 The Zero Mass Case

In this section we intend to find further restrictions for the entries of the connection matrix (32) by assuming mass $m = 0$. In this case the attractor $\mathcal{A}_\lambda^0$ is invariant under $\gamma_m : u \mapsto (-u)$. Nevertheless, γ_m acts nontrivially on the equilibria giving further restrictions for the entries in (34) and (35):

$$a = \tilde{a}\,,\ b = \tilde{b}\,,\ \alpha = \tilde{\alpha}\,,\ \beta = \tilde{\beta}\,,\ \gamma = \tilde{\gamma}\,,\ \mu = \tilde{\mu}\,,\ \text{and}\ \nu = \tilde{\nu}\,. \tag{37}$$

This leads to an almost unique connection matrix:

Theorem 5.3 *We assume again hypotheses (H1) to (H6) and consider the parameter range $m = 0$ and $\lambda \in (\lambda_{1,0}^*, \lambda_{2,0}^*]$.*
As in (29)

$$\mathcal{M}_\lambda^0 = \{\mathbf{x}_j^0, \mathbf{d}_j^{0,+}, \mathbf{d}_j^{0,-}, \mathbf{d}_j^{0,*}, \mathbf{c}_i^0;\ M_3 :\ i = 0, 1\,,\ j = 0, ..., 3\} \tag{38}$$

is a Morse decomposition of the attractor $\mathcal{A}_\lambda^0$ with energy induced order. Then any possible connection matrix Δ_λ^0 for $\lambda_{1,0}^* < \lambda \leq \lambda_{2,0}^*$ has the form

$\mathbf{x}_0^0$	$\mathbf{x}_1^0$	$\mathbf{x}_2^0$	$\mathbf{x}_3^0$	$\mathbf{d}_0^{0,-}$	$\mathbf{d}_1^{0,-}$	$\mathbf{d}_2^{0,-}$	$\mathbf{d}_3^{0,-}$	$\mathbf{d}_0^{0,+}$	$\mathbf{d}_1^{0,+}$	$\mathbf{d}_2^{0,+}$	$\mathbf{d}_3^{0,+}$	$\mathbf{d}_0^{0,*}$	$\mathbf{d}_1^{0,*}$	$\mathbf{d}_2^{0,*}$	$\mathbf{d}_3^{0,*}$	$\mathbf{c}_0^0$	$\mathbf{c}_1^0$	M_3	
				1	0	0	1	1	0	0	1								$\mathbf{x}_0^0$
				1	1	0	0	1	1	0	0								$\mathbf{x}_1^0$
				0	1	1	0	0	1	1	0								$\mathbf{x}_2^0$
				0	0	1	1	0	0	1	1								$\mathbf{x}_3^0$
												1	0	0	0	μ	ν		$\mathbf{d}_0^{0,-}$
												0	1	0	0	ν	μ		$\mathbf{d}_1^{0,-}$
												0	0	1	0	μ	ν		$\mathbf{d}_2^{0,-}$
												0	0	0	1	ν	μ		$\mathbf{d}_3^{0,-}$
												1	0	0	0	ν	μ		$\mathbf{d}_0^{0,+}$
												0	1	0	0	μ	ν		$\mathbf{d}_1^{0,+}$
												0	0	1	0	ν	μ		$\mathbf{d}_2^{0,+}$
												0	0	0	1	μ	ν		$\mathbf{d}_3^{0,+}$
																		1	$\mathbf{d}_0^{0,*}$
																		1	$\mathbf{d}_1^{0,*}$
																		1	$\mathbf{d}_2^{0,*}$
																		1	$\mathbf{d}_3^{0,*}$
																		1	$\mathbf{c}_0^0$
																		1	$\mathbf{c}_1^0$
																			M_3

(39)

with

$$\mu \ + \ \nu \ = \ 1 \ . \tag{40}$$

Proof: We start with $\lambda > \lambda^*_{1,0}$, but close to $\lambda^*_{1,0}$, so that we can use the result of Proposition 5.2. In particular, we get $\alpha = s = 1$ and $\beta = \gamma = 0$ from (36).

ad $a = 1$: For $\lambda \leq \lambda^*_{1,0}$, $I = \{\mathbf{x}_0^0, \mathbf{d}_0^0\}$ is an interval and therefore M_I is an isolated invariant set with isolating neighborhood N at $\lambda = \lambda^*_{1,0}$ (cf. Figure 15) and

$$CH_*\Big(Inv(N, \varphi_{\lambda^*_{1,0}})\Big) \ \approx \ 0 \tag{41}$$

due to (C3) and the respective entry in the connection matrix of Proposition 4.6.

We use N as isolating neighborhood for λ slightly larger than $\lambda^*_{1,0}$. The equilibria contained in I contribute after the bifurcation to $J := \{\mathbf{x}_0^0,\, \mathbf{d}_0^{0,\pm},\, \mathbf{d}_0^{0,*}\}$ (cf. Figure 15). J is not an interval in the Morse decomposition (38) with energy induced order. We therefore have to switch for the moment to the flow induced order $>_\varphi$. Clearly, by Lemma 3.3, the set of possible connection matrices $\{\Delta_\lambda^{0,>_\varphi}\}$ with respect to the flow induced order is always a subset of the set of possible connection matrices $\{\Delta_\lambda^{0,>_E}\}$ with respect to the energy induced order. Hence, since $\Delta_{\lambda^*_{1,0}}^{0,>_E}$ in Proposition 4.6 was unique, so is $\Delta_{\lambda^*_{1,0}}^{0,>_\varphi}$ and therefore they are in fact equal with entries given in (28). It follows from Proposition 3.7 that the isolating neighborhood N given in (41) persists for $\lambda > \lambda^*_{1,0}$ close by with J still being an interval for $>_\varphi$ and $Inv(N, \varphi_\lambda) = M_J = M_J^\lambda$ (cf. (19)). The connection matrix $\Delta = \Delta_\lambda^{0,>_\varphi}$ satisfies

$$\Delta(J) \;=\; \begin{array}{c|cccc} & \mathbf{x}_0^0 & \mathbf{d}_0^{0,-} & \mathbf{d}_0^{0,+} & \mathbf{d}_0^{0,*} \\ \hline \mathbf{x}_0^0 & & a & a & \\ \mathbf{d}_0^{0,-} & & & & \alpha \\ \mathbf{d}_0^{0,+} & & & & \alpha \\ \mathbf{d}_0^{0,*} & & & & \end{array}$$

where $\alpha = 1$ has already been determined before and $a = 1$ follows from (C3) and (41). Let us emphasize that until later we keep discussing entries of possible connection matrices with respect to $>_\varphi$ only.

ad $b = 0$: Assuming $b = 1$ all entries of D_0 in (34) would be 1, violating the rank condition $\dim(\text{im } D_0) = 3$ (see (33)).

ad $\mu + \nu = 1$: Both cases $\mu = \nu = 0$ or $\mu = \nu = 1$ yield $\dim(\text{im } D_1) = 4$ contradicting again the rank condition.

ad $r = 1$: From $D_1 \circ D_2 = 0$ we obtain $r \cdot \alpha + 1 = 0$ with $\alpha = 1$ already determined before.

Therefore we have determined the desired form for $\Delta_\lambda^0 = \Delta_\lambda^{0,>_\varphi}$ and $\lambda > \lambda^*_{1,0}$ close to the bifurcation point. At that point we have to switch back to the energy induced order, because only with respect to this order we can guarantee that the Morse decomposition (38) persists on the whole interval $(\lambda^*_{1,0}, \lambda^*_{2,0}]$. Having determined $\Delta_\lambda^{0,>_\varphi}$ as in (39) this clearly gives at least one connection matrix $\Delta_\lambda^0 = \Delta_\lambda^{0,>_E}$ for the energy induced order (see again Lemma 3.3). Using a transition matrix argument (see Proposition 3.5), we get for Δ_λ^0 with arbitrary $\lambda \in (\lambda^*_{1,0}, \lambda^*_{2,0}]$ no further possibilities than the two already indicated, because the set of transition matrices takes the form

$$T \;=\; \begin{bmatrix} T_0 & 0 & 0 & 0 \\ 0 & T_1 & 0 & 0 \\ 0 & 0 & T_2 & 0 \\ 0 & 0 & 0 & T_3 \end{bmatrix}$$

with $T_0 = T_1 = T_3 = Id$, since all equilibria on the respective level share the same energy value and, due to symmetry,

$$T_2 = \begin{array}{|cccccc|c} \hline \mathbf{d}_0^{0,*} & \mathbf{d}_1^{0,*} & \mathbf{d}_2^{0,*} & \mathbf{d}_3^{0,*} & \mathbf{c}_0^0 & \mathbf{c}_1^0 & \\ \hline 1 & 0 & 0 & 0 & \psi & \psi & \mathbf{d}_0^{0,*} \\ 0 & 1 & 0 & 0 & \psi & \psi & \mathbf{d}_1^{0,*} \\ 0 & 0 & 1 & 0 & \psi & \psi & \mathbf{d}_2^{0,*} \\ 0 & 0 & 0 & 1 & \psi & \psi & \mathbf{d}_3^{0,*} \\ 0 & 0 & 0 & 0 & 1 & 0 & \mathbf{c}_0^0 \\ 0 & 0 & 0 & 0 & 0 & 1 & \mathbf{c}_1^0 \\ \hline \end{array}$$

with $\psi = 0$ or $\psi = 1$. Since all connection matrices for $\lambda_{1,0}^* < \lambda \leq \lambda_{2,0}^*$ may be obtained via $\tilde{\Delta} = T\Delta T^{-1}$ only the role of μ and ν might change, but we always recover only the two possible connection matrices already known. ◇

At this point we seemingly have exhausted the possibilities of the algebra. Given only the abstract hypotheses (H1) to (H6) depending on the underlying dynamical system it might be possible that $\mathbf{c}_0^0$ connects to $\mathbf{d}_0^{0,-}$ (case $\mu = 1$ and $\nu = 0$) or to $\mathbf{d}_0^{0,+}$ (case $\mu = 0$ and $\nu = 1$). As an ungeneric case in between, $\mathbf{c}_0^0$ might even connect to $\mathbf{d}_0^{0,*}$ which would be a saddle–saddle connection since both equilibria have Morse index 2. In this case the set of connection matrices Δ_λ^0 given in Theorem 5.3 would have to be non unique with both cases for $\mu + \nu = 1$ occurring.

For the Cahn–Hilliard dynamics, however, numerical simulations have revealed that in the whole interval $\lambda_{1,*}^0 < \lambda \leq \lambda_{2,*}^0$ the connection $\mathbf{c}_0^0$ to $\mathbf{d}_0^{0,+}$ is always present corresponding to a unique connection matrix Δ_λ^0 in Theorem 5.3 with $\mu = 0$ and $\nu = 1$. Although this is not a rigorous computation, we are quite confident that the heteroclinic connection exists, since it was in fact found in the fixed point set $Fix(\gamma_a) = \{u\colon \gamma_a u = u\}$ of the reflection γ_a at the diagonal $\{y = x\}$. In $Fix(\gamma_a)$ the equilibria $\mathbf{d}_0^{0,\pm}$ are stable and $\mathbf{c}_0^0$ has Morse index 1, whereas the equilibria $\mathbf{x}_0^0, ..., \mathbf{x}_3^0$ are no longer present. Furthermore, by symmetry the other connection of $\mathbf{c}_0^0$ connects to $\mathbf{d}_2^{0,+}$. This suggests the hypothesis in the following corollary.

Corollary 5.4 *Assume the situation of Theorem 5.3 for $m = 0$ and $\lambda_0 \in (\lambda_{1,0}^*, \lambda_{2,0}^*]$ with additionally*

at λ_0 the set $I = \{\mathbf{d}_0^{0,+}, \mathbf{c}_0^0\}$ is an interval with respect to the flow induced order and there exists a unique transverse heteroclinic connection from $\mathbf{c}_0^0$ to $\mathbf{d}_0^{0,+}$. (42)

Then the connection matrix $\Delta_{\lambda_0}^0$ of the flow induced order $>_\varphi$ is unique and has the form (39) with $\mu = 0$ and $\nu = 1$.

Proof: Since $I = \{\mathbf{d}_0^{0,+}, \mathbf{c}_0^0\}$ is an interval we obtain that

$$M_I \;=\; \{\mathbf{d}_0^{0,+}, \mathbf{c}_0^0\} \;\cup\; \mathcal{C}(\mathbf{c}_0^0, \mathbf{d}_0^{0,+})$$

is an isolated invariant set for φ_{λ_0}. By assumption the heteroclinic orbit consists of the transverse intersection of $W^u(\mathbf{c}_0^0)$ and $W^s(\mathbf{d}_0^{0,+})$. Hence an explicit geometrical construction yields a trivial Conley index for M_I. Therefore by (C3) the connection matrix for I gives $\nu = 1$.

◇

Note that the assumption (42) could in principle be verified numerically in a rigorous way. For instance to confirm that $I = \{\mathbf{d}_0^{0,+}, \mathbf{c}_0^0\}$ is an interval, one would have to exclude connections from $\mathbf{c}_0^0$ to $\mathbf{d}_j^{0,*}$ (cf. Figure 10). To see that, one could consider a small ball around $\mathbf{c}_0^0$ and evolve it in time. We expect that all initial values in that ball besides $\mathbf{c}_0^0$ reach an energy value less that $E_{\lambda_0}(\mathbf{d}_j^{0,*})$ in finite time, without coming close to any $\mathbf{d}_j^{0,*}$. Since such a property is robust it can be verified rigorously.

In the following we sketch parts of the attractor $\mathcal{A}_{\lambda_0}^0$ suggested by the above obtained connection matrix. We focus on the part of the attractor shown in Figure 16, cf. also Figure 13.

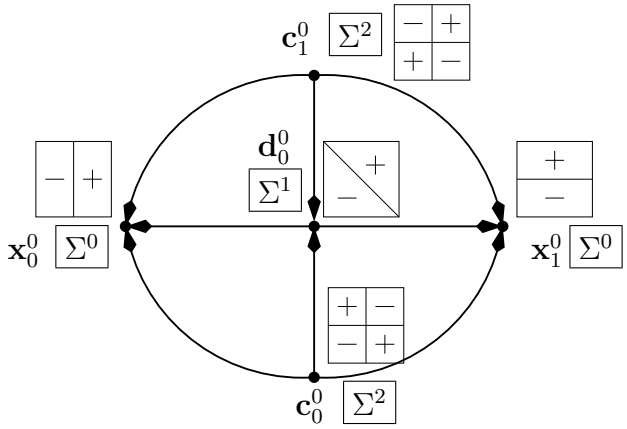


Figure 16: Parts of $\mathcal{A}_\lambda^0$ for $\lambda \in (\lambda_{2,0}, \lambda_{1,0}^*)$

After the bifurcation, i.e. for $\lambda \in (\lambda_{1,0}^*, \lambda_{2,0}^*]$ the connection matrix in Corollary 5.4 suggests a flow as shown in Figure 17.

Remark 5.5 *Although the attractor in Figures 16 and 17 is certainly more than two–dimensional (we have suppressed all unstable directions coming from $m = 0$), it seems that the bifurcation at $\lambda = \lambda_{1,0}^*$ did not change the dimension of the attractor.*

We would like to bolster this remark with a heuristic argument. Consider the gradient

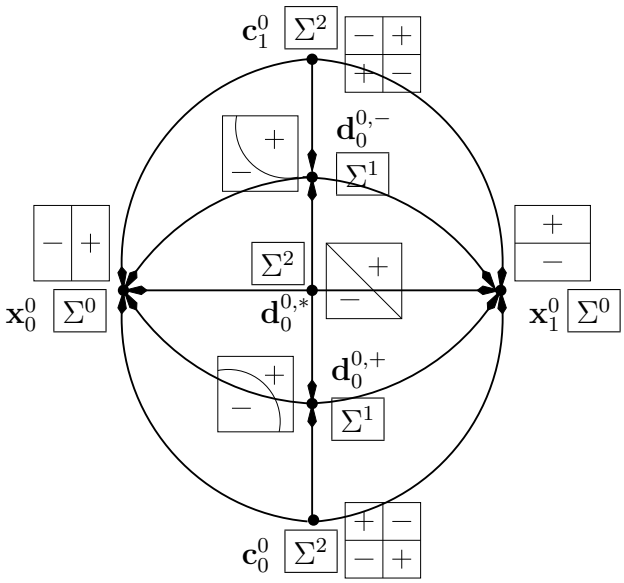


Figure 17: Parts of $\mathcal{A}_\lambda^0$ for $\lambda \in (\lambda_{1,0}^*, \lambda_{2,0}^*)$

flow $z' = -\nabla V(z)$ for the potential

$$\begin{array}{rcl} V\colon \mathbb{R}^2 & \to & \mathbb{R} \\ z \;=\; (x,y) & \mapsto & \dfrac{1}{4}\,y^4 \;+\; \cos x\;. \end{array} \tag{43}$$

In this example we have saddle points with Morse index 1, e.g. at $(x_0,\, y_0) = (0,0)$ and $(x_1, y_1) = (2\pi, 0)$ and a stable fixed point at $(x_2,\, y_2) = (\pi, 0)$. This reflects roughly the situation of Figure 16 when restricted to the fixed point space $Fix(\gamma_a)$ with two saddles $\mathbf{c}_0^0$ and $\mathbf{c}_1^0$, and $\mathbf{d}_0^0$ as stable equilibrium before the bifurcation. The attractor corresponding to (43) is clearly $\{y = 0\}$ which is one–dimensional. We now assume the potential $V_\delta = V + \delta\tilde{V}$ depends on a parameter δ and at $\delta = 0$ the stable fixed point $(x_2, y_2) = (\pi, 0)$ undergoes a generic pitchfork bifurcation yielding two new stable equilibria nearby and leaving (x_2, y_2) with Morse index 1. For small δ the level sets of V_δ will typically change only slightly nearby $(\pi, 0)$. We illustrate this for

$$\tilde{V} = -\left(a\,(x-\pi) + by\right)^2 \cdot \text{Heaviside}\big(2 - (x-\pi)^2 - y^2\big)\, e^{-\left(2-(x-\pi)^2-y^2\right)^{-1}}\;.$$

In Figure 18 we consider the case $a = 0.4$, $b = 0.6$, and $\delta = 1.4$, and in Figure 19 we consider $a = 0$, $b = 1$, and $\delta = 0.7$.

The dimension of the attractor stays one–dimensional (cf. Figure 20) after the bifurcation, since the unstable equilibria have only Morse index one. A saddle-saddle connection is only created in case the two new equilibria bifurcate orthogonally to the $\{y = 0\}$ axis (see Figure 21). This last situation is apparently not very likely.

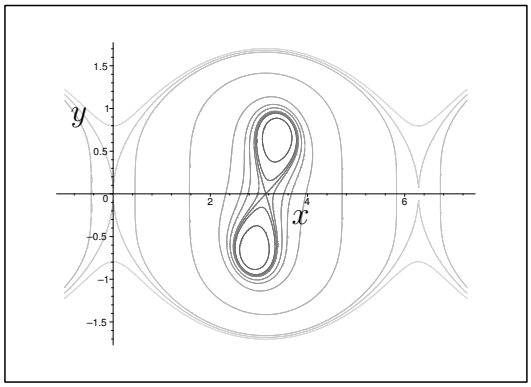


Figure 18: Level sets for V_δ, Case I

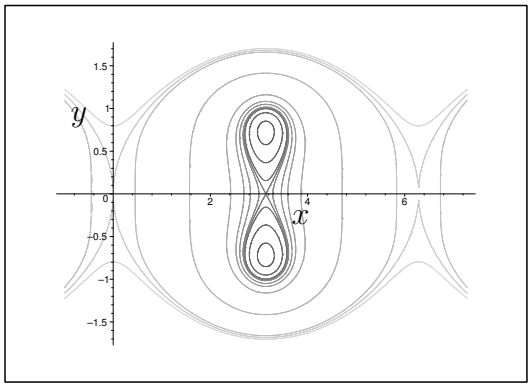


Figure 19: Level sets for V_δ, Case II

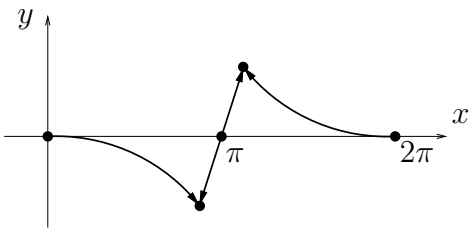


Figure 20: Generic 1d attractor for V_δ

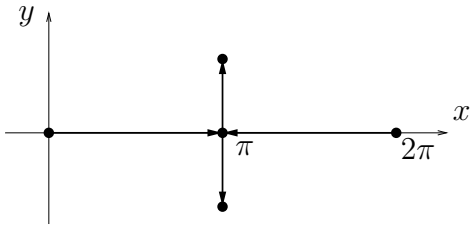


Figure 21: Ungeneric saddle–saddle connection for V_δ

5.3 Global Bifurcations

The aim of this subsection is to extend the knowledge of the last subsection on possible connection matrices in the region $m = 0$ and $\lambda \in (\lambda^*_{1,0}, \lambda^*_{2,0}]$ to parameter values $m \neq 0$. As long as the Morse decomposition (29) persists we may use Proposition 3.5 to get the set of all possible connection matrices via transition matrices. We begin with a connection matrix that has the form

$$D = \begin{bmatrix} 0 & D_0 & 0 & 0 \\ 0 & 0 & D_1 & 0 \\ 0 & 0 & 0 & D_2 \\ 0 & 0 & 0 & 0 \end{bmatrix}$$

where $D_i \colon \bigoplus_{p\in\mathcal{P}} CH_{i+1}(M_p) \to \bigoplus_{p\in\mathcal{P}} CH_i(M_p)$ and M_p, $p \in \mathcal{P}$, are our Morse sets. Let

$$D_0 = \begin{array}{|cccccccc|c|} \hline \mathbf{d}_0^{0,-} & \mathbf{d}_1^{0,-} & \mathbf{d}_2^{0,-} & \mathbf{d}_3^{0,-} & \mathbf{d}_0^{0,+} & \mathbf{d}_1^{0,+} & \mathbf{d}_2^{0,+} & \mathbf{d}_3^{0,+} & \\ \hline 1 & 0 & 0 & 1 & 1 & 0 & 0 & 1 & \mathbf{x}_0^0 \\ 1 & 1 & 0 & 0 & 1 & 1 & 0 & 0 & \mathbf{x}_1^0 \\ 0 & 1 & 1 & 0 & 0 & 1 & 1 & 0 & \mathbf{x}_2^0 \\ 0 & 0 & 1 & 1 & 0 & 0 & 1 & 1 & \mathbf{x}_3^0 \\ \hline \end{array} \qquad D_2 = \begin{array}{|c|c|} \hline M_3 & \\ \hline 1 & \mathbf{d}_0^{0,*} \\ 1 & \mathbf{d}_1^{0,*} \\ 1 & \mathbf{d}_2^{0,*} \\ 1 & \mathbf{d}_3^{0,*} \\ 1 & \mathbf{c}_0^0 \\ 1 & \mathbf{c}_1^0 \\ \hline \end{array}$$

$$D_{1+} = \begin{array}{|cccccc|c|} \hline \mathbf{d}_0^{0,*} & \mathbf{d}_1^{0,*} & \mathbf{d}_2^{0,*} & \mathbf{d}_3^{0,*} & \mathbf{c}_0^0 & \mathbf{c}_1^0 & \\ \hline 1 & 0 & 0 & 0 & 0 & 1 & \mathbf{d}_0^{0,-} \\ 0 & 1 & 0 & 0 & 1 & 0 & \mathbf{d}_1^{0,-} \\ 0 & 0 & 1 & 0 & 0 & 1 & \mathbf{d}_2^{0,-} \\ 0 & 0 & 0 & 1 & 1 & 0 & \mathbf{d}_3^{0,-} \\ 1 & 0 & 0 & 0 & 1 & 0 & \mathbf{d}_0^{0,+} \\ 0 & 1 & 0 & 0 & 0 & 1 & \mathbf{d}_1^{0,+} \\ 0 & 0 & 1 & 0 & 1 & 0 & \mathbf{d}_2^{0,+} \\ 0 & 0 & 0 & 1 & 0 & 1 & \mathbf{d}_3^{0,+} \\ \hline \end{array} \qquad D_{1-} = \begin{array}{|cccccc|c|} \hline \mathbf{d}_0^{0,*} & \mathbf{d}_1^{0,*} & \mathbf{d}_2^{0,*} & \mathbf{d}_3^{0,*} & \mathbf{c}_0^0 & \mathbf{c}_1^0 & \\ \hline 1 & 0 & 0 & 0 & 1 & 0 & \mathbf{d}_0^{0,-} \\ 0 & 1 & 0 & 0 & 0 & 1 & \mathbf{d}_1^{0,-} \\ 0 & 0 & 1 & 0 & 1 & 0 & \mathbf{d}_2^{0,-} \\ 0 & 0 & 0 & 1 & 0 & 1 & \mathbf{d}_3^{0,-} \\ 1 & 0 & 0 & 0 & 0 & 1 & \mathbf{d}_0^{0,+} \\ 0 & 1 & 0 & 0 & 1 & 0 & \mathbf{d}_1^{0,+} \\ 0 & 0 & 1 & 0 & 0 & 1 & \mathbf{d}_2^{0,+} \\ 0 & 0 & 0 & 1 & 1 & 0 & \mathbf{d}_3^{0,+} \\ \hline \end{array}$$

and set

$$D^+ = \begin{bmatrix} 0 & D_0 & 0 & 0 \\ 0 & 0 & D_{1+} & 0 \\ 0 & 0 & 0 & D_2 \\ 0 & 0 & 0 & 0 \end{bmatrix} \quad \text{and} \quad D^- = \begin{bmatrix} 0 & D_0 & 0 & 0 \\ 0 & 0 & D_{1-} & 0 \\ 0 & 0 & 0 & D_2 \\ 0 & 0 & 0 & 0 \end{bmatrix}.$$

Note that these are the matrices which may occur for $m = 0$ and $\lambda \in (\lambda^*_{1,0}, \lambda^*_{2,0}]$ (cf. Theorem 5.3). D_{1+} and D_{1-} are the pair of possible matrix entries.

We now apply transition matrices to these connection matrices to determine the set of all possible connection matrices as m is varied and the other parameter λ is kept fixed. To avoid the change of notation we assume from now on $m \leq 0$. Using Lemma 5.1 we can easily determine the set of connection matrices for $m > 0$, once we have done so for $m < 0$. Similarly, we could keep $m \neq 0$ fixed and vary λ as long as the Morse decomposition persists. The advantage of $m < 0$ is that in this case $\mathbf{d}_i^{m,-} < \mathbf{d}_j^{m,+}$ for all $i, j = 0, ..., 3$. This follows from the energy assumptions in Figure 11 and the symmetries in (N3). Using this order we can for instance stick to the column notation of D_0 even for $m < 0$ and obtain

$$D_0 = D_{0,m} = \begin{array}{|cccccccc|c|} \hline \mathbf{d}_0^{m,-} & \mathbf{d}_1^{m,-} & \mathbf{d}_2^{m,-} & \mathbf{d}_3^{m,-} & \mathbf{d}_0^{m,+} & \mathbf{d}_1^{m,+} & \mathbf{d}_2^{m,+} & \mathbf{d}_3^{m,+} & \\ \hline & & & & & & & & \mathbf{x}_0^m \\ & & & & & & & & \mathbf{x}_1^m \\ & & & & & & & & \mathbf{x}_2^m \\ & & & & & & & & \mathbf{x}_3^m \\ \hline \end{array}$$

whose entries will now be determined.

The set of transition matrices takes the form

$$\begin{bmatrix} T_0 & 0 & 0 & 0 \\ 0 & T_1 & 0 & 0 \\ 0 & 0 & T_2 & 0 \\ 0 & 0 & 0 & T_3 \end{bmatrix},$$

with $T_i \colon \bigoplus_{p \in \mathcal{P}} CH_i(M_p) \to \bigoplus_{p \in \mathcal{P}} CH_i(M_p)$. Since the Morse sets with index Σ^0 are all attractors, T_0 has to be the identity and by symmetry we have that

$$T_0 = \begin{array}{|cccc|c} \multicolumn{4}{c}{\mathbf{x}_0^m\ \mathbf{x}_1^m\ \mathbf{x}_2^m\ \mathbf{x}_3^m} & \\ \hline 1&0&0&0 & \mathbf{x}_0^m \\ 0&1&0&0 & \mathbf{x}_1^m \\ 0&0&1&0 & \mathbf{x}_2^m \\ 0&0&0&1 & \mathbf{x}_3^m \\ \hline \end{array} \qquad T_2 = \begin{array}{|cccccc|c} \multicolumn{6}{c}{\mathbf{d}_0^{m,*}\ \mathbf{d}_1^{m,*}\ \mathbf{d}_2^{m,*}\ \mathbf{d}_3^{m,*}\ \mathbf{c}_0^m\ \mathbf{c}_1^m} & \\ \hline 1&0&0&0&x&y & \mathbf{d}_0^{m,*} \\ 0&1&0&0&y&x & \mathbf{d}_1^{m,*} \\ 0&0&1&0&x&y & \mathbf{d}_2^{m,*} \\ 0&0&0&1&y&x & \mathbf{d}_3^{m,*} \\ 0&0&0&0&1&0 & \mathbf{c}_0^m \\ 0&0&0&0&0&1 & \mathbf{c}_1^m \\ \hline \end{array}$$

and

$$T_1 = \begin{array}{|cccccccc|c} \multicolumn{8}{c}{\mathbf{d}_0^{m,-}\ \mathbf{d}_1^{m,-}\ \mathbf{d}_2^{m,-}\ \mathbf{d}_3^{m,-}\ \mathbf{d}_0^{m,+}\ \mathbf{d}_1^{m,+}\ \mathbf{d}_2^{m,+}\ \mathbf{d}_3^{m,+}} & \\ \hline 1&0&0&0&a&b&c&b & \mathbf{d}_0^{m,-} \\ 0&1&0&0&b&a&b&c & \mathbf{d}_1^{m,-} \\ 0&0&1&0&c&b&a&b & \mathbf{d}_2^{m,-} \\ 0&0&0&1&b&c&b&a & \mathbf{d}_3^{m,-} \\ 0&0&0&0&1&0&0&0 & \mathbf{d}_0^{m,+} \\ 0&0&0&0&0&1&0&0 & \mathbf{d}_1^{m,+} \\ 0&0&0&0&0&0&1&0 & \mathbf{d}_2^{m,+} \\ 0&0&0&0&0&0&0&1 & \mathbf{d}_3^{m,+} \\ \hline \end{array} \qquad T_3 = \begin{array}{|c|} \hline M_3 \\ \hline 1 \\ \hline \end{array} M_3$$

Upper triangularity of transition matrices demands for instance the form of T_i (cf. (C1)). Here it is essential to know $\mathbf{d}_i^{m,-} < \mathbf{d}_j^{m,+}$. We adopt the point of view that global bifurcations of the saddle–saddle type, i.e. connections between equilibria of the same Morse index, will most likely happen on an individual basis and so we will build a graph whose vertices are connection matrices and whose edges are the transition matrices obtained by setting exactly one of the entries a, b, c, x, y equal to 1 and letting the rest be 0. With this in mind we will label the transition matrices by T^a, $T^b, \ldots, T^y$.

Conjugating $D^{\pm}$ with these transition matrices, we obtain the set of possible connection matrices $D^{i\pm} = (T^i)^{-1}\, D^{\pm} T^i$. Let

$$D_0^{b\pm} = \begin{bmatrix} 1&0&0&1&0&1&1&0 \\ 1&1&0&0&0&0&1&1 \\ 0&1&1&0&1&0&0&1 \\ 0&0&1&1&1&1&0&0 \end{bmatrix}$$

$$D_1^{b+} = \begin{bmatrix} 1&1&0&1&0&1 \\ 1&1&1&0&1&0 \\ 0&1&1&1&0&1 \\ 1&0&1&1&1&0 \\ 1&0&0&0&1&0 \\ 0&1&0&0&0&1 \\ 0&0&1&0&1&0 \\ 0&0&0&1&0&1 \end{bmatrix} \quad D_1^{b-} = \begin{bmatrix} 1&1&0&1&1&0 \\ 1&1&1&0&0&1 \\ 0&1&1&1&1&0 \\ 1&0&1&1&0&1 \\ 1&0&0&0&0&1 \\ 0&1&0&0&1&0 \\ 0&0&1&0&0&1 \\ 0&0&0&1&1&0 \end{bmatrix} \quad D_2^{b\pm} = \begin{bmatrix} 1 \\ 1 \\ 1 \\ 1 \\ 1 \\ 1 \end{bmatrix},$$

which defines $D^{b\pm}$. Similarly $D^{a\pm}$ is built by

$$D_0^{a\pm} = \begin{bmatrix} 1 & 0 & 0 & 1 & 0 & 0 & 0 & 0 \\ 1 & 1 & 0 & 0 & 0 & 0 & 0 & 0 \\ 0 & 1 & 1 & 0 & 0 & 0 & 0 & 0 \\ 0 & 0 & 1 & 1 & 0 & 0 & 0 & 0 \end{bmatrix}$$

$$D_1^{a+} = \begin{bmatrix} 0 & 0 & 0 & 0 & 1 & 1 \\ 0 & 0 & 0 & 0 & 1 & 1 \\ 0 & 0 & 0 & 0 & 1 & 1 \\ 0 & 0 & 0 & 0 & 1 & 1 \\ 1 & 0 & 0 & 0 & 1 & 0 \\ 0 & 1 & 0 & 0 & 0 & 1 \\ 0 & 0 & 1 & 0 & 1 & 0 \\ 0 & 0 & 0 & 1 & 0 & 1 \end{bmatrix} \quad D_1^{a-} = \begin{bmatrix} 0 & 0 & 0 & 0 & 1 & 1 \\ 0 & 0 & 0 & 0 & 1 & 1 \\ 0 & 0 & 0 & 0 & 1 & 1 \\ 0 & 0 & 0 & 0 & 1 & 1 \\ 1 & 0 & 0 & 0 & 0 & 1 \\ 0 & 1 & 0 & 0 & 1 & 0 \\ 0 & 0 & 1 & 0 & 0 & 1 \\ 0 & 0 & 0 & 1 & 1 & 0 \end{bmatrix} \quad D_2^{a\pm} = \begin{bmatrix} 1 \\ 1 \\ 1 \\ 1 \\ 1 \\ 1 \end{bmatrix}$$

Observe that because $\mathbf{d}_j^{m,\pm}$ have a one–dimensional unstable manifold, $D_0^{a\pm}$ is impossible (see Proposition 3.4). Proposition 3.4 is applicable since $\mathbf{d}_j^{m,\pm}$ and $\mathbf{x}_i^m$ are all adjacent due to the assumption that between bifurcations there are no saddle–saddle connections present. Here we also need to exclude that $\mathbf{d}_j^{m,\pm}$ connect to some single $\mathbf{x}_i^m$ with two connections, which would also result in a 0 entry in $D_0^{a,\pm}$, because connections are counted modulo 2. However, the above described situation is impossible, since $\mathcal{C}(\mathbf{d}_j^{m,\pm}, \mathbf{x}_i^m) \neq \emptyset$ implies a connection to some different $\mathbf{x}_k^m$, $i \neq k$, by the diagonal symmetry of $\mathbf{d}_j^{m,\pm}$.

Therefore the T^a transition matrix cannot occur and as long as we restrict ourselves to codimension 1 heteroclinic connections $D^{a\pm}$ is impossible. Let

$$D_0^{c\pm} = \begin{bmatrix} 1 & 0 & 0 & 1 & 1 & 1 & 1 & 1 \\ 1 & 1 & 0 & 0 & 1 & 1 & 1 & 1 \\ 0 & 1 & 1 & 0 & 1 & 1 & 1 & 1 \\ 0 & 0 & 1 & 1 & 1 & 1 & 1 & 1 \end{bmatrix}$$

$$D_1^{c+} = \begin{bmatrix} 1 & 0 & 1 & 0 & 1 & 1 \\ 0 & 1 & 0 & 1 & 1 & 1 \\ 1 & 0 & 1 & 0 & 1 & 1 \\ 0 & 1 & 0 & 1 & 1 & 1 \\ 1 & 0 & 0 & 0 & 1 & 0 \\ 0 & 1 & 0 & 0 & 0 & 1 \\ 0 & 0 & 1 & 0 & 1 & 0 \\ 0 & 0 & 0 & 1 & 0 & 1 \end{bmatrix} \quad D_1^{c-} = \begin{bmatrix} 1 & 0 & 1 & 0 & 1 & 1 \\ 0 & 1 & 0 & 1 & 1 & 1 \\ 1 & 0 & 1 & 0 & 1 & 1 \\ 0 & 1 & 0 & 1 & 1 & 1 \\ 1 & 0 & 0 & 0 & 0 & 1 \\ 0 & 1 & 0 & 0 & 1 & 0 \\ 0 & 0 & 1 & 0 & 0 & 1 \\ 0 & 0 & 0 & 1 & 1 & 0 \end{bmatrix} \quad D_2^{c\pm} = \begin{bmatrix} 1 \\ 1 \\ 1 \\ 1 \\ 1 \\ 1 \end{bmatrix}$$

Again relying on the fact that the $\mathbf{d}_j^{m,\pm}$ have a one–dimensional unstable manifold, $D_0^{c\pm}$ is impossible and therefore the T^c transition matrix also cannot occur. Let

$$D_0^{x\pm} = \begin{bmatrix} 1 & 0 & 0 & 1 & 1 & 0 & 0 & 1 \\ 1 & 1 & 0 & 0 & 1 & 1 & 0 & 0 \\ 0 & 1 & 1 & 0 & 0 & 1 & 1 & 0 \\ 0 & 0 & 1 & 1 & 0 & 0 & 1 & 1 \end{bmatrix}$$

$$D_1^{x+} = \begin{bmatrix} 1 & 0 & 0 & 0 & 1 & 1 \\ 0 & 1 & 0 & 0 & 1 & 1 \\ 0 & 0 & 1 & 0 & 1 & 1 \\ 0 & 0 & 0 & 1 & 1 & 1 \\ 1 & 0 & 0 & 0 & 0 & 0 \\ 0 & 1 & 0 & 0 & 0 & 0 \\ 0 & 0 & 1 & 0 & 0 & 0 \\ 0 & 0 & 0 & 1 & 0 & 0 \end{bmatrix} \quad D_1^{x-} = \begin{bmatrix} 1 & 0 & 0 & 0 & 0 & 0 \\ 0 & 1 & 0 & 0 & 0 & 0 \\ 0 & 0 & 1 & 0 & 0 & 0 \\ 0 & 0 & 0 & 1 & 0 & 0 \\ 1 & 0 & 0 & 0 & 1 & 1 \\ 0 & 1 & 0 & 0 & 1 & 1 \\ 0 & 0 & 1 & 0 & 1 & 1 \\ 0 & 0 & 0 & 1 & 1 & 1 \end{bmatrix} \quad D_2^{x\pm} = \begin{bmatrix} 0 \\ 0 \\ 0 \\ 0 \\ 1 \\ 1 \end{bmatrix}$$

and

$$D_0^{y\pm} = \begin{bmatrix} 1 & 0 & 0 & 1 & 1 & 0 & 0 & 1 \\ 1 & 1 & 0 & 0 & 1 & 1 & 0 & 0 \\ 0 & 1 & 1 & 0 & 0 & 1 & 1 & 0 \\ 0 & 0 & 1 & 1 & 0 & 0 & 1 & 1 \end{bmatrix}$$

$$D_1^{y+} = \begin{bmatrix} 1 & 0 & 0 & 0 & 0 & 0 \\ 0 & 1 & 0 & 0 & 0 & 0 \\ 0 & 0 & 1 & 0 & 0 & 0 \\ 0 & 0 & 0 & 1 & 0 & 0 \\ 1 & 0 & 0 & 0 & 1 & 1 \\ 0 & 1 & 0 & 0 & 1 & 1 \\ 0 & 0 & 1 & 0 & 1 & 1 \\ 0 & 0 & 0 & 1 & 1 & 1 \end{bmatrix} \quad D_1^{y-} = \begin{bmatrix} 1 & 0 & 0 & 0 & 1 & 1 \\ 0 & 1 & 0 & 0 & 1 & 1 \\ 0 & 0 & 1 & 0 & 1 & 1 \\ 0 & 0 & 0 & 1 & 1 & 1 \\ 1 & 0 & 0 & 0 & 0 & 0 \\ 0 & 1 & 0 & 0 & 0 & 0 \\ 0 & 0 & 1 & 0 & 0 & 0 \\ 0 & 0 & 0 & 1 & 0 & 0 \end{bmatrix} \quad D_2^{y\pm} = \begin{bmatrix} 0 \\ 0 \\ 0 \\ 0 \\ 1 \\ 1 \end{bmatrix},$$

we observe that $D^{x+} = D^{y-}$ and $D^{x-} = D^{y+}$. Hence it suffices to continue with $D^{x\pm}$ and $D^{b\pm}$. To complete the picture, we still need to conjugate $D^{x\pm}$ with T^b. Let

$$D_0^{bx\pm} = \begin{bmatrix} 1 & 0 & 0 & 1 & 0 & 1 & 1 & 0 \\ 1 & 1 & 0 & 0 & 0 & 0 & 1 & 1 \\ 0 & 1 & 1 & 0 & 1 & 0 & 0 & 1 \\ 0 & 0 & 1 & 1 & 1 & 1 & 0 & 0 \end{bmatrix}$$

$$D_1^{bx+} = \begin{bmatrix} 1 & 1 & 0 & 1 & 1 & 1 \\ 1 & 1 & 1 & 0 & 1 & 1 \\ 0 & 1 & 1 & 1 & 1 & 1 \\ 1 & 0 & 1 & 1 & 1 & 1 \\ 1 & 0 & 0 & 0 & 0 & 0 \\ 0 & 1 & 0 & 0 & 0 & 0 \\ 0 & 0 & 1 & 0 & 0 & 0 \\ 0 & 0 & 0 & 1 & 0 & 0 \end{bmatrix} \quad D_1^{bx-} = \begin{bmatrix} 1 & 1 & 0 & 1 & 0 & 0 \\ 1 & 1 & 1 & 0 & 0 & 0 \\ 0 & 1 & 1 & 1 & 0 & 0 \\ 1 & 0 & 1 & 1 & 0 & 0 \\ 1 & 0 & 0 & 0 & 1 & 1 \\ 0 & 1 & 0 & 0 & 1 & 1 \\ 0 & 0 & 1 & 0 & 1 & 1 \\ 0 & 0 & 0 & 1 & 1 & 1 \end{bmatrix} \quad D_2^{bx\pm} = \begin{bmatrix} 0 \\ 0 \\ 0 \\ 0 \\ 1 \\ 1 \end{bmatrix}.$$

From this we get the following graph

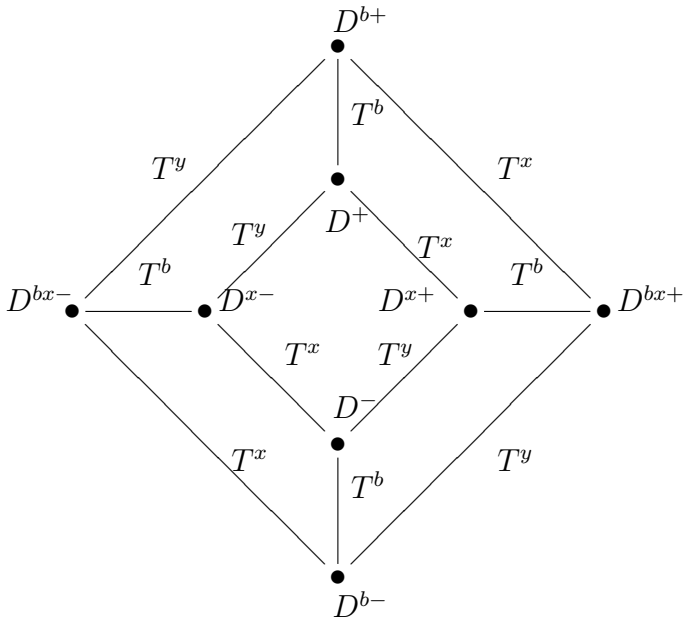


Figure 22: Codimension one connections

Thus, we have established the following result.

Theorem 5.6 *Assume that $\overline{m} \geq 0$ and $\overline{\lambda} > 0$ is a parameter value up to which the Morse decomposition of (29) starting at some point $m = 0$ and $\lambda \in (\lambda^*_{1,0}, \lambda^*_{2,0}]$ persists. Then the graph in Figure 22 indicates all possible codimension one heteroclinic connections that might occur and the resulting changes in the connection matrices.*

Therefore,

$$\text{if only co–dimension one bifurcations occur for saddle–saddle connections}\ , \tag{44}$$

the set of possible connection matrices with respect to the energy induced order at $(\overline{m}, \overline{\lambda})$ is a subset of

$$\{D^{\pm},\, D^{x\pm},\, D^{b\pm},\, D^{bx\pm}\}\ . \tag{45}$$

Since saddle–saddle connections are generically a codimension one phenomenon in parameter space, we expect that any point $(\overline{m}, \overline{\lambda})$ in parameter space up to which the Morse decomposition (29) persists can be connected to $m = 0$, $\lambda \in (\lambda^*_{1,0}, \lambda^*_{2,0}]$ by a path avoiding double saddle–saddle connections. That means, the assumption in (44) is most likely satisfied for all parameter values in question.

An immediate question for further research would be to search the parameter space and decide which of the connection matrices in (45) actually occur for the flow induced order. Any occurrence of a connection matrix besides the known D^+ would rigorously prove a saddle–saddle connection somewhere on the way in parameter space.

6 The Attractor with stable Quarter Circle Solutions

In this section we intend to determine the fine structure of the Cahn–Hilliard attractor $\mathcal{A}^0_\lambda$ in parameter regions when the quarter circle solutions $\mathbf{d}^{0,\pm}_j$ become stable. We pursue this effort for simplicity only for $m = 0$, although any (unique) connection matrix we find has a continuation for m sufficiently close to zero. The latter holds true since the chosen Morse decomposition continues.

6.1 Numerically Motivated Hypotheses

As already indicated in Figure 10 at $\lambda^*_{2,0}$ there is a symmetry breaking bifurcation of the chessboard solutions $\mathbf{c}^0_0$ and $\mathbf{c}^0_1$. At this point, however, we ignore this bifurcation by choosing Morse sets $M_{\mathbf{c}^0_i}$, $i = 0, 1$, which contain $\mathbf{c}^0_i$ and all equilibria bifurcating from this branch, together with their connecting orbits. In the following we formulate hypotheses similar to (H1) to (H6) from Section 2 which allow us to go beyond the point $\lambda^*_{2,0}$. As with all the hypotheses before, numerical evidence supports our hypotheses. We formulate them for the parameter range $\lambda^*_{2,0} \le \lambda \le \lambda^*_{4,0}$ where $\lambda^*_{4,0}$ could in fact be very large, if not infinity. But we currently do not know exactly how far these hypotheses hold true. Nevertheless, $\lambda^*_{4,0}$ should be reasonably larger than $\lambda^*_{3,0}$, the bifurcation point where the quarter circle solutions $\mathbf{d}^{0,\pm}_j$ become stable.

(H1)' We still consider the Cahn–Hilliard equation (1) on the unit square $\Omega = (0, 1)^2 \subset \mathbb{R}^2$ for $f(u) = u - u^3$ and total mass $m = 0$.

(H2)' As described in (H2), $D_4 = \{\gamma_k,\, k = 0, ..., 3\} \cup \{\gamma_x, \gamma_y, \gamma_a, \gamma_b\}$ acts on the solutions of (1) and furthermore $\gamma_m : u \mapsto -u$ yields also an action leaving the attractor $\mathcal{A}^0_\lambda$ invariant.

(H3a)' **(Structure of the x^0_j–branches)**
The solution branches $\mathbf{x}^0_j$, $j = 0, ..., 3$, (described in (N2)) continue as smooth curves with Morse index Σ^0 for $\lambda_{1,0} < \lambda \le \lambda^*_{4,0}$ without secondary bifurcation.

(H3b)' **(Structure of the c^0_i–branches)**
The solution branches $\mathbf{c}^0_i$, $i = 0, 1$, (described in (N1)) continue as smooth curves for $\lambda_{2,0} < \lambda < \lambda^*_{2,0}$ with a secondary bifurcation happening at $\lambda^*_{2,0}$.
For $\lambda^*_{2,0} \le \lambda \le \lambda^*_{4,0}$ and $i = 0, 1$ there exists an isolated invariant set $M_{\mathbf{c}^0_i} = M_{\mathbf{c}^0_i}(\lambda)$ with Conley index Σ^2 and the same symmetries as $\mathbf{c}^{0,*}_i$. $M_{\mathbf{c}^0_i}$ contains the equilibrium $\mathbf{c}^{0,*}_i$ as well as all equilibria bifurcating from this branch, including possible ternary bifurcations and all connecting orbits in between. For all $\lambda^*_{2,0} \le \lambda \le \lambda^*_{4,0}$ the energies of all elements in $M_{\mathbf{c}^0_i}$ respect the order

$$\mathbf{d}^{0,*}_j \;<\; M_{\mathbf{c}^0_i} \;<\; M_3 \;, \tag{46}$$

and, furthermore, there exist no heteroclinic connections between $M_{\mathbf{c}^0_0}$ and $M_{\mathbf{c}^0_1}$.

(H4)' **(Structure of the d_j^0–branches)**
The solution branches corresponding to $\mathbf{d}_j^0$ (described in (N3)) continue as smooth curves for $\lambda_{1,0} < \lambda \leq \lambda_{1,0}^*$ when at $\lambda_{1,0}^*$ the branches $\mathbf{d}_j^{0,*}$ with Morse index Σ^2 and $\mathbf{d}_j^{0,\pm}$ with Morse index Σ^1 are created. The branch $\mathbf{d}_j^{0,*}$ exists for all $\lambda_{1,0}^* < \lambda \leq \lambda_{4,0}^*$ without secondary bifurcation, whereas the quarter circle solutions $\mathbf{d}_j^{0,\pm}$ exist only for $\lambda_{1,0}^* < \lambda \leq \lambda_{3,0}^*$ as smooth curves and undergo a further bifurcation at $\lambda_{3,0}^*$, which is described in (H7)' below.

(H5)' **(Continuation of the trivial Morse set)**
Similar to (H5), for every $\lambda_{2,0} < \lambda \leq \lambda_{4,0}^*$ there exists an isolated invariant set $M_3 = M_3(\lambda)$ with Conley index Σ^3 containing $u \equiv 0$ and all equilibria bifurcating from the trivial solution to the right of $\lambda_{2,0}$, including heteroclinic connections between them. Furthermore, M_3 has all symmetries of $u \equiv 0$, i.e. $D_4 \oplus < \gamma_m >$ and satisfies the order relation (46).

(H6)' **(Completeness of the bifurcation diagram)**
The bifurcation diagram shown in Figure 23 is complete for all $0 < \lambda \leq \lambda_{4,0}^*$, where the $\mathbf{a}_0^{0,\pm}$ and $\mathbf{b}_0^{0,\pm}$ branches are described in (H7)' below.

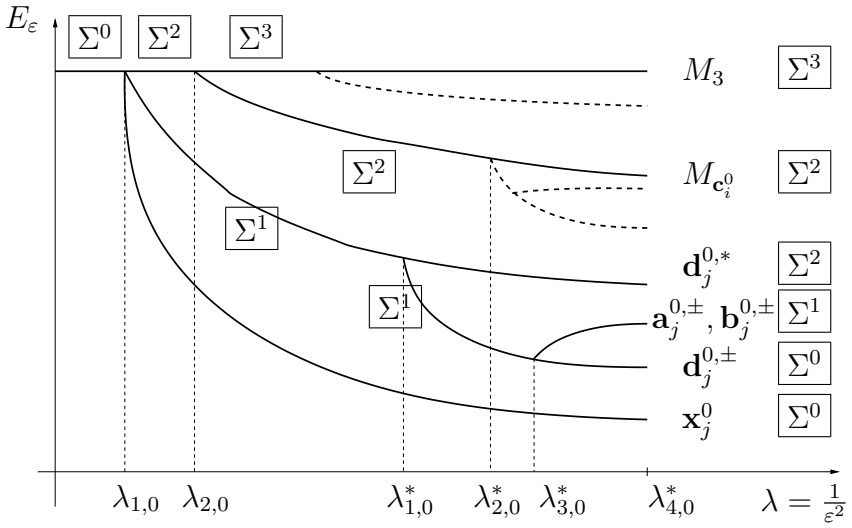


Figure 23: Bifurcation diagram and energy values for $m = 0$

The following lemma is an immediate consequence of our assumptions.

Lemma 6.1 *Assuming (H1)' to (H6)' we obtain for $\lambda_{2,0}^* < \lambda \leq \lambda_{3,0}^*$ a Morse decomposition*

$$\mathcal{M}_\lambda^0 \;=\; \{\mathbf{x}_j^0,\, \mathbf{d}_j^{0,\pm},\, \mathbf{d}_j^{0,*},\; M_{\mathbf{c}_i^0},\; M_3 \colon\; i = 0, 1,\; j = 0, ..., 3\} \text{ of } \mathcal{A}_\lambda^0 \tag{47}$$

with energy induced order which is admissible due to (46) (there is no relation between $M_{\mathbf{c}_0^0}$ and $M_{\mathbf{c}_1^0}$).

The order of the energies (46) was already observed in Maier–Paape and Miller [27], Figure 4 for $0 < \lambda \leq 230$, but we conjecture it holds for all $\lambda > \lambda^*_{2,0}$. For instance, comparing the solutions $\mathbf{c}^{0,\pm}_i$ bifurcating from $\mathbf{c}^0_i$ at $\lambda^*_{2,0}$ (cf. (N1)) with $\mathbf{d}^{0,*}_j$, it is easy to see from the interface length that $E_\lambda(\mathbf{d}^{0,*}_j) < E_\lambda(\mathbf{c}^{0,\pm}_i)$ for λ sufficiently large (see Figure 24).

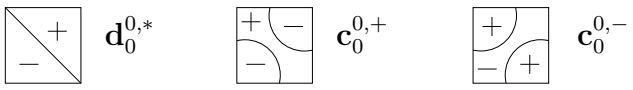


Figure 24: Interfaces of $\mathbf{d}^{0,*}_0$ versus $\mathbf{c}^{0,\pm}_0$

On the upper side we have to compare the energies of $\mathbf{c}^{0,*}_0$ and the ODE branch with 2 internal interfaces, which seems also reasonable for λ sufficiently large, although here the interface length it actually equal (see Figure 25).

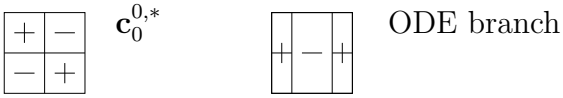


Figure 25: Interfaces of $\mathbf{c}^{0,*}_0$ versus ODE branch with 2 internal layers

Since we did not resolve the bifurcation of $\mathbf{c}^{0,*}_i$ further, we immediately obtain the following consequence of Theorem 5.3.

Corollary 6.2 *Under the hypotheses (H1)' to (H6)' and with the Morse decomposition $\mathcal{M}^0_\lambda$ of the attractor $\mathcal{A}^0_\lambda$ given in (47) and energy induced order, any connection matrix Δ^0_λ for $\lambda^*_{2,0} < \lambda \leq \lambda^*_{3,0}$ has the same form as described in Theorem 5.3 with only $\mathbf{c}^0_i$ replaced by $M_{\mathbf{c}^0_i}$.*

We conclude that the structure of $\mathcal{A}^0_\lambda$, $\lambda \in (\lambda^*_{2,0}\,,\,\lambda^*_{3,0}]$ is still as in Figure 17 with $\mathbf{c}^0_i$ replaced by $M_{\mathbf{c}^0_i}$, respectively. However, the decision which of the two possible connection matrices occurs is more subtle for $\lambda \in (\lambda^*_{2,0}\,,\,\lambda^*_{3,0}]$, because it involves more than just checking one heteroclinic connection. This is even more so, since the $\mathbf{c}^{0,\pm}_i$ undergo ternary bifurcations just after $\lambda^*_{2,0}$ (cf. (N1) and [11]).

To proceed to $\lambda^*_{3,0} < \lambda \leq \lambda^*_{4,0}$ we have to describe the bifurcation of the quarter circle solutions for $m = 0$.

(H7)' **(The $\mathbf{a}^{0,\pm}_j$– and $\mathbf{b}^{0,\pm}_j$–branches)**
The quarter circle solutions $\mathbf{d}^{0,\pm}_j$ undergo a generic symmetry–breaking supercritical pitchfork bifurcation at $\lambda^*_{3,0}$ which results in two new, completely asymmetric branches $\mathbf{a}^{0,\pm}_j$ and $\mathbf{b}^{0,\pm}_j$ with Morse index Σ^1 for $\lambda^*_{3,0} < \lambda \leq \lambda^*_{4,0}$ (see Figure 26). The quarter circle solutions $\mathbf{d}^{0,\pm}_j$ have Morse index Σ^0 for $\lambda > \lambda^*_{3,0}$. Within the range $\lambda^*_{3,0} < \lambda \leq \lambda^*_{4,0}$ no further bifurcations occur off any of these branches.

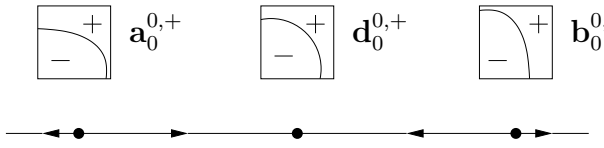


Figure 26: $\mathbf{d}_0^{0,+}$ bifurcates to $\mathbf{a}_0^{0,+}$ and $\mathbf{b}_0^{0,+}$

To fix notation we use $\gamma_j \mathbf{d}_0^{0,+} = \mathbf{d}_j^{0,+},\ j = 1, ..., 3$ and $\mathbf{d}_0^{0,-} = -\mathbf{d}_2^{0,+}$. We therefore set $\mathbf{a}_0^{0,-} := -\mathbf{a}_2^{0,+},\ \mathbf{b}_0^{0,-} := -\mathbf{b}_2^{0,+}$ and $\mathbf{a}_j^{0,\pm} := \gamma_j \mathbf{a}_0^{0,\pm},\ \mathbf{b}_j^{0,\pm} := \gamma_j \mathbf{b}_0^{0,\pm},\ j = 1, ..., 3$. This concludes the description of our setup.

6.2 Situation with Non–resolved Chessboard Solutions

In the following we want to build the connection matrix assuming that (H1)' to (H7)' holds. For all $\lambda_{3,0}^* < \lambda \leq \lambda_{4,0}^*$ we obtain a Morse decomposition $\mathcal{M}_\lambda^0$ of $\mathcal{A}_\lambda^0$

$$\mathcal{M}_\lambda^0 \ := \ \{\mathbf{x}_j^0,\, \mathbf{d}_j^{0,\pm},\, \mathbf{a}_j^{0,\pm},\, \mathbf{b}_j^{0,\pm},\, \mathbf{d}_j^{0,*},\ M_{\mathbf{c}_i^0},\, M_3,\ j = 0, ..., 3,\ i = 0, 1\} \tag{48}$$

with energy induced admissible order. Any connection matrix Δ_λ^0 has to be of the form

$$\Delta \ = \ \begin{bmatrix} 0 & D_0 & 0 & 0 \\ 0 & 0 & D_1 & 0 \\ 0 & 0 & 0 & D_2 \\ 0 & 0 & 0 & 0 \end{bmatrix}, \tag{49}$$

where by (C3) the matrices

$$D_2 : \mathbb{Z}_2 \to \mathbb{Z}_2^6, D_1 : \mathbb{Z}_2^6 \to \mathbb{Z}_2^{16}, \text{and } D_0 \colon \mathbb{Z}_2^{16} \to \mathbb{Z}_2^{12} \text{ have ranks } 1, 5, \text{and } 11, \tag{50}$$

respectively. Using symmetry (see Remark 3.6) we obtain for D_0

$\mathbf{a}_0^{0,-}$	$\mathbf{b}_0^{0,-}$	$\mathbf{a}_1^{0,-}$	$\mathbf{b}_1^{0,-}$	$\mathbf{a}_2^{0,-}$	$\mathbf{b}_2^{0,-}$	$\mathbf{a}_3^{0,-}$	$\mathbf{b}_3^{0,-}$	$\mathbf{a}_0^{0,+}$	$\mathbf{b}_0^{0,+}$	$\mathbf{a}_1^{0,+}$	$\mathbf{b}_1^{0,+}$	$\mathbf{a}_2^{0,+}$	$\mathbf{b}_2^{0,+}$	$\mathbf{a}_3^{0,+}$	$\mathbf{b}_3^{0,+}$	
a	b	c	d	d	c	b	a	a	b	c	d	d	c	b	a	$\mathbf{x}_0^0$
b	a	a	b	c	d	d	c	b	a	a	b	c	d	d	c	$\mathbf{x}_1^0$
d	c	b	a	a	b	c	d	d	c	b	a	a	b	c	d	$\mathbf{x}_2^0$
c	d	d	c	b	a	a	b	c	d	d	c	b	a	a	b	$\mathbf{x}_3^0$
s	s	t	u	v	v	u	t	w	w	x	y	z	z	y	x	$\mathbf{d}_0^{0,-}$
u	t	s	s	t	u	v	v	y	x	w	w	x	y	z	z	$\mathbf{d}_1^{0,-}$
v	v	u	t	s	s	t	u	z	z	y	x	w	w	x	y	$\mathbf{d}_2^{0,-}$
t	u	v	v	u	t	s	s	x	y	z	z	y	x	w	w	$\mathbf{d}_3^{0,-}$
w	w	x	y	z	z	y	x	s	s	t	u	v	v	u	t	$\mathbf{d}_0^{0,+}$
y	x	w	w	x	y	z	z	u	t	s	s	t	u	v	v	$\mathbf{d}_1^{0,+}$
z	z	y	x	w	w	x	y	v	v	u	t	s	s	t	u	$\mathbf{d}_2^{0,+}$
x	y	z	z	y	x	w	w	t	u	v	v	u	t	s	s	$\mathbf{d}_3^{0,+}$

(51)

and

$$D_1 \;=\; \begin{array}{|cccccc|l} \hline \mathbf{d}_0^{0,*} & \mathbf{d}_1^{0,*} & \mathbf{d}_2^{0,*} & \mathbf{d}_3^{0,*} & M_{\mathbf{c}_0^0} & M_{\mathbf{c}_1^0} & \\ \hline \alpha & \beta & \gamma & \delta & \mu & \nu & \mathbf{a}_0^{0,-} \\ \alpha & \delta & \gamma & \beta & \mu & \nu & \mathbf{b}_0^{0,-} \\ \delta & \alpha & \beta & \gamma & \nu & \mu & \mathbf{a}_1^{0,-} \\ \beta & \alpha & \delta & \gamma & \nu & \mu & \mathbf{b}_1^{0,-} \\ \gamma & \delta & \alpha & \beta & \mu & \nu & \mathbf{a}_2^{0,-} \\ \gamma & \beta & \alpha & \delta & \mu & \nu & \mathbf{b}_2^{0,-} \\ \beta & \gamma & \delta & \alpha & \nu & \mu & \mathbf{a}_3^{0,-} \\ \delta & \gamma & \beta & \alpha & \nu & \mu & \mathbf{b}_3^{0,-} \\ \alpha & \beta & \gamma & \delta & \nu & \mu & \mathbf{a}_0^{0,+} \\ \alpha & \delta & \gamma & \beta & \nu & \mu & \mathbf{b}_0^{0,+} \\ \delta & \alpha & \beta & \gamma & \mu & \nu & \mathbf{a}_1^{0,+} \\ \beta & \alpha & \delta & \gamma & \mu & \nu & \mathbf{b}_1^{0,+} \\ \gamma & \delta & \alpha & \beta & \nu & \mu & \mathbf{a}_2^{0,+} \\ \gamma & \beta & \alpha & \delta & \nu & \mu & \mathbf{b}_2^{0,+} \\ \beta & \gamma & \delta & \alpha & \mu & \nu & \mathbf{a}_3^{0,+} \\ \delta & \gamma & \beta & \alpha & \mu & \nu & \mathbf{b}_3^{0,+} \\ \hline \end{array} \qquad D_2 \;=\; \begin{array}{|c|l} \hline M_3 & \\ \hline \xi & \mathbf{d}_0^{0,*} \\ \xi & \mathbf{d}_1^{0,*} \\ \xi & \mathbf{d}_2^{0,*} \\ \xi & \mathbf{d}_3^{0,*} \\ \eta & M_{\mathbf{c}_0^0} \\ \eta & M_{\mathbf{c}_1^0} \\ \hline \end{array} \tag{52}$$

Theorem 6.3 *We assume (H1)' to (H7)' yielding the Morse decomposition (47) of $\mathcal{A}_\lambda^0$ for $\lambda_{3,0}^* < \lambda \le \lambda_{4,0}^*$ with energy induced admissible order. Then any connection matrix Δ_λ^0 for $\lambda_{3,0}^* < \lambda \le \lambda_{4,0}^*$ has the form (49) with (51) and (52), where*

(i) *$s = 1$ and $a + b = 1$; all other entries of D_0 are zero.*

(ii) *$\alpha = 1,\ \beta = \gamma = \delta = 0$ and $\mu + \nu = 1$.*

(iii) *$\xi = \eta = 1$.*

If in addition

$$\text{there exists a heteroclinic connection from } \mathbf{b}_0^{0,-} \text{ to } \mathbf{x}_0^0 \tag{53}$$

for all $\lambda \in (\lambda_{3,0}^*\,,\ \lambda_{3,0}^* + \delta]$ and for some $\delta > 0$, then

(iv) *$a = 0$ and $b = 1$.*

Notice that (53) is also numerically motivated.

Proof: We start by considering $\lambda > \lambda_{3,0}^*$ sufficiently close to $\lambda_{3,0}^*$, where we can use information from $\Delta_{\lambda_{3,0}^*}^0$ of Corollary 6.2.

ad (i)

For $\lambda \le \lambda_{3,0}^*$ the index set $I = \{\mathbf{x}_0^0\,,\ \mathbf{d}_0^{0,-}\}$ is an interval with $CH_*(M_I) \approx 0$ obtained from (C3) and the respective entry in $\Delta_{\lambda_{3,0}^*}^0$. In particular, there exists an

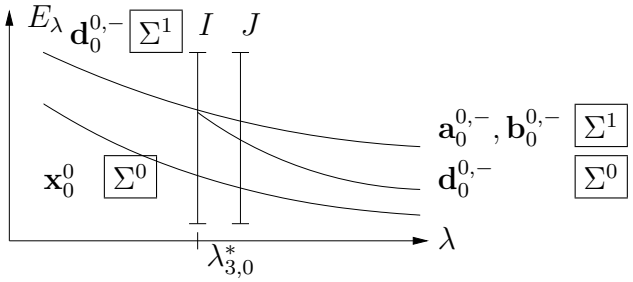


Figure 27: Energy diagram with intervals

isolating neighborhood N of M_I at $\lambda = \lambda^*_{3,0}$ which persists for $\lambda > \lambda^*_{3,0}$. To build the connection matrix Δ^0_λ for $\lambda > \lambda^*_{3,0}$ but close by, we switch to the flow induced order as in the proof of Theorem 5.3. Similarly we find that $\mathcal{M}^0_\lambda$ from (48) is a Morse decomposition of $\mathcal{A}^0_\lambda$ with respect to the flow induced order and by Proposition 3.7 we obtain that $J = \{\mathbf{x}_0^0\,,\, \mathbf{d}_0^{0,-},\, \mathbf{a}_0^{0,-},\, \mathbf{b}_0^{0,-}\}$ is an interval for $\lambda > \lambda^*_{3,0}$ sufficiently close to $\lambda^*_{3,0}$ (see Figure 27). We get $Inv(N, \varphi_\lambda) = M^\lambda_J$ and the connection matrix $\Delta = \Delta^{0,>_\varphi}_\lambda$ satisfies:

$$\Delta(J) \;=\; \begin{array}{c|cc|cc|l} & \mathbf{x}_0^0 & \mathbf{d}_0^{0,-} & \mathbf{a}_0^{0,-} & \mathbf{b}_0^{0,-} & \\ \hline & & & a & b & \mathbf{x}_0^0 \\ & & & s & s & \mathbf{d}_0^{0,-} \\ \hline & & & & & \mathbf{a}_0^{0,-} \\ & & & & & \mathbf{b}_0^{0,-} \end{array}$$

Letting $B = \left(\begin{smallmatrix} a & b \\ s & s \end{smallmatrix}\right)$, from (C3) we obtain $\dim(\mathrm{im}\, B) = 2$ yielding $s = 1$ and $a + b = 1$. In particular either $\mathbf{a}_0^{0,-}$ or $\mathbf{b}_0^{0,-}$ connects to both $\mathbf{x}_0^0$ and $\mathbf{d}_0^{0,-}$. To see this say we have $a = 1$ and $b = 0$. Clearly $\{\mathbf{d}_0^{0,-}, \mathbf{a}_0^{0,-}\}$ is an interval and from (C4) and $s = 1$ we obtain $\mathcal{C}(\mathbf{a}_0^{0,-}, \mathbf{d}_0^{0,-}) \neq \emptyset$. The same reasoning gives $\mathcal{C}(\mathbf{a}_0^{0,-}, \mathbf{x}_0^0) \neq \emptyset$ from $a = 1$ since $\{\mathbf{x}_0^0\,,\, \mathbf{a}_0^{0,-}\}$ is also an interval for the flow induced order. This holds true since the only possible equilibria in between are $\mathbf{d}_j^{0,\pm}$ which are all stable. Since $\mathbf{a}_0^{0,-}$ has Morse index one, we have found all its heteroclinic connections. We conclude

$$c \;=\; d \;=\; t \;=\; u \;=\; v \;=\; w \;=\; x \;=\; y \;=\; z \;=\; 0\,, \tag{54}$$

because by (C4) each of these entries being one would cause an additional heteroclinic connection.

ad (iv) Notice, furthermore, (53) implies $a = 0$ and $b = 1$, since otherwise $a = 1$ and $b = 0$ yields that $\mathbf{b}_0^{0,-}$ connects to $\mathbf{x}_1^0$ and $\mathbf{d}_0^{0,-}$ and no other equilibria; a contradiction.

ad (ii) We start by showing $\alpha = 1$.

Observe that $I = \{\mathbf{d}_0^{0,-}, \mathbf{d}_0^{0,*}\}$ is an interval for $\lambda = \lambda^*_{3,0}$ with $CH_*(M_I) \approx 0$. Arguing as before we may consider the interval $J = \{\mathbf{d}_0^{0,-}, \mathbf{a}_0^{0,-}, \mathbf{b}_0^{0,-}, \mathbf{d}_0^{0,*}\}$ in the flow

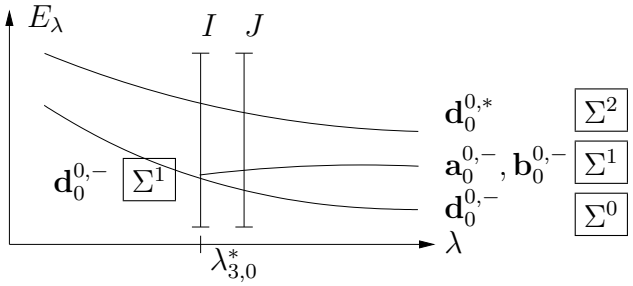


Figure 28: Energy diagram with intervals

induced order (see Figure 28) for $\lambda > \lambda^*_{3,0}$ close to $\lambda^*_{3,0}$ with

$$\Delta(J) \;=\; \begin{array}{|c|cc|c|l} \hline \mathbf{d}_0^{0,-} & \mathbf{a}_0^{0,-} & \mathbf{b}_0^{0,-} & \mathbf{d}_0^{0,*} & \\ \hline & 1 & 1 & & \mathbf{d}_0^{0,-} \\ \cline{2-4} & & & \alpha & \mathbf{a}^{0,-} \\ & & & \alpha & \mathbf{b}^{0,-} \\ \cline{3-4} & & & & \mathbf{d}^{0,*} \\ \hline \end{array}$$

and (C3) gives immediately $\alpha = 1$. To consider β and δ we can use the situation in Figure 28 with just $\mathbf{d}_0^{0,*}$ exchanged by $\mathbf{d}_1^{0,*}$. Again $I = \{\mathbf{d}_0^{0,-}, \mathbf{d}_1^{0,*}\}$ is an interval for $\lambda = \lambda^*_{3,0}$ with

$$CH_k(M_I) \;\approx\; \begin{cases} \mathbb{Z}_2\,, & k \,=\, 1,2 \\ 0\,, & \text{else,} \end{cases}$$

and the flow induced interval $J = \{\mathbf{d}_0^{0,-}, \mathbf{a}_0^{0,-}, \mathbf{b}_0^{0,-}, \mathbf{d}_1^{0,*}\}$ may be used for $\lambda > \lambda^*_{3,0}$ close to $\lambda^*_{3,0}$ with

$$\Delta(J) \;=\; \begin{array}{|c|cc|c|l} \hline \mathbf{d}_0^{0,-} & \mathbf{a}_0^{0,-} & \mathbf{b}_0^{0,-} & \mathbf{d}_1^{0,*} & \\ \hline & 1 & 1 & & \mathbf{d}_0^{0,-} \\ \cline{2-4} & & & \beta & \mathbf{a}_0^{0,-} \\ & & & \delta & \mathbf{b}_0^{0,-} \\ \cline{3-4} & & & & \mathbf{d}_1^{0,*} \\ \hline \end{array}$$

and $\beta = \delta = 0$ follow again from (C3). $\gamma = 0$ follows analogously when we exchange $\mathbf{d}_1^{0,*}$ by $\mathbf{d}_2^{0,*}$. To conclude case **(ii)** we are left to just show $\mu + \nu = 1$. Both cases $\mu = \nu = 0$ or $\mu = \nu = 1$ would imply $\dim(\text{im } D_1) = 4$ which contradicts the rank condition of D_1 (cf. (50)).

ad (iii) We obtain $\eta = 1$ from the respective entry in $\Delta^0_{\lambda^*_{3,0}}$ of Corollary 6.2 since the interval $I = \{M_{\mathbf{c}_1^0}, M_3\}$ persists. Finally $\xi = 1$ follows from $D_1 \circ D_2 = 0$ (see (C2)). Therefore, all assertions are verified for $\lambda > \lambda^*_{3,0}$ sufficiently close to $\lambda^*_{3,0}$. We have calculated the entries for Δ^0_λ with respect to the flow induced order. To go even

further, we return to the energy induced order which is admissible for all $\lambda \in (\lambda^*_{3,0}, \lambda^*_{4,0}]$. As before we employ transition matrices and Proposition 3.5 to obtain the set of all possible connection matrices. Note that by Lemma 3.3 the above–derived flow induced connection matrix is one possible connection matrix for the energy induced order. The set of all possible transition matrices is given by

$$T = \begin{bmatrix} T_0 & 0 & 0 & 0 \\ 0 & T_1 & 0 & 0 \\ 0 & 0 & T_2 & 0 \\ 0 & 0 & 0 & T_3 \end{bmatrix}$$

with $T_1 = Id$ and $T_3 = Id$, because all equilibria with Morse index 1 and 3 have the same energy. Also $T_0 = Id$, because all equilibria with Morse index 0 are attractors (cf. Franzosa and Mischaikow [17]). The only nontrivial part takes the form

$$T_2 = \begin{array}{|cccccc|l} \multicolumn{6}{c}{} & \multicolumn{1}{c}{} \\ \hline \mathbf{d}_0^{0,*} & \mathbf{d}_1^{0,*} & \mathbf{d}_2^{0,*} & \mathbf{d}_3^{0,*} & M_{\mathbf{c}_0^0} & M_{\mathbf{c}_1^0} & \\ \hline 1 & 0 & 0 & 0 & \psi & \psi & \mathbf{d}_0^{0,*} \\ 0 & 1 & 0 & 0 & \psi & \psi & \mathbf{d}_1^{0,*} \\ 0 & 0 & 1 & 0 & \psi & \psi & \mathbf{d}_2^{0,*} \\ 0 & 0 & 0 & 1 & \psi & \psi & \mathbf{d}_3^{0,*} \\ 0 & 0 & 0 & 0 & 1 & 0 & M_{\mathbf{c}_0^0} \\ 0 & 0 & 0 & 0 & 0 & 1 & M_{\mathbf{c}_1^0} \\ \hline \end{array}$$

with $\psi = 0$ or $\psi = 1$. Since all possible connection matrices for $\lambda^*_{3,0} < \lambda \leq \lambda^*_{4,0}$ may be obtained by conjugation of the old connection matrix with T (cf. Proposition 3.5) only the role of μ and ν get exchanged. Therefore the proof is complete.

◇

To illustrate this result with $a = 0$ and $b = 1$ we depict in Figure 29 the upper part of the attractor $\mathcal{A}^0_\lambda$ given in Figure 17, assuming the role of μ and ν has not yet changed (i.e. $\mu = 0$ and $\nu = 1$).

6.3 Resolved Chessboard Solutions in a Fixed Point Space

Although the view of $\mathcal{A}^0_\lambda$ given in Figure 29 is already very illuminating, it has its drawbacks. The isolating invariant sets $M_{\mathbf{c}_i^0}$ which turned out so favorably so far, cause problems when it comes to deciding the open entries in the connection matrix of Theorem 6.3, in particular μ and ν are only determined up to $\mu + \nu = 1$. It is not clear to us how these entries might be decided by just looking at relatively simple to compute objects such as heteroclinic orbits.

To resolve this problem to some extend, we now study the attractor $\mathcal{A}^0_\lambda$ restricted to the fixed point space $Fix(\gamma_a) = \{u : \gamma_a u = u\}$ of the reflection at the diagonal $\{x = y\}$.

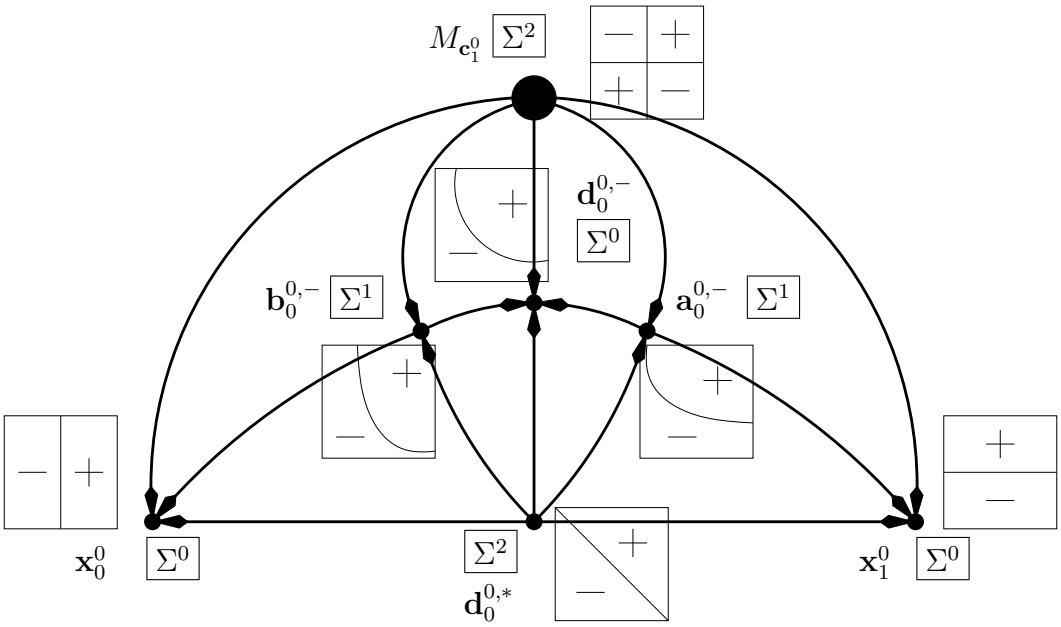


Figure 29: Parts of $\mathcal{A}_\lambda^0$ for $\lambda \in (\lambda_{3,0}^*, \lambda_{4,0}^*]$

For the sake of simplicity, instead of formulating completely new hypotheses for solutions in $Fix(\gamma_a)$, we build on notation given in hypotheses (H1)' to (H6)' and state differences only.

(H6)" **(Completeness of the bifurcation diagram in $Fix(\gamma_a)$)**
The bifurcation diagram for equilibria in $Fix(\gamma_a)$ shown in Figure 30 for $0 < \lambda \leq \lambda_{4,0}^*$ is complete.

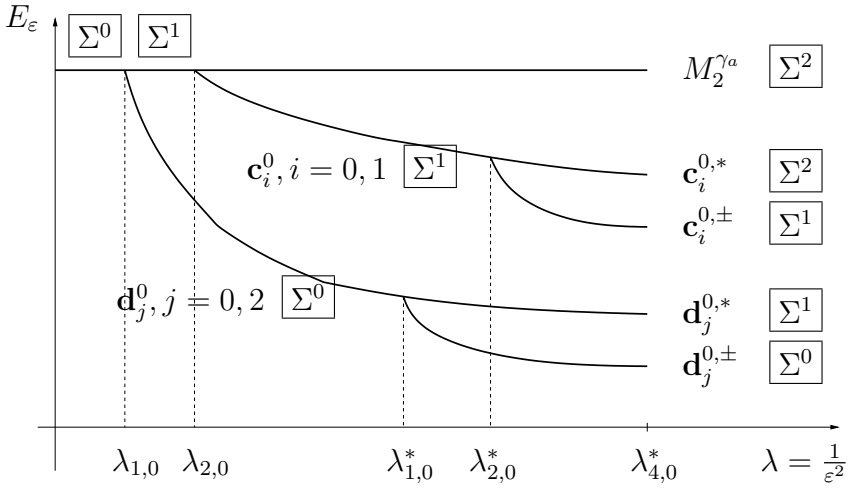


Figure 30: Bifurcation diagram and energy values in $Fix(\gamma_a)$ for $m = 0$

Obviously there are no $\mathbf{x}_j^0$–branches in $Fix(\gamma_a)$ and also the $\mathbf{d}_j^0$–branches for $j = 1, 3$ are missing, as are the $\mathbf{a}_j^{0,\pm}$ and $\mathbf{b}_j^{0,\pm}$ branches. Notice that the Morse indices are also reduced. This gives the following changes:

(H3)" **(Structure of the $\mathbf{c}_i^0$–branch in $Fix(\gamma_a)$)**
The solution branches $\mathbf{c}_i^0$, $i = 0, 1$, present for λ with $\lambda_{2,0} < \lambda < \lambda_{2,0}^*$ undergo a generic symmetry breaking pitchfork bifurcation at $\lambda_{2,0}^*$ which results in two new branches $\mathbf{c}_i^{0,\pm}$ with Morse index Σ^1 in $Fix(\gamma_a)$ as described in (N1). $\mathbf{c}_i^0$ changes index from Σ^1 to Σ^2 in $Fix(\gamma_a)$ and is denoted by $\mathbf{c}_i^{0,*}$ after the bifurcation. All branches exist in $Fix(\gamma_a)$ for $\lambda_{2,0}^* < \lambda \leq \lambda_{4,0}^*$ as smooth curves without secondary bifurcation.

(H4)" **(Structure of the $\mathbf{d}_j^0$–branches in $Fix(\gamma_a)$)**
As before we have the $\mathbf{d}_j^0$–branches, $j = 0, 2$, in $Fix(\gamma_a)$ for $\lambda_{1,0} < \lambda < \lambda_{1,0}^*$, now with Morse index Σ^0. These solution branches bifurcate at $\lambda_{1,0}^*$ to $\mathbf{d}_j^{0,*}$ and $\mathbf{d}_j^{0,\pm}$, $j = 0, 2$, with index Σ^1 and Σ^0 in $Fix(\gamma_a)$, respectively, and continue as smooth curves in $\lambda_{1,0}^* < \lambda \leq \lambda_{4,0}^*$ without secondary bifurcation.

(H5)" **(Continuation of the trivial Morse set in $Fix(\gamma_a)$)**
For $\lambda_{2,0} < \lambda \leq \lambda_{4,0}^*$ there exists an isolating invariant set $M_2^{\gamma_a} = M_2^{\gamma_a}(\lambda)$ with Conley index Σ^2 in $Fix(\gamma_a)$ which contains $u \equiv 0$ and all branches of equilibria in $Fix(\gamma_a)$ bifurcating from the trivial solution to the right of $\lambda_{2,0}$, including heteroclinic connections. Furthermore $M_2^{\gamma_a}$ has all symmetries of $u \equiv 0$ in $Fix(\gamma_a)$, i.e. $< \gamma_b > \ \oplus \ < \gamma_m >$, and for $\lambda \in (\lambda_{2,0}\,,\, \lambda_{4,0}^*]$ the energies of all elements in $M_2^{\gamma_a}$ respect the order

$$\mathbf{c}_i^0 \ < \ M_2^{\gamma_a} \ \text{ or } \ \mathbf{c}_i^{0,*} < \ M_2^{\gamma_a}\,, \ \text{respectively}\,. \tag{55}$$

Note that $M_2^{\gamma_a}$ is not invariant under γ_1, because γ_a and γ_1 do not commute. The analogous reasoning that led to Theorem 5.3 gives immediately

Theorem 6.4 *Assuming hypotheses (H1)', (H2)', and (H3)" to (H6)", we obtain for total mass $m = 0$ and all $\lambda \in (\lambda_{1,0}^*\,,\, \lambda_{2,0}^*]$ a Morse decomposition*

$$\mathcal{M}_\lambda^{0,\gamma_a} \ = \ \{\mathbf{d}_j^{0,\pm},\, \mathbf{d}_j^{0,*},\ \mathbf{c}_i^0,\ M_2^{\gamma_a},\ j \,=\, 0, 2\,,\ i \,=\, 0, 1\}$$

of $\mathcal{A}_\lambda^{0,\gamma_a} := \mathcal{A}_\lambda^0 \cap Fix(\gamma_a)$ with energy induced admissible order. Any connection matrix $\Delta_\lambda^{0,\gamma_a}$ has the form

$\mathbf{d}_0^{0,-}$	$\mathbf{d}_2^{0,-}$	$\mathbf{d}_0^{0,+}$	$\mathbf{d}_2^{0,+}$	$\mathbf{d}_0^{0,*}$	$\mathbf{d}_2^{0,*}$	$\mathbf{c}_0^0$	$\mathbf{c}_1^0$	$M_2^{\gamma_a}$	
				1	0	μ	ν		$\mathbf{d}_0^{0,-}$
				0	1	μ	ν		$\mathbf{d}_2^{0,-}$
				1	0	ν	μ		$\mathbf{d}_0^{0,+}$
				0	1	ν	μ		$\mathbf{d}_2^{0,+}$
								1	$\mathbf{d}_0^{0,*}$
								1	$\mathbf{d}_2^{0,*}$
								1	$\mathbf{c}_0^0$
								1	$\mathbf{c}_1^0$
									$M_2^{\gamma_a}$

(56)

with $\mu + \nu = 1$.

Corollary 6.5 *Assume the situation of Theorem 6.4. If in addition*

$$\text{there exists a heteroclinic connection from } \mathbf{c}_0^0 \text{ to } \mathbf{d}_0^{0,+} \text{ in } Fix(\gamma_a) \tag{57}$$

for some $\lambda_0 \in (\lambda_{1,0}^*\,,\, \lambda_{2,0}^*]$*, then the connection matrix* $\Delta_{\lambda_0}^{0,\gamma_a}$ *with respect to the flow induced order* $>_\varphi$ *is unique and has the form (56) with* $\mu = 0$ *and* $\nu = 1$*.*

As already noted before Corollary 5.4, there is numerical evidence that the connection in (57) exists for all $\lambda_{1,0}^* < \lambda \le \lambda_{2,0}^*$. We note that the heteroclinic connection in (57) for $\lambda \in (\lambda_{1,0}^*\,,\, \lambda_{2,0}^*)$, if it exists, is automatically unique, because $\mathbf{c}_0^0$ has Morse index Σ^1 and symmetry gives a second connection from $\mathbf{c}_0^0$ to $\mathbf{d}_2^{0,+}$. Moreover, the heteroclinic connection is transverse, because $\mathbf{d}_0^{0,+}$ is stable in $Fix(\gamma_a)$.

Proof: The problem in deciding the entries μ and ν arises (even though we assume that the heteroclinic connection exists), since $I := \{\mathbf{d}_0^{0,+}, \mathbf{c}_0^0\}$ is not an interval with respect to the energy induced order. However, I is an interval with respect to the flow induced order. For this, we have to distinguish two cases.

Case (i): $\lambda_0 \in (\lambda_{1,0}^*\,,\, \lambda_{2,0}^*)$. Note that $\mathcal{C}(\mathbf{c}_0^0\,,\, \mathbf{d}_j^{0,*}) = \emptyset$, since the two directions leaving $\mathbf{c}_0^0$ connect to $\mathbf{d}_j^{0,+}$, $j = 0, 2$. As a consequence $M_I = I \cup \mathcal{C}(\mathbf{c}_0^0\,,\, \mathbf{d}_0^{0,+})$ is an isolated invariant set and its Conley index $CH_*(M_I)$ is trivial. Using this and (C3) we obtain

$$\Delta(I) \;=\; \begin{array}{|c|c|l}\hline \mathbf{d}_0^{0,+} & \mathbf{c}_0^0 & \\ \hline & 1 & \mathbf{d}_0^{0,+} \\ \hline & & \mathbf{c}_0^0 \\ \hline \end{array}$$

giving $\nu = 1$.

Case (ii): $\lambda_0 = \lambda_{2,0}^*$. Here we make use of the assumed heteroclinic connection from $\mathbf{c}_0^0$ to $\mathbf{d}_0^{0,+}$ at $\lambda_{2,0}^*$. The Cahn–Hilliard equation supplemented with $\lambda' = 0$ has a two–dimensional center manifold at $(\mathbf{c}_0^0\,,\, \lambda_{2,0}^*)$. Using a generalized Hartman–Grobman theorem it can be shown that the stable/unstable directions and the center directions decouple to a system that is nonlinear only in the center directions. More precisely, our flow is locally topologically equivalent to

$$\begin{aligned} x' &= A^+ x \\ y' &= A^0 y \;+\; c(y) \\ z' &= A^- z\;. \end{aligned} \tag{58}$$

In our case x is one–dimensional and y is two–dimensional. Notice that the eigenspaces are orthogonal since the linearized Cahn–Hilliard operator is selfadjoint. The generic pitchfork bifurcation which we assumed in (H3)" looks in decoupled coordinates exactly as shown in Figure 31.

We conclude that there are exactly two orbits leaving $\mathbf{c}_0^0$ for $\lambda_0 = \lambda_{2,0}^*$ which by assumption connect to $\mathbf{d}_0^{0,+}$ and $\mathbf{d}_2^{0,+}$, respectively. In particular, $I = \{\mathbf{d}_0^{0,+}, \mathbf{c}_0^0\}$ is an

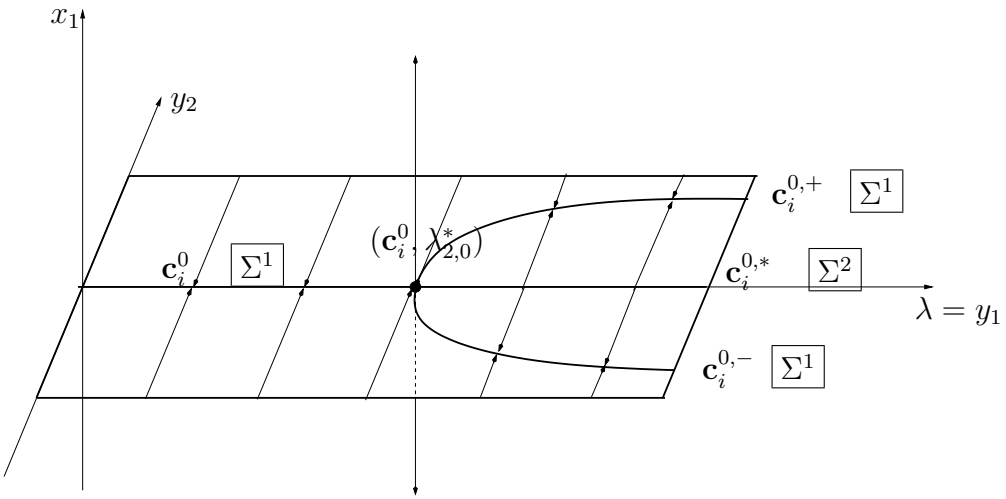


Figure 31: The decoupled generic supercritical pitchfork bifurcation

interval for the flow induced order at $\lambda_0 = \lambda_{2,0}^*$, its Conley index is $CH_*(M_I) \approx 0$, and the same conclusion as in Case (i) holds. Hence the proof is complete.

$\diamond$

The above result establishes the following qualitative picture, where we show the situation with $\nu = 1$ and $\mu = 0$.

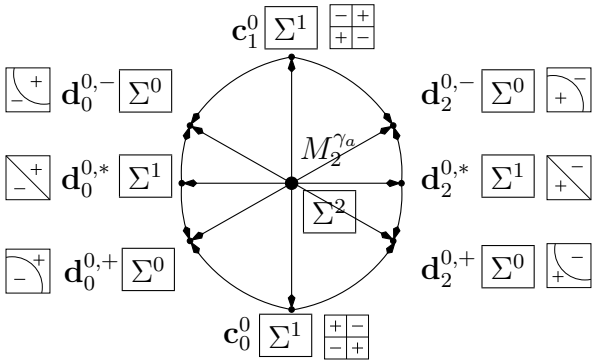


Figure 32: The attractor $\mathcal{A}_\lambda^{0,\gamma_a}$ in $Fix(\gamma_a)$ for $\lambda_{1,0}^* < \lambda \leq \lambda_{2,0}^*$

We now turn our attention to the situation after the bifurcation at $\lambda_{2,0}^*$. The assumption in (H3)" to (H6)" guarantees that

$$\mathcal{M}_\lambda^{0,\gamma_a} \;=\; \{\mathbf{d}_j^{0,\pm},\, \mathbf{d}_j^{0,*},\; \mathbf{c}_i^{0,\pm},\, \mathbf{c}_i^{0,*},\; M_2^{\gamma_a},\; j = 0, 2,\; i = 0, 1\} \tag{59}$$

is a Morse decomposition for $\lambda_{2,0}^* < \lambda \leq \lambda_{4,0}^*$ with energy induced admissible order. Using the symmetry of the involved Morse sets we obtain that any connection matrix

$\Delta_\lambda^{0,\gamma_a}$ has to be of the form

$\mathbf{d}_0^{0,-}$	$\mathbf{d}_2^{0,-}$	$\mathbf{d}_0^{0,+}$	$\mathbf{d}_2^{0,+}$	$\mathbf{d}_0^{0,*}$	$\mathbf{d}_2^{0,*}$	$\mathbf{c}_0^{0,-}$	$\mathbf{c}_1^{0,-}$	$\mathbf{c}_0^{0,+}$	$\mathbf{c}_1^{0,+}$	$\mathbf{c}_0^{0,*}$	$\mathbf{c}_1^{0,*}$	$M_2^{\gamma_a}$	
				a	b	c	f	e	d				$\mathbf{d}_0^{0,-}$
				b	a	c	f	e	d				$\mathbf{d}_2^{0,-}$
				a	b	d	e	f	c				$\mathbf{d}_0^{0,+}$
				b	a	d	e	f	c				$\mathbf{d}_2^{0,+}$
										σ	σ	γ	$\mathbf{d}_0^{0,*}$
										σ	σ	γ	$\mathbf{d}_2^{0,*}$
										α	β	ψ	$\mathbf{c}_0^{0,-}$
										β	α	φ	$\mathbf{c}_1^{0,-}$
										α	β	φ	$\mathbf{c}_0^{0,+}$
										β	α	ψ	$\mathbf{c}_1^{0,+}$
													$\mathbf{c}_0^{0,*}$
													$\mathbf{c}_1^{0,*}$
													$M_2^{\gamma_a}$

(60)

Notice that besides the two obvious symmetries, γ_m and γ_b, operating on the above Morse sets there is also a more subtle one. For instance $\tilde{\gamma} := \gamma_1 \circ \gamma_m$ operates on $\mathbf{c}_1^{0,\pm}$, and even leaves $\mathbf{c}_1^{0,*}$ invariant. It cannot, however, be used on any other Morse set, since the image is no longer in $Fix(\gamma_a)$.

Theorem 6.6 *We assume hypotheses (H1)', (H2)', (H3)" to (H6)" and consider total mass $m = 0$ and the parameter range $\lambda > \lambda_{2,0}^*$, but close to $\lambda_{2,0}^*$. Then $\mathcal{M}_\lambda^{0,\gamma_a}$ in (59) is a Morse decomposition for $\mathcal{A}_\lambda^{0,\gamma_a} = \mathcal{A}_\lambda^0 \cap Fix(\gamma_a)$ with energy induced admissible order. Any connection matrix $\Delta_\lambda^{0,\gamma_a}$ for $\lambda \in (\lambda_{2,0}^*\,,\, \lambda_{2,0}^* + \delta]$ and some sufficiently small $\delta > 0$ has to be of the form (60) with*

(i) $a = 1$ *and* $b = 0$.

(ii) $\alpha = 1$ *and* $\beta = 0$.

For further assertions we assume that at $\lambda_{2,0}^*$

$$\text{there exists a heteroclinic connection from } \mathbf{c}_0^0 \text{ to } \mathbf{d}_0^{0,+} \text{ in } Fix(\gamma_a)\ . \tag{61}$$

Then for $\lambda \in (\lambda_{2,0}^*\,,\, \lambda_{2,0}^* + \tilde{\delta}]$ and some $0 < \tilde{\delta} \le \delta$ any connection matrix $\Delta_\lambda^{0,\gamma_a}$ with respect to the flow induced order is as in (60) and satisfies in addition to (i) and (ii) the identities

(iii) $d = f = 1 \quad$ *and* $\quad e = c = 0$.

(iv) $\gamma = 1$.

(v) $\psi + \varphi = 1 \quad$ *and* $\quad \sigma = 0$.

Proof: Using Theorem 6.4 we obtain a connection matrix $\Delta^{0,\gamma_a}_{\lambda^*_{2,0}}$ with $\mu + \nu = 1$. The entries a and b in (60) correspond to intervals in the energy induced order. Hence the respective entries of (56) continue unchanged yielding **(i)**. The argument leading to $\alpha = 1$ and $\beta = 0$ and thus **(ii)** has been given already in Proposition 5.2, where $\mathbf{d}^{0,\pm}_j$ and $\mathbf{d}^{0,*}_j$ played the role of $\mathbf{c}^{0,\pm}_i$ and $\mathbf{c}^{0,*}_i$ here (see $m = 0$; α and β have the same meaning as here).

ad (iii): The assumption (61) has already been used in the proof of Corollary 6.5, Case (ii). In particular we found that the flow of the Cahn–Hilliard equation near $(\mathbf{c}^0_0, \lambda^*_{2,0})$ is homeomorphic to the decoupled system (58) depicted in Figure 31 with two unique orbits leaving $\mathbf{c}^0_0$ for $\lambda = \lambda^*_{2,0}$ connecting to $\mathbf{d}^{0,+}_0$ and $\mathbf{d}^{0,+}_2$.

Since $\mathbf{d}^{0,+}_0$ and $\mathbf{d}^{0,+}_2$ have Morse index Σ^0 in $Fix(\gamma_a)$ they are local attractors and the heteroclinic connections from $\mathbf{c}^0_0$ to $\mathbf{d}^{0,+}_j$, $j = 0, 2$, survive for $\lambda > \lambda^*_{2,0}$ close to $\lambda^*_{2,0}$ (cf. Figure 33).

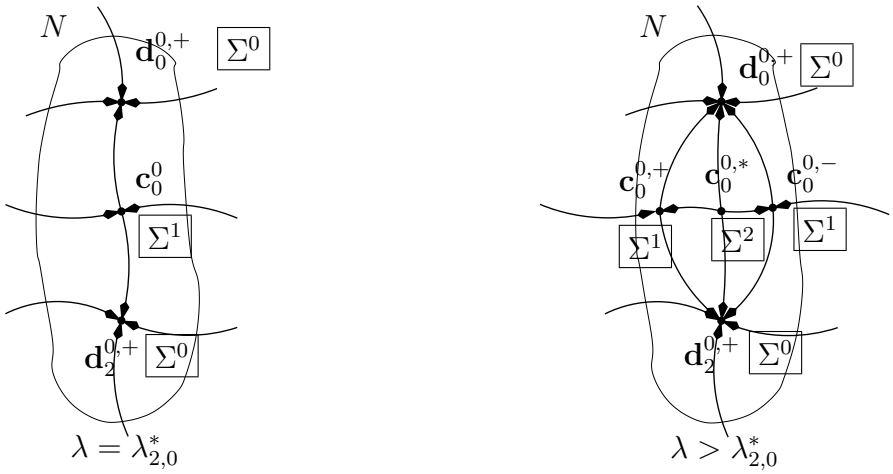


Figure 33: Isolating neighborhood of the heteroclinic connections of $\mathbf{c}^0_0$ to $\mathbf{d}^{0,+}_j$ in $Fix(\gamma_a)$

Therefore $I = \{\mathbf{d}^{0,+}_0, \mathbf{d}^{0,+}_2, \mathbf{c}^0_0\}$ is an interval for the flow induced order and $CH_*(M_I) \approx \Sigma^0$ at $\lambda^*_{2,0}$ with some isolating neighborhood N which is positively invariant. By Proposition 3.7 $J = \{\mathbf{d}^{0,+}_0, \mathbf{d}^{0,+}_2, \mathbf{c}^{0,\pm}_0, \mathbf{c}^{0,*}_0\}$ is also an interval with respect to the flow induced order for $\lambda > \lambda^*_{2,0}$ close to $\lambda^*_{2,0}$ with

$$\Delta(J) \;=\; \begin{array}{|cc|ccc|l}
\multicolumn{2}{c|}{\mathbf{d}^{0,+}_0 \quad \mathbf{d}^{0,+}_2} & \mathbf{c}^{0,-}_0 & \mathbf{c}^{0,+}_0 & \mathbf{c}^{0,*}_0 & \\
\hline
 & & d & f & & \mathbf{d}^{0,+}_0 \\
 & & d & f & & \mathbf{d}^{0,+}_2 \\
\hline
 & & & & \alpha = 1 & \mathbf{c}^{0,-}_0 \\
 & & & & \alpha & \mathbf{c}^{0,+}_0 \\
\hline
\multicolumn{5}{|c|}{} & \mathbf{c}^{0,*}_0 \\
\hline
\end{array}$$

Using again the generalized Hartman–Grobman argument that led to Figure 31, combined with $E(\mathbf{c}_0^{0,\pm}) < E(\mathbf{c}_0^{0,*})$ and symmetry, we conclude that shortly after the bifurcation there exist unique heteroclinic connections from $\mathbf{c}_0^{0,\pm}$ to $\mathbf{d}_j^{0,+}$, $j = 0, 2$. Hence $(\mathbf{d}_j^{0,+}, \mathbf{c}_0^{0,\pm})$ are adjacent in the flow–defined order for $\lambda \in (\lambda_{2,0}^*, \lambda_{2,0}^* + \tilde{\delta}]$ and some $\tilde{\delta} > 0$.

Using a result of McCord (see Proposition 3.4) this implies $d = f = 1$. A similar argument using the isolated invariant neighborhood N from above together with a similar neighborhood of the connections from $\mathbf{c}_1^0$ to $\mathbf{d}_0^{0,-}$ and $\mathbf{d}_2^{0,-}$ and again McCord's proposition gives $c = e = 0$.

ad (iv): At $\lambda_{2,0}^*$ the set $\tilde{I} = \{\mathbf{d}_0^{0,*}, M_2^{\gamma_a}\}$ is an interval with respect to the flow induced order since the only possible equilibria in between, $\mathbf{c}_i^0$, $i = 0, 1$, only connect to $\mathbf{d}_j^{0,\pm}$, $j = 0, 2$. Hence $\tilde{I}$ persists as an interval in the flow induced order for $\lambda > \lambda_{2,0}^*$ sufficiently close to $\lambda_{2,0}^*$. Using (C3) we obtain from (56) that $CH_*(M_I) \approx 0$ and with (C3) for $\lambda > \lambda_{2,0}^*$ again $\gamma = 1$.

ad (v): By (C2) $D_0 \circ D_1 = 0$ and we get $\sigma = 0$ (first row times first column) and $\psi + \varphi = 1$ (first row times last column).

◇

We illustrate the situation of Theorem 6.6 in Figure 34. For comparison, the solid lines are the connections which were already present before the bifurcation, see Figure 32.

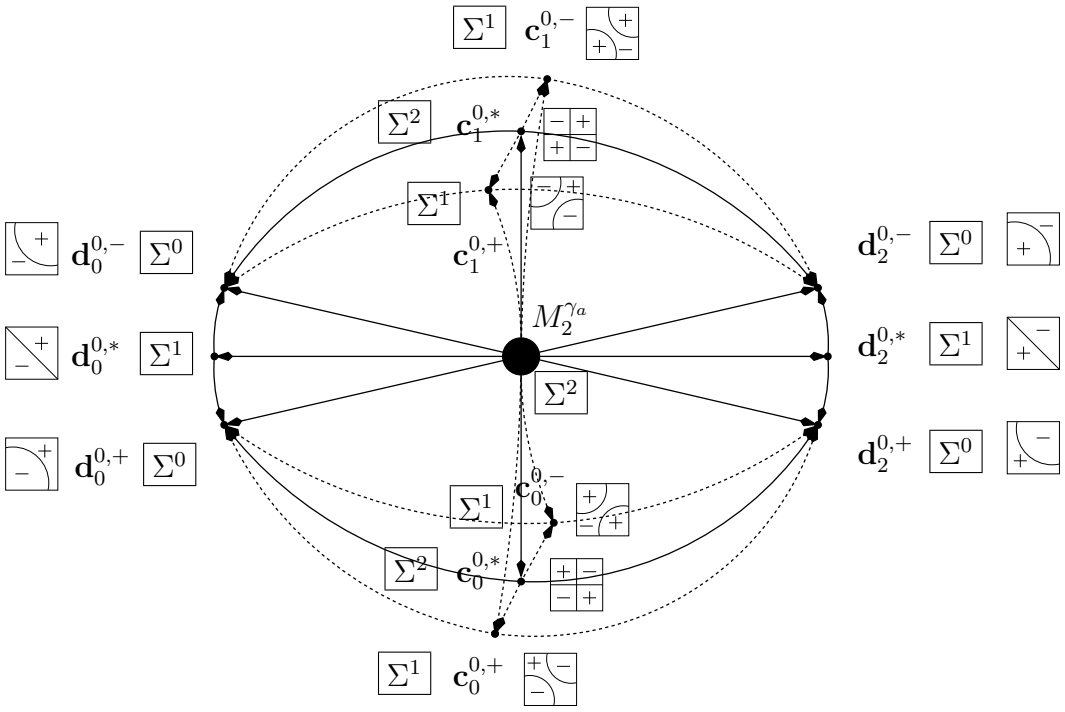


Figure 34: The attractor $\mathcal{A}_\lambda^{0,\gamma_a}$ for $\lambda > \lambda_{2,0}^*$

Remark 6.7 *In the next subsection we will see that there are connections from $M_2^{\gamma_a}$ to $\mathbf{c}_i^{0,*}$ as well as to $\mathbf{c}_i^{0,\pm}$. We think that therefore the connection matrix $\Delta_\lambda^{0,\gamma_a}$ in Theorem 6.6 of the flow induced order is nonunique (with $\psi+\varphi=1$). The fact that $\mathcal{C}(M_2^{\gamma_a}, \mathbf{c}_i^{0,*}) \neq \emptyset$ gives rise to a saddle–saddle connection between Morse sets. However, it probably does not imply a saddle–saddle connection between hyperbolic equilibria (see also the results of the next subsection). Furthermore, we note that the nonuniqueness is not immediately a consequence of symmetry, because $M_2^{\gamma_a}$ is not invariant under γ_1.*

Finally we use a transition matrix argument to gain control over the possible connection matrices $\Delta_\lambda^{0,\gamma_a}$ for $\lambda_{2,0}^* < \lambda \leq \lambda_{4,0}^*$. To this end, we switch back to the energy induced order of the Morse decomposition (59) of $\mathcal{A}_\lambda^{0,\gamma_a}$ valid on $\lambda_{2,0}^* < \lambda \leq \lambda_{4,0}^*$. The connection matrix $\Delta_\lambda^{0,\gamma_a} = \Delta_\lambda^{0,\gamma_a,>_\varphi}$ determined in Theorem 6.6 gives at least one connection matrix $\Delta_\lambda^{0,\gamma_a,>_E}$ for the energy induced order (see Lemma 3.3). Any transition matrix has the form

$$T \;=\; \begin{bmatrix} T_0 & & \\ & T_1 & \\ & & T_2 \end{bmatrix}, \quad \text{with } T_0 \;=\; Id\,,$$

since $\mathbf{d}_0^{0,\pm}$ and $\mathbf{d}_2^{0,\pm}$ have all the same energy and

$$T_1 \;=\; \begin{array}{|cccccc|l} \multicolumn{6}{l}{\mathbf{d}_0^{0,*}\ \mathbf{d}_2^{0,*}\ \mathbf{c}_0^{0,-}\ \mathbf{c}_1^{0,-}\ \mathbf{c}_0^{0,+}\ \mathbf{c}_1^{0,+}} & \\ \hline 1 & & \varrho & \eta & \eta & \varrho & \mathbf{d}_0^{0,*} \\ & 1 & \varrho & \eta & \eta & \varrho & \mathbf{d}_2^{0,*} \\ & & 1 & & & & \mathbf{c}_0^{0,-} \\ & & & 1 & & & \mathbf{c}_1^{0,-} \\ & & & & 1 & & \mathbf{c}_0^{0,+} \\ & & & & & 1 & \mathbf{c}_1^{0,+} \\ \hline \end{array} \qquad T_2 \;=\; \begin{array}{|ccc|l} \multicolumn{3}{l}{\mathbf{c}_0^{0,*}\ \mathbf{c}_1^{0,*}\ M_2^{\gamma_a}} & \\ \hline 1 & & \Phi & \mathbf{c}_0^{0,*} \\ & 1 & \Phi & \mathbf{c}_1^{0,*} \\ & & 1 & M_2^{\gamma_a} \\ \hline \end{array}$$

with missing entries being zero. Using again $\tilde{\Delta} = T^{-1}\Delta T$ and Proposition 3.5 we obtain all possible connection matrices.

Notice that we can ignore T_2 since it only exchanges the roles of ψ and φ, which have not yet been determined anyway in Theorem 6.4.

Corollary 6.8 *Let hypotheses (H1)', (H2)', (H3)" to (H6)" be satisfied and consider $m=0$ and $\lambda \in (\lambda_{2,0}^*\,,\, \lambda_{4,0}^*]$, as well as the Morse decomposition M_λ^{0,γ_a} in (59) of $\mathcal{A}_\lambda^{0,\gamma_a}$ with energy induced admissible order. Furthermore, assume (61) at $\lambda_{2,0}^*$. Then any connection matrix $\Delta_\lambda^{0,\gamma_a}$ with respect to the energy induced order and $\lambda_{2,0}^* < \lambda \leq \lambda_{4,0}^*$ has the form*

$\mathbf{d}_0^{0,-}$	$\mathbf{d}_2^{0,-}$	$\mathbf{d}_0^{0,+}$	$\mathbf{d}_2^{0,+}$	$\mathbf{d}_0^{0,*}$	$\mathbf{d}_2^{0,*}$	$\mathbf{c}_0^{0,-}$	$\mathbf{c}_1^{0,-}$	$\mathbf{c}_0^{0,+}$	$\mathbf{c}_1^{0,+}$	$\mathbf{c}_0^{0,*}$	$\mathbf{c}_1^{0,*}$	$M_2^{\gamma_a}$	
				1	0	ϱ	$1+\eta$	η	$1+\varrho$				$\mathbf{d}_0^{0,-}$
				0	1	ϱ	$1+\eta$	η	$1+\varrho$				$\mathbf{d}_2^{0,-}$
				1	0	$1+\varrho$	η	$1+\eta$	ϱ				$\mathbf{d}_0^{0,+}$
				0	1	$1+\varrho$	η	$1+\eta$	ϱ				$\mathbf{d}_2^{0,+}$
										$\varrho+\eta$	$\varrho+\eta$	1	$\mathbf{d}_0^{0,*}$
										$\varrho+\eta$	$\varrho+\eta$	1	$\mathbf{d}_0^{2,*}$
										1	0	ψ	$\mathbf{c}_0^{0,-}$
										0	1	φ	$\mathbf{c}_1^{0,-}$
										1	0	φ	$\mathbf{c}_0^{0,+}$
										0	1	ψ	$\mathbf{c}_1^{0,+}$
													$\mathbf{c}_0^{0,*}$
													$\mathbf{c}_1^{0,*}$
													$M_2^{\gamma_d}$

with $\psi + \varphi = 1$ *and* $\varrho, \eta \in \{0, 1\}$.

As in Theorem 5.3 the entries ϱ and η may be monitored by looking at the heteroclinic connections leaving $\mathbf{c}_i^{0,\pm}$ as λ varies. Our numerical investigations suggest the following assumptions.

Corollary 6.9 *Assume the situation of Corollary 6.8 for* $m = 0$ *and* $\lambda_0 \in (\lambda_{2,0}^*\,,\ \lambda_{4,0}^*]$, *and additionally suppose that*

> *at* λ_0 *the sets* $I_1 = \{\mathbf{d}_0^{0,+},\, \mathbf{c}_0^{0,-}\}$ *and* $I_2 = \{\mathbf{d}_0^{0,+},\, \mathbf{c}_0^{0,+}\}$ *are intervals with respect to the flow induced order and there exist unique heteroclinic connections from* $\mathbf{c}_0^{0,-}$ *to* $\mathbf{d}_0^{0,+}$ *and from* $\mathbf{c}_0^{0,+}$ *to* $\mathbf{d}_0^{0,+}$.
>
> (62)

Then the connection matrix $\Delta_{\lambda_0}^0$ *of the flow induced order* $>_\varphi$ *has the form (60) as derived in Theorem 6.6, i.e. with entries*

$$a = \alpha = d = f = \gamma = 1\ ,\ b = \beta = e = c = \sigma = 0 \quad \textit{and} \quad \psi + \varphi = 1\ .$$

Remark 6.10 *We think this indicates that also* $\mu = 0$ *and* $\nu = 1$ *in the situation of Figure 29 persists. The problem there was that the entries* μ *and* ν *in the corresponding connection matrix (51) and (52) could not be decided because we have no information on for instance* $\mathcal{C}(M_{\mathbf{c}_1^0},\, \mathbf{a}_0^{0,-})$ *and* $\mathcal{C}(M_{\mathbf{c}_1^0},\, \mathbf{b}_0^{0,-})$*; see again Figure 29. This problem cannot be resolved here, but in the above corollary we have information on for instance* $\mathcal{C}(\mathbf{c}_1^{0,\pm},\, \mathbf{d}_0^{0,-})$, *which is close.*

6.4 Symmetry with respect to Both Diagonals

This last subsection of the paper is devoted to verifying the existence of connections in $\mathcal{C}(M_2^{\gamma_a}, \mathbf{c}_i^{0,*})$ and $\mathcal{C}(M_2^{\gamma_a}, \mathbf{c}_i^{0,\pm})$ (cf. Remark 6.7). For this, we have to resolve the structure of $M_2^{\gamma_a}$ further, and therefore discuss the attractor $\mathcal{A}_\lambda^0$ restricted to the fixed point space $Fix(\gamma_{a,b}) := Fix(\gamma_a) \cap Fix(\gamma_b) = \{u : \gamma_a u = \gamma_b u = u\}$. Thus, we only consider solutions which are invariant with respect to the reflections at both diagonals of the square. Again we build our hypotheses on the ones given earlier.

(H6)‴ **(Completeness of the bifurcation diagram in $Fix(\gamma_{a,b})$)**
The bifurcation diagram for equilibria in $Fix(\gamma_{a,b})$ shown in Figure 35 for $0 < \lambda \le \lambda_{4,0}^*$ is complete.

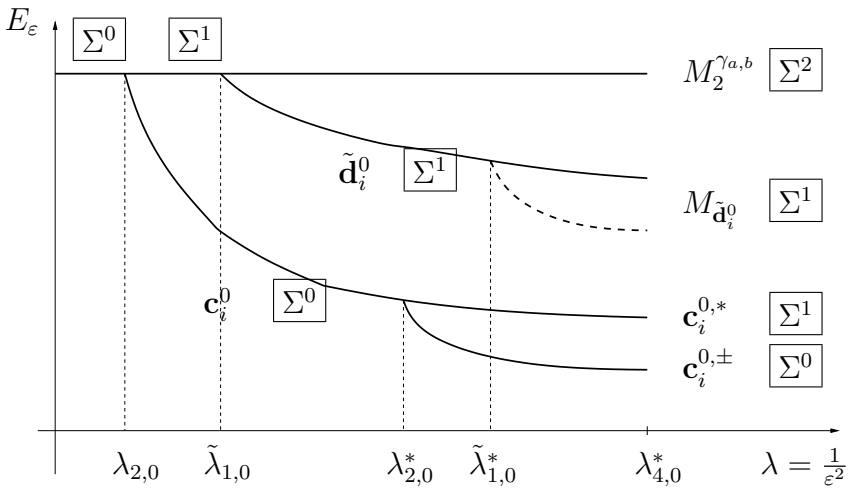


Figure 35: Bifurcation diagram and energy values in $Fix(\gamma_{a,b})$ for $m = 0$

Compared to the situation in $Fix(\gamma_a)$ we have removed all the $\mathbf{d}_j^0$ branches. Parts of $M_2^{\gamma_a}$ were removed as well, yet other parts will be resolved finer as described below.

(H3)‴ **(Structure of the $\mathbf{c}_i^0$–branch in $Fix(\gamma_{a,b})$)**
The solution branches $\mathbf{c}_i^0$, $i = 0, 1$, present in $\lambda_{2,0} < \lambda < \lambda_{2,0}^*$ undergo a generic symmetry breaking pitchfork bifurcation at $\lambda_{2,0}^*$ which generate two new branches $\mathbf{c}_i^{0,\pm}$ with Morse index Σ^0 in $Fix(\gamma_{a,b})$ as described in (N1). $\mathbf{c}_i^0$ changes index from Σ^0 to Σ^1 in $Fix(\gamma_{a,b})$ and is denoted $\mathbf{c}_i^{0,*}$ after the bifurcation. All branches exist in $Fix(\gamma_{a,b})$ for $\lambda_{2,0}^* < \lambda \le \lambda_{4,0}^*$ as smooth curves without secondary bifurcation.

(H4)‴ **(Structure of the $\tilde{\mathbf{d}}_i^0$–branch in $Fix(\gamma_{a,b})$)**
The $\tilde{\mathbf{d}}_i^0$ branches, $i = 0, 1$ are obtained by rescaling the $\mathbf{d}_i^0$ branches, and are depicted in Figure 36. These branches bifurcate from the trivial solution at $\tilde{\lambda}_{1,0} = 4\lambda_{1,0} = 4\pi^2$ with Morse index Σ^1 and undergo a supercritical pitchfork bifurcation at $\tilde{\lambda}_{1,0}^* = 4\lambda_{1,0}^* \approx 200$. However, since we do not want to resolve this

solution branch any further, we denote these Morse sets by $M_{\tilde{\mathbf{d}}_i^0}$ for $\lambda \in (\tilde{\lambda}^*_{1,0}\,,\,\lambda^*_{4,0}]$ and assume for the involved energies

$$\mathbf{c}_i^{0,*} \;<\; M_{\tilde{\mathbf{d}}_i^0}\;. \tag{63}$$

Furthermore, we suppose that there exist no heteroclinic connections between $M_{\tilde{\mathbf{d}}_0^0}$ and $M_{\tilde{\mathbf{d}}_1^0}$.

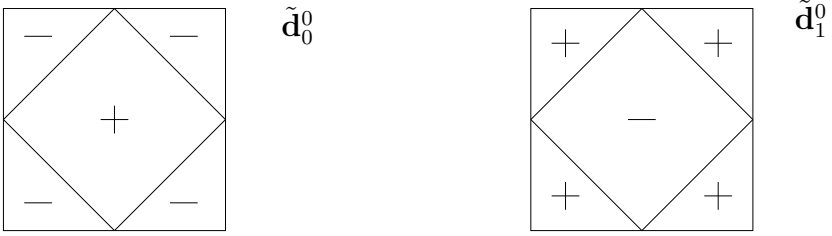


Figure 36: The $\tilde{d}_i^0$ branches in $Fix(\gamma_{a,b})$ for $m = 0$

(H5)''' **(Continuation of the trivial Morse set in $Fix(\gamma_{a,b})$)**
For $\tilde{\lambda}_{1,0} < \lambda \le \lambda^*_{4,0}$ there exists an isolating invariant set $M_2^{\gamma_{a,b}} = M_2^{\gamma_{a,b}}(\lambda)$ with Conley index Σ^2 in $Fix(\gamma_{a,b})$ containing $u \equiv 0$ and all branches of equilibria in $Fix(\gamma_{a,b})$ bifurcating from the trivial solution to the right of $\tilde{\lambda}_{1,0}$, including heteroclinic connections. Furthermore $M_2^{\gamma_{a,b}}$ has all symmetries of $u \equiv 0$ in $Fix(\gamma_{a,b})$, i.e. $<\gamma_1> \oplus <\gamma_m>$, and for $\lambda \in (\tilde{\lambda}_{1,0}\,,\,\lambda^*_{4,0}]$ the energies of all elements in $M_2^{\gamma_{a,b}}$ respect the order

$$\tilde{\mathbf{d}}_i^0 \;<\; M_2^{\gamma_{a,b}} \;\text{ or }\; M_{\tilde{\mathbf{d}}_i^0} \;<\; M_2^{\gamma_{a,b}}\,,\ \text{respectively}\,. \tag{64}$$

The trivial solution $u \equiv 0$ has Morse index Σ^1 for $\lambda_{2,0} < \lambda \le \tilde{\lambda}_{1,0}$.

We note that $M_2^{\gamma_{a,b}}$ is now symmetric with respect to γ_1 which was not the case for $M_2^{\gamma_a}$. One just has to use the identity $\gamma_a\gamma_1 = \gamma_1\gamma_b$. Then the following result can easily be established.

Proposition 6.11 *Assuming hypotheses (H1)', (H2)', and (H3)''' to (H6)''', we obtain for total mass $m = 0$ and $\lambda \in (\lambda_{2,0}\,,\,\tilde{\lambda}_{1,0}]$ a Morse decomposition*

$$\mathcal{M}_\lambda^{0,\gamma_{a,b}} \;=\; \{\mathbf{c}_0^0\,,\,\mathbf{c}_1^0\,,\,0\}$$

of $\mathcal{A}_\lambda^{0,\gamma_{a,b}} := \mathcal{A}_\lambda^0 \cap Fix(\gamma_{a,b})$ with energy induced admissible order and connection matrix:

$\mathbf{c}_0^0$	$\mathbf{c}_1^0$	0	
		1	$\mathbf{c}_0^0$
		1	$\mathbf{c}_1^0$
			0

For all $\lambda \in (\tilde{\lambda}_{1,0}\,,\, \lambda^*_{2,0}]$ *we obtain the Morse decomposition*

$$\mathcal{M}_\lambda^{0,\gamma_{a,b}} \;=\; \left\{\mathbf{c}_i^0\,,\, \tilde{\mathbf{d}}_i^0\,,\, M_2^{\gamma_{a,b}},\; i\,=\,0,1\right\}$$

with energy induced admissible order and connection matrix

$\mathbf{c}_0^0$	$\mathbf{c}_1^0$	$\tilde{\mathbf{d}}_0^0$	$\tilde{\mathbf{d}}_1^0$	$M_2^{\gamma_{a,b}}$	
		1	1		$\mathbf{c}_0^0$
		1	1		$\mathbf{c}_1^0$
				1	$\tilde{\mathbf{d}}_0^0$
				1	$\tilde{\mathbf{d}}_1^0$
					$M_2^{\gamma_{a,b}}$

. (65)

After the bifurcation point $\lambda^*_{2,0}$ we get the following Morse decomposition

$$\mathcal{M}_\lambda^{0,\gamma_{a,b}} \;=\; \left\{\mathbf{c}_i^{0,\pm},\, \mathbf{c}_i^{0,*},\, \tilde{\mathbf{d}}_i^0\,,\, M_2^{\gamma_{a,b}},\; i\,=\,0,1\right\} \tag{66}$$

with energy induced admissible order. Using symmetry one can easily see that any connection matrix $\Delta_\lambda^{0,\gamma_{a,b}}$ has to be of the form

$\mathbf{c}_0^{0,-}$	$\mathbf{c}_1^{0,-}$	$\mathbf{c}_0^{0,+}$	$\mathbf{c}_1^{0,+}$	$\mathbf{c}_0^{0,*}$	$\mathbf{c}_1^{0,*}$	$\tilde{\mathbf{d}}_0^0$	$\tilde{\mathbf{d}}_1^0$	$M_2^{\gamma_{a,b}}$	
				α	β	γ	δ		$\mathbf{c}_0^{0,-}$
				β	α	γ	δ		$\mathbf{c}_1^{0,-}$
				α	β	δ	γ		$\mathbf{c}_0^{0,+}$
				β	α	δ	γ		$\mathbf{c}_1^{0,+}$
								a	$\mathbf{c}_0^{0,*}$
								a	$\mathbf{c}_1^{0,*}$
								b	$\tilde{\mathbf{d}}_0^0$
								b	$\tilde{\mathbf{d}}_1^0$
									$M_2^{\gamma_{a,b}}$

(67)

Theorem 6.12 *Assume the hypotheses (H1)', (H2)', and (H3)''' to (H6)''' for total mass* $m = 0$ *and* $\lambda \in (\lambda^*_{2,0}\,,\, \tilde{\lambda}^*_{1,0}]$. *Then (66) with energy induced order is admissible and the connection matrix in (67) has the entries*

(i) $\alpha \,=\, 1$ *and* $\beta \,=\, 0$.

(ii) $\gamma \,+\, \delta \,=\, 1$.

(iii) $a \,=\, b \,=\, 1$.

Proof: We start by considering $\lambda \in (\lambda^*_{2,0}\,,\, \lambda^*_{2,0} + \delta]$ for $\delta > 0$ sufficiently small.

ad (i): The local bifurcation at $(\mathbf{c}_i^0\,,\,\lambda_{2,0}^*)$ implies $\alpha = 1$ and $\beta = 0$ with arguments similar to the ones used before.

ad (ii): Consider the interval $I = \{\mathbf{c}_0^0\,,\,\tilde{\mathbf{d}}_0^0\}$ a $\lambda_{2,0}^*$. The respective entry in the connection matrix of Proposition 6.11 yields $CH_*(M_I) \approx 0$. To go beyond the bifurcation point we use again Proposition 3.7. Thus, $J = \{\mathbf{c}_0^{0,\pm}, \mathbf{c}_0^{0,*}, \tilde{\mathbf{d}}_0^0\}$ is an interval with respect to the flow induced order and

$$\Delta(J) \;=\; \begin{array}{c|cc|cc|l} & \mathbf{c}_0^{0,-} & \mathbf{c}_0^{0,+} & \mathbf{c}_0^{0,*} & \tilde{\mathbf{d}}_0^0 & \\ \hline & & & 1 & \gamma & \mathbf{c}_0^{0,-} \\ & & & 1 & \delta & \mathbf{c}_0^{0,+} \\ \hline & & & & & \mathbf{c}_0^{0,*} \\ & & & & & \tilde{\mathbf{d}}_0^0 \end{array}$$

From the above index information we obtain that $\left(\begin{smallmatrix} 1 & \gamma \\ 1 & \delta \end{smallmatrix}\right)$ has full rank, i.e. $\gamma + \delta = 1$.

ad (iii): $b = 1$ follows immediately, since the respective entry in the connection matrix of Proposition 6.11 persists. Finally, (C2) furnishes $a + b(\gamma + \delta) = 0$, and therefore $a = 1$.

So far we have determined possible connection matrices for the flow induced order near the bifurcation point. Using transition matrices we see that the entries γ and δ might be exchanged, but the structure of the connection matrix with respect to the energy induced order on $\lambda \in (\lambda_{2,0}^*\,,\,\tilde{\lambda}_{1,0}^*]$ stays as in (i) – (iii).

$\diamond$

Remark 6.13 *With our assumptions we can go even further. For* $\lambda \in \left(\tilde{\lambda}_{1,0}^*\,,\,\lambda_{4,0}^*\right]$ *we have the notation changing from* $\tilde{\mathbf{d}}_i^0$ *to* $M_{\tilde{\mathbf{d}}_i^0}$*, but apart from that, Theorem 6.12 remains unchanged.*

Robust numerical computations indicate that $\gamma = 0$ and $\delta = 1$. This implies an attractor as shown in Figure 37.

Remark 6.14 *The nontrivial connections* $\mathcal{C}(\tilde{\mathbf{d}}_1^0\,,\,\mathbf{c}_i^{0,-})\,,\,\mathcal{C}(\tilde{\mathbf{d}}_0^0\,,\,\mathbf{c}_i^{0,+})$ *and* $\mathcal{C}(M_2^{\gamma_a,b}, \mathbf{c}_i^{0,*})$ *show that* $\mathcal{C}(M_2^{\gamma_a}, \mathbf{c}_i^{0,*}) \neq \emptyset$ *and* $\mathcal{C}(M_2^{\gamma_a}, \mathbf{c}_i^{0,\pm}) \neq \emptyset$ *as stated in Remark 6.7.*

List of Figures

1 Sketch of the bifurcation diagram and energy values for $m = 0$ 5
2 Contour plots of the four main branches at $\lambda = 150$ 5
3 Dynamics near the bifurcation point $\varepsilon = \varepsilon_{2,m}$ for $m = 0$ 10
4 Dynamics near the bifurcation point $\varepsilon = \varepsilon_{1,m}$ for $m = 0$ 12
5 $\mathbf{c}_0^{0,*}$ bifurcates to $\mathbf{c}_0^{0,+}$ and $\mathbf{c}_0^{0,-}$ at $\lambda_{2,0}^*$ 15
6 $\mathbf{c}_0^{m,+}$ and the saddle node branch ($\mathbf{c}_0^{m,*}$ and $\mathbf{c}_0^{m,-}$) for $m > 0$ 15

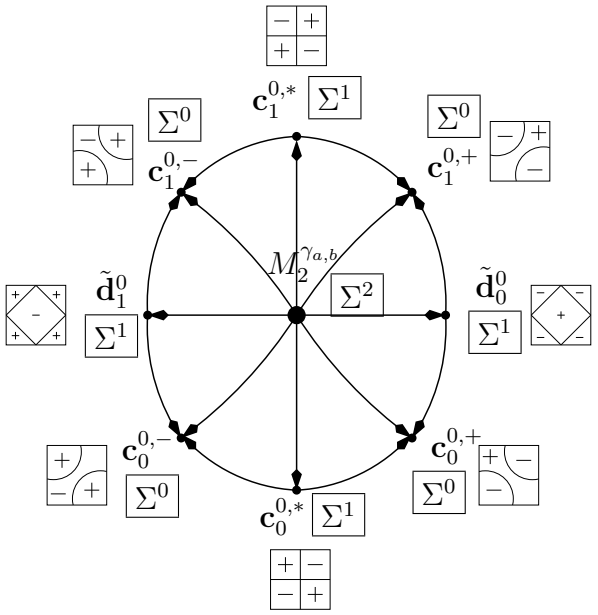


Figure 37: The attractor $\mathcal{A}_\lambda^{0,\gamma_{a,b}}$ for $\lambda \in (\lambda_{2,0}^*, \tilde{\lambda}_{1,0}^*)$

7 Nodal line structure of x_0^m, x_0^0 and x_0^{-m} for $m > 0$ 15
8 $\mathbf{d}_0^{0,*}$ bifurcates to $\mathbf{d}_0^{0,+}$ and $\mathbf{d}_0^{0,-}$ at $\lambda_{1,0}^*$ 16
9 $\mathbf{d}_0^{m,+}$ and the saddle node branch ($\mathbf{d}_0^{m,*}$ and $\mathbf{d}_0^{m,-}$) for $m > 0$ 16
10 Partial bifurcation diagram and energy values for $m = 0$ 17
11 Partial bifurcation diagram and energy values for $m > 0$ 17
12 Intervals near the bifurcation point λ_0 23
13 Sketch of the attractor $\mathcal{A}_\lambda^0$ for $\lambda \in (\lambda_{2,0}, \lambda_{1,0}^*)$ 29
14 $\mathbf{d}_0^{0,*}$ and $\mathbf{d}_0^{0,\pm}$, $i = 0, 1$ intervals 33
15 Intervals between $\mathbf{x}_0^0$ and $\mathbf{d}_0^{0,*}$ 33
16 Parts of $\mathcal{A}_\lambda^0$ for $\lambda \in (\lambda_{2,0}, \lambda_{1,0}^*)$ 38
17 Parts of $\mathcal{A}_\lambda^0$ for $\lambda \in (\lambda_{1,0}^*, \lambda_{2,0}^*)$ 39
18 Level sets for V_δ, Case I 40
19 Level sets for V_δ, Case II 40
20 Generic 1d attractor for V_δ 40
21 Ungeneric saddle–saddle connection for V_δ 40
22 Codimension one connections 45
23 Bifurcation diagram and energy values for $m = 0$ 47
24 Interfaces of $\mathbf{d}_0^{0,*}$ versus $\mathbf{c}_0^{0,\pm}$ 48
25 Interfaces of $\mathbf{c}_0^{0,*}$ versus ODE branch with 2 internal layers 48
26 $\mathbf{d}_0^{0,+}$ bifurcates to $\mathbf{a}_0^{0,+}$ and $\mathbf{b}_0^{0,+}$ 49
27 Energy diagram with intervals 51
28 Energy diagram with intervals 52
29 Parts of $\mathcal{A}_\lambda^0$ for $\lambda \in (\lambda_{3,0}^*, \lambda_{4,0}^*]$ 54
30 Bifurcation diagram and energy values in $Fix(\gamma_a)$ for $m = 0$ 54
31 The decoupled generic supercritical pitchfork bifurcation 57

32 The attractor $\mathcal{A}_\lambda^{0,\gamma_a}$ in $Fix(\gamma_a)$ for $\lambda_{1,0}^* < \lambda \le \lambda_{2,0}^*$ 57
33 Isolating neighborhood of the heteroclinic connections of $\mathbf{c}_0^0$ to $\mathbf{d}_j^{0,+}$ in $Fix(\gamma_a)$ 59
34 The attractor $\mathcal{A}_\lambda^{0,\gamma_a}$ for $\lambda > \lambda_{2,0}^*$ 60
35 Bifurcation diagram and energy values in $Fix(\gamma_{a,b})$ for $m = 0$ 63
36 The $\tilde{d}_i^0$ branches in $Fix(\gamma_{a,b})$ for $m = 0$ 64
37 The attractor $\mathcal{A}_\lambda^{0,\gamma_{a,b}}$ for $\lambda \in (\lambda_{2,0}^*, \tilde{\lambda}_{1,0}^*)$ 67

References

[1] A. V. Babin and M. I. Vishik. *Attractors of Evolution Equations*. North-Holland, Amsterdam, 1992. Translated and revised from the 1989 Russian original by Babin.

[2] F. Bai, C. M. Elliott, A. Gardiner, A. Spence, and A. M. Stuart. The viscous Cahn-Hilliard equation. Part I: Computations. *Nonlinearity*, 8:131–160, 1995.

[3] P. Brunovský and B. Fiedler. Connecting orbits in scalar reaction diffusion equations. In *Dynamics reported, Vol. 1*, pages 57–89. Teubner, Stuttgart, 1988.

[4] P. Brunovský and B. Fiedler. Connecting orbits in scalar reaction diffusion equations. II. The complete solution. *Journal of Differential Equations*, 81(1):106–135, 1989.

[5] J. W. Cahn. Free energy of a nonuniform system. II. Thermodynamic basis. *Journal of Chemical Physics*, 30:1121–1124, 1959.

[6] J. W. Cahn and J. E. Hilliard. Free energy of a nonuniform system I. Interfacial free energy. *Journal of Chemical Physics*, 28:258–267, 1958.

[7] S.-N. Chow and J. K. Hale. *Methods of Bifurcation Theory*. Springer-Verlag, New York – Berlin – Heidelberg, 1982.

[8] C. Conley. *Isolated invariant sets and the Morse index*. American Mathematical Society, Providence, R.I., 1978.

[9] M. G. Crandall and P. H. Rabinowitz. Bifurcation from simple eigenvalues. *Journal of Functional Analysis*, 8:321–340, 1971.

[10] S. Day, Y. Hiraoka, K. Mischaikow, and T. Ogawa. Rigorous numerics for global dynamics: A study of the Swift–Hohenberg equation. *SIAM J. Applied Dynamical Systems*, 4(1):1–31, 2005.

[11] J. E. Deering, S. Maier-Paape, U. Miller, and T. Wanner. Secondary bifurcations of the equilibria of the Cahn–Hilliard equation on the square, in preparation.

[12] C. M. Elliott and A. M. Stuart. Viscous Cahn-Hilliard equation. Part II: Analysis. *Journal of Differential Equations*, 128:387–414, 1996.

[13] B. Fiedler and C. Rocha. Orbit equivalence of global attractors of semilinear parabolic differential equations. *Transactions of the American Mathematical Society*, 352(1):257–284, 2000.

[14] P. C. Fife. Models for phase separation and their mathematics. *Electronic Journal of Differential Equations*, 2000(48):1–26, 2000.

[15] P. C. Fife, H. Kielhöfer, S. Maier-Paape, and T. Wanner. Perturbation of doubly periodic solution branches with applications to the Cahn-Hilliard equation. *Physica D*, 100(3–4):257–278, 1997.

[16] R. Franzosa. The connection matrix theory for Morse decompositions. *Transactions of the American Mathematical Society*, 311(2):561–592, 1989.

[17] R. Franzosa and K. Mischaikow. Algebraic transition matrices in the Conley index theory. *Transactions of the American Mathematical Society*, 350(3):889–912, 1998.

[18] M. Grinfeld and A. Novick-Cohen. Counting stationary solutions of the Cahn-Hilliard equation by transversality arguments. *Proceedings of the Royal Society of Edinburgh*, 125A:351–370, 1995.

[19] M. Grinfeld and A. Novick-Cohen. The viscous Cahn-Hilliard equation: Morse decomposition and structure of the global attractor. *Transactions of the American Mathematical Society*, 351(6):2375–2406, 1999.

[20] J. K. Hale. *Asymptotic Behavior of Dissipative Systems*. American Mathematical Society, Providence, Rhode Island, 1988.

[21] D. Henry. *Geometric Theory of Semilinear Parabolic Equations*, volume 840 of *Lecture Notes in Mathematics*. Springer-Verlag, Berlin – Heidelberg – New York, 1981.

[22] W. Kalies, K. Mischaikow, and R. Vandervorst. in preparation.

[23] H. Kielhöfer. Pattern formation of the stationary Cahn-Hilliard model. *Proceedings of the Royal Society of Edinburgh*, 127A:1219–1243, 1997.

[24] H. Kielhöfer. Minimizing sequences selected via singular perturbations, and their pattern formation. *Arch. Ration. Mech. Anal.*, 155(4):261–276, 2000.

[25] H. Kokubu, K. Mischaikow, Y. Nishiura, H. Oka, and T. Takaishi. Connecting orbit structure of monotone solutions in the shadow system. *Journal of Differential Equations*, 140(2):309–364, 1997.

[26] V. R. Korostyshevskiy. *A Hermite Spectral Approach to Homoclinic Solutions of Ordinary Differential Equations*. University of Maryland, Baltimore County, PhD thesis, 2005.

[27] S. Maier-Paape and U. Miller. Path-following the equilibria of the Cahn-Hilliard equation on the square. *Computing and Visualization in Science*, 5(3):115–138, 2002.

[28] S. Maier-Paape, U. Miller, K. Mischaikow, and T. Wanner. Rigorous numerics for the Cahn–Hilliard equation on the unit square. 2005.

[29] S. Maier-Paape and T. Wanner. Solutions of nonlinear planar elliptic problems with triangle symmetry. *Journal of Differential Equations*, 136(1):1–34, 1997.

[30] C. McCord. The connection map for attractor-repeller pairs. *Transactions of the American Mathematical Society*, 307(1):195–203, 1988.

[31] C. McCord. Simplicial models for the global dynamics of attractors. *Journal of Differential Equations*, 167(2):316–356, 2000.

[32] C. McCord and K. Mischaikow. On the global dynamics of attractors for scalar delay equations. *Journal of the American Mathematical Society*, 9(4):1095–1133, 1996.

[33] K. Mischaikow. Conley index theory. In R. Johnson, editor, *Dynamical Systems (Montecatini Terme, 1994), Lecture Notes in Mathematics 1609*, pages 119–207. Springer-Verlag, Berlin – Heidelberg – New York, 1995.

[34] K. Mischaikow. Global asymptotic dynamics of gradient-like bistable equations. *SIAM Journal on Mathematical Analysis*, 26:1199–1224, 1995.

[35] K. Mischaikow and M. Mrozek. Conley index theory. In B. Fiedler, editor, *Handbook of Dynamical Systems*, volume 2, pages 393–460. Elsevier, 2002.

[36] B. Nicolaenko, B. Scheurer, and R. Temam. Some global dynamical properties of a class of pattern formation equations. *Communications in Partial Differential Equations*, 14:245–297, 1989.

[37] K. P. Rybakowski. *The Homotopy Index and Partial Differential Equations*. Springer-Verlag, Berlin, 1987.

[38] P. Rybka and K.-H. Hoffmann. Convergence of solutions to Cahn-Hilliard equation. *Communications in Partial Differential Equations*, 24(5-6):1055–1077, 1999.

[39] D. Salamon. Connected simple systems and the Conley index of isolated invariant sets. *Transactions of the American Mathematical Society*, 291(1):1–41, 1985.

[40] J. Smoller. *Shock Waves and Reaction-Diffusion Equations*. Springer-Verlag, New York, second edition, 1994.

[41] R. Temam. *Infinite-Dimensional Dynamical Systems in Mechanics and Physics*. Springer-Verlag, New York, second edition, 1997.

[42] P. Zgliczyński and K. Mischaikow. Riogorous numerics for partial differential equations: the Kuramoto–Shivashinsky equation. *Found. Comput. Math.*, 1(3):255–288, 2001.

[43] S. Zheng. Asymptotic behavior of solutions to the Cahn-Hilliard equation. *Applicable Analysis*, 23:165–184, 1986.